THE STRUCTURAL GEOLOGY OF THE OLD BOOLCOOMATA AREA, SOUTH AUSTRALIA

By

ROBERT GRAHAM WILTSHIRE

B.Sc. (Hons), Sydney

A THESIS SUBMITTED IN ACCORDANCE WITH THE REQUIREMENTS OF THE DEGREE OF DOCTOR OF PHILOSOPHY.

DEPARTMENT OF GEOLOGY AND MINERALOGY

UNIVERSITY OF ADELAIDE

October, 1975

CONTENTS

Page

Page

SUMMARY

Two major groups of rocks can be recognised in the Old Boolcoomata area: an older basement which is part of the Willyama Complex, and a younger cover sequence which is part of the Adelaide System.

In this area the Willyama Complex consists of schists and gneisses intruded by basic dykes, pegmatites and granitic bodies. The schist sequence contains micaceous schists with interlayered quartzites and calcareous rocks, and shows evidence of being a meta-sedimentary sequence. The gneisses included layered gneiss, migmatite and granitic gneiss. The origin of the layered gneiss is obscure, but the migmatite and granitic gneiss are thought to have formed during high-grade metamorphism.

The cover sequence in this area is approximately 3,300 m thick and consists of siltstone, quartzite, tillite and conglomerate. The cover rests unconformably on the Willyama Complex, but in this area, the cover sequence has been faulted against the basement by the MacDonald Fault.

At least three metamorphic and deformational episodes have affected the basement rocks, the most recent of these also having affected the cover rocks. Mineralogical evidence for conditions of temperature and pressure during the first metamorphic event (M_1) has been obscured by the later metamorphic events. However, the presence of granitic gneiss and associated migmatites (thought to have been produced by melting during the first metamorphism) suggests that the temperature reached at least 650^{o}C. Mineral assemblages produced during the second metamorphic event (M_2) are indicative of the amphibolite

facies. The stability ranges of these minerals suggest that temperature was in the range of 500°C to 650°C and load pressure was between 0.4 GPa and 0.6 GPa, with high water pressure and low carbon dioxide pressure. The Boolcoomata Adamellite which intrudes Willyama Complex schists in the Old Boolcoomata area was formed by melting of gneisses during this metamorphic event (M_2).

After deposition of the cover, metamorphism (M_3), associated with the synchronous deformation of the basement and cover, caused retrogression of many of the high-grade minerals in the basement rocks and produced greenschist facies mineral assemblages in the cover rocks. During this metamorphism, temperature was of the order of 400°C and load pressure was approximately 0.4 GPa, with a high pressure of carbon dioxide.

Three periods of deformation can be recognised in the basement schists. The first period of deformation (D_1) has caused isoclinal folding, but most of the evidence for this deformation has been obliterated by the second period of deformation (D_2) which has produced tight folds with strongly developed schistosity parallel to their axial planes. Folds produced during the third period of deformation (D_3) are, in general, not as tight as the earlier folds and in the schists, have crenulation foliation developed parallel to their axial planes. The macroscopic structure of the basement in this area is dominated by an easterly plunging third generation synform which has been superimposed on tight first and second generation folds.

In most parts of the cover, only one period of deformation is evident which has produced tight folds with slaty cleavage subparallel to their axial planes. These folds have a similar orientation and style to third generation folds in the basement, suggesting that they have been formed during the same period of deformation (D_3).

Crenulations are developed in the cover rocks only adjacent to the MacDonald Fault, suggesting that these crenulations have developed in association with the faulting and that fault movement took place after folding of the cover. However, the trace of the MacDonald Fault (which separates the basement from the cover in the Old Boolcoomata area) is curved, suggesting that the fault has been folded.

Strain estimates from pebbles in conglomerates and tillites in the cover indicate that strain is generally low in the cover and that foliation has developed approximately perpendicular to the direction of maximum finite shortening. Cover rocks with the highest strain occur in a narrow, fault-bound zone flanked by basement rocks.

Deformation of the basement and the cover during the third period of deformation (D_3) has taken place in response to crustal shortening. This has resulted in the cover rocks being folded into a series of tight synclines and broad anticlines, this pattern being due to differences in competency between the basement and the cover. The tight synclines were probably sites of higher strain and so were the likely sites for the development of faults (e.g., the MacDonald Fault). Further shortening during this deformation caused localised folding of the MacDonald Fault.

This thesis contains no material which has been accepted for the award of any other degree or diploma in any University nor, to the best of my knowledge and belief, does it contain any material previously published or written by another person, except where due reference is made in the text.

R. G. Wiltshire

ACKNOWLEDGEMENTS

This project was suggested by Dr T.P.Hopwood, who supervised the early stages of the investigation and he is thanked for his help. Dr R.L.Oliver is thanked for supervising the remainder of the study, for discussions in the field and laboratory and for reading and commenting on draft versions of the thesis.

Drs T.H.Bell, M.P.Coward and M.A.Etheridge contributed to this study with fruitful discussions in the field and laboratory. Dr M.P.Coward is especially thanked fo encouraging the work on strain. Drs C.D.Branch and P.R.James are thanked for reading and commenting on draft versions of the thesis.

Thanks are also extended to Mr D.Bruce who prepared many of the thin sections, Mr R.Barrett who prepared the photographic plates and Miss A.P.Boos who typed the thesis. I am especially grateful to my wife, Helen, for her patience during the preparation of this thesis, and for typing and editing draft copies of the thesis.

CHAPTER 1

INTRODUCTION

1.1. REGIONAL GEOLOGICAL SETTING

The Olary Province lies in the northeast of South Australia (Fig. 1.1), adjacent to the New South Wales border, and contains Proterozoic Willyama Complex metamorphics, overlain unconformably by Adelaidean metasediments.

The Willyama Complex extends from 30 km east of Broken Hill in New South Wales, west for 200 km to Mount Victoria in South Australia. It crops out in the Olary Province as a series of blocks, each with its eastern margin unconformably overlain by Adelaidean metasediments and its western margin in faulted contact with Adelaidean metasediments (Campana, 1955, and Thomson, 1969, fig. 8). The Willyama Complex is composed of schists and gneisses which have been metamorphosed and deformed a number of times, and have been intruded by granitic rocks. The grade of metamorphism ranges from granulite and upper amphibolite facies in the Broken Hill district (Binns, 1964) to greenschist facies in the west, but the lower grades are probably due to retrograde metamorphism (Talbot, 1962). Radiometric dating indicates that the age of the high grade metamorphism in the Broken Hill district is about 1,700 m.y. (Compston and Arriens, 1968) and that the age of the Boolcoomata Adamellite, which intrudes the Willyama Complex schists and gneisses in the Olary region, is 1,580 m.y. (Compston, et al., 1966, specimen GA388).

At least three periods of deformation are recognisable in parts of the Willyama Complex (e.g., Hobbs, 1966; Talbot, 1962; Parker, 1972). In many areas, and especially in the Broken Hill district, early deformations have resulted in the development of tight to isoclinal folds and transposition of lithological layering (Anderson, 1965; Hobbs, 1966; Williams, 1967), and in the Olary region similar structures are seen (Talbot, 1962; Parker, 1972).

The rocks of the Adelaide System unconformably overlie the Willyama Complex in the Olary Province, and are representative of the Burra, Umberatana and Wilpena Groups. The base of the Burra Group is marked by a well developed conglomerate which rests unconformably on the Willyama Complex and allows the easy distinction between the basement and cover rocks in many areas (Campana and King, 1958). This conglomerate is overlain by slates, dolomites and quartzites of the Burra Group, followed unconformably by tillites and slates of the Umberatana Group (Talbot, 1967), though this unconformity is apparent in only a few places.

The Adelaidean metasediments have been folded into broad synclines and anticlines and show greenschist facies mineral assemblages (Talbot, 1962). They retain most of their sedimentary characteristics and only in the finer grained rocks, or in local zones of more intensive deformation, is cleavage evident.

1.2. PREVIOUS INVESTIGATIONS

The first geological mapping in the Olary Province was carried out by Mawson (1912), who delineated the unconformity between the Willyama Complex and the Adelaidean metasediments, and described some of the Willyama Complex rock types, but did not map their distribution.

The first subdivision of the Willyama Complex in the Olary Province was by Campana (1952, 1956a, 1956b, and Campana and King, 1958) who divided these rocks into two groups: a group of metasediments consisting of (from oldest to youngest) the Weekeroo-Billeroo Schists, the Ethiudna Calcsilicates and the Outalpa Quartzites, and a younger group consisting of migmatites, granite gneisses and 'anatectic' granites.

Talbot (1967) suggested that Campana's sequence of metasediments should be inverted and that the Ethiudna Calcsilicates were not a valid unit. Work by Pitt (1971b) and Parker (1972) have supported the inversion of the sequence, but both have reinstated the Ethiudna Calcsilicates.

Talbot (1962), Parker (1972), Berry (1973) and Flint (1974) have carried out detailed structural investigations of the Willyama Complex in parts of the Olary Province. Talbot (1962) and Parker (1972) recognised three periods of deformation, but Berry (1973) recognised four, and Flint (1974) recognised five periods of deformation. In all cases, first generation folds are obscure, but there is a well developed early schistosity, which is nearly everywhere parallel to lithological layering, and these two are folded by later deformations.

The Adelaidean succession was first subdivided by Campana (see Campana and King, 1958) who divided the sequence into the Torrensian, Sturtian and Marinoan Series. Talbot (1967) recognised the presence of an unconformity between the Torrensian and Sturtian Series (or between the Burra and Umberatana Groups).

Talbot (1962), Berry (1973) and Flint (1974) have examined the structure of the Adelaidean metasediments and found that, in general, these cover rocks have been folded only once, but have suffered two periods of deformation in some restricted areas, especially near faulted contacts with the basement.

Basement-cover relationships in the Olary Province have been investigated by Sprigg (1954), Campana and King (1958) and Talbot (1962). Sprigg considered that folding in the cover and basement was accomplished

by movement on faults, whereas Campana considered that faulting was of only minor importance, and that folding of the basement and cover took place at the same time. From studies in the Whey Whey Creek area, Talbot (1962) concluded that folding in the cover was achieved by "concentration of deformation in zones parallel to the foliation" in the basement rocks (ibid., p. 170). Thus there is no consensus of opinion on the basement-cover relationships in the Olary Province.

The Old Boolcoomata Area has been mapped previously by Whittle (1948) who did not recognise the presence of separate basement and cover sequences, and concluded that all the rocks in this area were part of the Willyama Complex.

There have been numerous reports on mineral occurrences in the Olary Province (see Campana and King, 1958) and other mapping in the Province has been carried out by Michelmore (1971), Waterhouse (1971) and Robertson (1972).

1.3. AIMS AND SCOPE OF INVESTIGATION

This study was undertaken to examine in detail the geology of a small part of the Olary Province and so contribute to the understanding of the region as a whole.

Two unresolved problems within the Olary Province which have received previous attention, and are considered specifically here, are:

(i) the relationship between the basement and cover rocks; and

(ii) the sequence within the basement rocks.

The investigation of these two problems has necessitated a detailed study of the structure and an investigation of the metamorphism of the basement and cover rocks. The area has been mapped

using enlarged aerial photographs and a geological map at a scale of 1:15,625 (Fig. 2.1) has been produced. References to locations on this map are given as six digit figures in the test and numbers prefixed by A470- refer to rock specimens housed in the Department of Geology collection. A structural analysis of the basement and cover rocks has been carried out to determine the macroscopic geometry of these rocks. Strain in parts of the cover sequence has been investigated to elucidate variations in strain during deformation of the cover. In presenting the results of these investigations, facts have been separated from interpretations: in each chapter, descriptive material is presented first and interpretations and synthesis of this material follow.

1.4. LOCATION, ACCESS AND PHYSIOGRAPHY

The area studied covers 90 sq. km around the Old Boolcoomata Homestead, which is situated 25 km north of Olary and about 350 km northeast of Adelaide (Fig. 1.1).

The Olary district has a semi-arid climate with an average annual rainfall of about 200 mm. Landforms in the area are typical of an arid area in a mature stage of erosion, with rounded hills separated by alluvial plains with dry creek beds.

Maximum relief in the area is in the north, where the Boolcoomata Adamellite rises to 500 m above sea level. Other hills rise to about 400 m above sea leval, whereas the alluvial plains are about 300 m above sea level. Outcrop on hills and in some of the large creek beds is good (up to 30%) but on the alluvial plains outcrop is sparse to absent.

The area is reached via the Barrier Highway from Adelaide to Olary and then by graded road to the Old Boolcoomata Homestead.

Within the southern part of the area, there are numerous tracks and the low relief and generally sparse vegetation make access easy.

CHAPTER 2

BASEMENT ROCK TYPES

2.1 INTRODUCTION

Campana and King (1958) divided rocks of the Willyama Complex within the Olary Province into two main groups: "Archaean Metasediments" and "Migmatites and Granite-Gneisses". Within the "Archaean Metasediments" they recognised a sequence which was (from the base) Weekeroo-Billeroo Schist, Ethiudna Calcsilicate Group and Outalpa Quartzites (or "Arkosic Quartzites, passing to granite-gneiss").

In the Old Boolcoomata area, the Willyama Complex consists of schists with interbedded calcareous rocks, geometrically below a group of quartzo-feldspathic rocks (which include layered gneisses, migmatites and granitic gneiss). Hence, in this area, the rock groups of Campana and King (1958) can be recognised, but, although the geometric order is the same, the limited facing evidence suggests that the sequence is overturned (Chapter 2.10). Within this area, no evidence exists to suggest that the layered gneisses have been derived directly from sediments, and so it may not be justified to equate them with the "Arkosic Quartzite" of Campana and King (1958).

The quartzo-feldspathic rocks in this area form the core of a major, easterly-plunging synform, around which the schists have been folded. In the north of the area, the schists are intruded by the Boolcoomata Adamellite, and elsewhere the schists and the quartzo-feldspathic rocks are intruded by pegmatites and amphibolites (see Fig. 2.1).

In this study, the Willyama Complex rocks have been subdivided using lithology. Descriptive names have been used for the rock units that have been mapped, and these names are distinguished in the text by use of capital letters (e.g., Fine-grained Mica Schist, Epidote

Schist, etc.). Rocks of the Willyama Complex in this area have been formed by metamorphism, deformation and, in some cases, metasomatism of pre-existing rock types. Hence, the same rock type occurring at two different locations need not necessarily represent the same stratigraphic horizon (see Chapter 2.2 for evidence of the original sedimentary character of some of these rocks). Conversely, rocks from the same stratigraphic horizon need not necessarily be represented by the same rock types now. Correlations can only be made by recognising the original rock type but where metasomatism has occurred this is not possible.

The relationships between the various rock types are shown on the geological map (Fig. 2.1) and in Table 2.1. The sequence of rock types recognised in this area and sequences recognised by other workers in different parts of the Olary Province are compared in Table 2.2.

2.1.1 Criteria for Distinguishing between Basement and Cover Rocks

In the area mapped, it is generally easy to distinguish between basement and cover rocks. However, in places, particularly near the MacDonald Fault, the cover rocks are schistose and structural features in the basement and cover rocks have similar orientations. This makes it difficult to distinguish between some basement and cover schists, and led Whittle (1948) to misinterpret the geology of the area.

There is no single criterion which can be used to distinguish between problematic basement and cover schists (see Table 2.3); the only mutually exclusive features are that:

(i) pegmatites are present only in the basement; and

(ii) pebbles are present only in the cover.

For the most part, basement schists have a well developed schistosity, are medium-to coarse-grained and are composed of muscovite, biotite and quartz. By comparison, cover rocks are generally slates with cleavage not strongly developed. Confusion over identification arises where the basement schists are fine-grained or where the cover rocks are schistose and do not contain pebbles.

Approximately 2 km east of the Old Boolcoomata Homestead (between 500600 and 700600) it is extremely difficult to distinguish between basement and cover rocks. The cover rocks here are schists with characteristics very similar to the adjacent basement schists, but can be distinguished from the basement in those places where pebbles are present in the cover rocks. About 0.5 km south of this location, an outcrop of fine-grained, quartz-rich phyllite occurs, in which bedding is well preserved. Because features of this phyllite are different from features of both adjacent basement and cover schists, it is not known to which of these groups this phyllite belongs.

2.2 SCHISTS

Mica schists with interlayered thin quartzites and calcareous rocks are the most abundant rocks of the Willyama Complex in this area. The schists crop out well, forming low hills which are elongate parallel to schistosity.

The schists can be divided into a number of different lithological types, namely:

Fine-grained Mica Schist

Medium-grained Mica Schist

Layered Schist

'Bedded" Schist

Epidote Schist

Chloritoid Schist

Graphite Schist

Piemontite Schist

Calcareous Rocks

Albite-rich Rocks

The relationships between these different rock types are shown in Fig. 2.1 and Table 2.1. In general, these rock types form discrete layers, and most of this layering is thought to reflect bedding for the following reasons:

(i) structures characteristic of transposition (Bishop, 1973) are absent from most of the schists in this area;

(ii) the gross lithological layering is continuous and mappable throughout much of the area, and forms a sequence that can be recognised in various parts of the area (see Fig. 2.1 and Table 2.1);

(iii) the mineral assemblages of many of the layers correspond to mineral assemblages produced by the metamorphism of sediments, suggesting that the layers have compositions compatible with a sedimentary origin (c.f. Turner and Weiss, 1963, p. 100);

(iv) quartz-rich layers within one schist unit contain cross-bedding (Fig. 2.2 and see Chapter 2.2.4).

However, some of the layers in the schist have probably been modified by metasomatism (e.g., albite-rich rocks) and therefore cannot be used in correlations, as they do not reflect their original composition. In addition, although these various rock types are fairly distinctive in the field, accurate mapping of their boundaries is difficult

because the boundaries are gradational, and in outcrop, schistosity, the most prominent feature, masks these boundaries.

As well as the gross lithological layering, fine scale lithological layering is present. In the Fine-grained Mica Schists the orientation of this fine scale lithological layering is independent of the orientation of schistosity, but is about parallel to gross lithological layering, hence it is thought to represent bedding.

On the other hand, in the Layered Schists, fine scale lithological layering is everywhere parallel to the strongly developed schistosity and is thought to have been produced by deformation and metamorphism (see Chapter 4.2).

2.2.1 Fine-grained Mica Schist

The main occurrence of Fine-grained Mica Schist is south of the Old Boolcoomata Homestead, where it is interbedded with 'Bedded' Schist and Calcareous Rocks.

The Fine-grained Mica Schist has a reasonably well developed schistosity with the micas evenly distributed throughout the rock. This schist is mainly a brown, muscovite-biotite schist. In places, grey, muscovite-rich laminations are parallel to the gross lithological layering, but are not necessarily parallel to the schistosity.

Under the microscope, this schist (e.g., A470-001) can be seen to be composed of polygonal grains of quartz (about 0.1 mm across) which are slightly elongate parallel to the schistosity, and fine-grained muscovite and biotite which are aligned defining the schistosity in the rock. The micas occur as small elongate grains about 0.2 mm x 0.05 mm, the biotite grains generally being slightly smaller than muscovite.

2.2.2 Medium-grained Mica Schist

The Medium-grained Mica Schist consists of grey, muscovite-rich schist interbedded with scattered quartz-rich layers ranging in thickness from a few millimetres to a few centimetres. The schist layers do not display a particularly strong schistosity in hand specimen.

In general, these schist layers are composed of polygonal quartz grains (about 0.5 mm across) with almost equant grains of muscovite which have a spread of orientations about a mean schistosity direction (e.g., A470-002). Grain-size of the muscovite ranges from about 0.5 mm x 0.2 mm to 1.0 mm x 0.5 mm. Some poorly aligned biotite is present and is finer grained than the muscovite.

Some schist layers consist of feldspar and muscovite, with only a small amount of quartz; both microcline- and albite-bearing varieties are present (e.g., A470-003 and A470-004 respectively). Grain-size and textures of these schists are generally similar to the quartz-rich variety described above.

2.2.3 Layered Schist

The Layered Schist is so called because it has, parallel to the schistosity, a layering defined by mica-rich and quartz-rich zones, each zone being 1 mm to 2 mm thick. The quartz-rich zones are generally lenticular and the mica-rich zones bifurcate around them (e.g., A470-005 and Fig. 2.3).

The mica-rich zones are composed predominantly of muscovite which occurs as small, elongate flakes (0.05 mm x 0.01 mm) strongly aligned parallel to the schistosity; some biotite and chlorite is present, also aligned parallel to the schistosity. Where garnet crystals occur, they are concentrated in these zones.

Quartz-rich lenses are generally composed of fine-grained granoblastic quartz (about 0.1 mm), together with some muscovite and chlorite grains which are not parallel to the schistosity in the rock. Some of the quartz-rich lenses are composed of single, large grains of quartz which show deformation bands and the development of sub-grains.

Some parts of the Layered Schist contain ellipsoidal aggregates of fine-grained muscovite and quartz. In one specimen (A470-007), remnants of andalusite, which poikiloblastically enclose small grains of quartz, are present in these aggregates (Fig. 2.4). This suggests that these aggregates have replaced original porphyroblasts.

Other parts of the Layered Schist contain prophyroblasts of muscovite (e.g., A470-006) which have their basal cleavage oblique to the schistosity (Fig. 2.5). Many of the muscovite porphyroblasts contain fine needles of sillimanite (Fig. 2.6).

2.2.4 'Bedded' Schist

The term 'Bedded' Schist is used here to refer to a unit of interbedded mica schists and quartzites. The unit has a thickness of about 50 m with both schist and quartzite interbeds ranging in thickness from 10 cm to 30 cm. Outcrops of this unit occur south of the Old Boolcoomata Homestead and in the centre of the area.

South of the Old Boolcoomata Homestead, the schist interbeds are fine-grained and show features similar to those of Fine-grained Mica Schist discussed in Chapter 2.2.1. The interbedded quartzites are fine-grained and contain biotite-rich laminations which in some cases outline cross-bedding (Fig. 2.2), indicating that the beds are facing upwards at this location.

Elsewhere, the schist interbeds are coarse-grained, contain some 'porphyroblasts' of muscovite and have a strongly developed schistosity (e.g., A470-008). Features of these schist interbeds are similar to those of the Layered Schist (Chapter 2.2.3). The quartzite interbeds are also coarse-grained and lack laminations.

2.2.5 Chloritoid Schist

A single layer of Chloritoid Schist occurs interbedded with Layered Schist, south of Cathedral Rock. The Chloritoid Schist is greenish, coarse-grained and has a strongly developed schistosity.

The rock (A470-009) is composed of muscovite-rich layers 0.3 mm to 2.0 mm thick, separated by quartz-rich lenses which are elongate parallel to the layer boundaries. The muscovite grains (up to 7.0 mm x 0.5 mm) which define the schistosity are also oriented parallel to this layering. Generally, the quartz-rich lenses are composed of aggregates of quartz with randomly oriented chlorite, though some of the lenses consist of single, large quartz grains (up to 4 mm long). Chlorite also occurs as lenticular clusters of grains (4 mm x 1 mm) which include scattered opaque minerals. In these clusters, chlorite grains have their basal cleavage aligned oblique to the schistosity (Fig. 2.7). Garnet and chloritoid (both with a grain size of about 1 mm) are scattered throughout the muscovite-rich layers. In some cases, the schistosity wraps around these grains, and in other cases, it is truncated by them (Fig. 2.8). There is a small amount of biotite in the rock, some grains of which are aligned with the muscovite, and other grains occur in the quartz-rich lenses.

2.2.6 Epidote Schist

Epidote Schist occurs at a number of localities in the area (see Fig. 2.1), always in close association with Calcareous Rocks. The Epidote Schist (e.g., A470-010) is a fine-grained, epidote-quartz-muscovite-biotite rock. In hand specimen, it appears similar to the Fine-grained Mica Schist, from which it can be distinguished by the presence of veins and patches (up to 30 cm long) of epidote.

Under the microscope the Epidote Schist is seen to be composed of equant grains of quartz (about 0.2 mm across) with aligned biotite grains (0.2 mm - 0.5 mm long) defining the schistosity. Muscovite and chlorite are present in small amounts, also aligned parallel to the schistosity. Epidote occurs as scattered grains ranging in size from 0.1 mm up to 1.0 mm. Other minerals occurring less commonly are garnet, albite and microcline.

2.2.7 Graphite Schist

A thin layer (3 m thick) of Graphite Schist occurs between the Black Maria and Lady Louise Mines, and another occurs southwest of Cathedral Rock. The position and strike of these layers suggest that they may be continuations of the same bed.

The Graphite Schist (A470-011) is a fine-grained, dark grey to black rock which generally has a well developed schistosity. However, near the Lady Louise Mine it displays weak schistosity and light coloured laminations.

The rocks, under the microscope, are seen to be composed of a mosaic of fine-grained quartz (0.05 mm - 0.1 mm) with biotite and some muscovite (0.1 mm) which are aligned to give the rock its schistosity. Small grains of graphite (0.01 mm) are abundant throughout

the rock and occur as inclusions within quartz and mica grains, as well as occurring between grains. The light coloured laminations are composed predominantly of quartz and contain less graphite than the rest of the rock.

2.2.8 Piemontite Schist

In the northeast of the area, a layer of Piemontite Schist about 2 m thick forms a distinctive horizon, but because it can only be traced for 1 km it is not a useful marker horizon.

The Piemontite Schist is a red, fine-grained, laminated rock with a weak schistosity. Layering, 1 mm to 15 mm thick, is defined by the relative abundances of quartz and piemontite. In thin section, these rocks (e.g., A470-012) are seen to consist of a mosaic of quartz grains (about 0.1 mm) with epidote and piemontite (grain-size 0.5 mm - 1.0 mm). Some layers also contain fine-grained (0.1 mm - 0.2 mm) biotite and garnet. Rare layers rich in opaques (e.g., A470-013) also contain fine-grained quartz and piemontite (0.5 mm - 1.0 mm) and poikiloblasts of garnet (up to 4 mm across) which enclose quartz and opaque grains, and retain the fine scale layering present in the opaque-rich layers.

2.3 CALCAREOUS ROCKS

Interbedded with the mica schists are two prominent horizons of Calcareous Rocks which crop out well and have a distinctive appearance, making them useful marker horizons. Their value as an aid in structural interpretation is enhanced by the fact that they generally have a well developed lithological layering and some have well developed lineations.

The Calcareous Rocks show mineralogical variations which are probably due to compositional differences within the original sediments,

but some of the mineralogical variations are due to differences in the grade of metamorphism throughout the area (see Chapter 7). The Calcareous Rocks in the area have a skarn-like appearance and include Epidote Quartzite, Quartz-Plagioclase-Hornblende Rock, Diopside Rock, Marble and Wollastonite-Vesuvianite-Garnet Rock. These various rock types appear to grade into one another laterally.

2.3.1 Epidote Quartzite

Epidote Quartzite is the most abundant calcareous rock type in the area. Its main occurrence is in the centre of the area where it crops out over a strike length of 1,500 m and has a thickness of about 2 m. The rock varies from a dark, uniform, flinty type (e.g., A470-014) to one with alternating quartz-rich and epidote-rich layers between 1 cm and 2 cm thick (e.g., A470-015). Both types contain prominent lineations defined by the alignment of biotite and aggregates of epidote, the layered variety also contains a conspicuous foliation.

The non-layered Epidote Quartzite is composed of a fine-grained mosaic of quartz (grain-size about 0.2 mm) with abundant, evenly distributed epidote grains (about 0.5 mm across) and equant grains of green-brown biotite (about 0.2 mm).

The layered varieties consist of a mosaic of quartz (0.1 mm - 0.5 mm) with epidote abundant in some layers. The grains of epidote are larger (grain-size up to 0.5 mm) in the epidote-rich layers than in the quartz-rich layers, where epidote has a grain-size of about 0.02 mm. A small amount of biotite is present and is more abundant in the quartz-rich layers than in epidote-rich layers. Calcite and albite are also present in small amounts.

2.3.2 Quartz-Plagioclase-Hornblende Rock

In hand specimen, the Quartz-Plagioclase-Hornblende Rock resembles in many respects the layered variety of the Epidote Quartzite and has a similar outcrop thickness (about 2 m).

The Quartz-Plagioclase-Hornblende Rock (e.g., A470-016) is composed of a mosaic of quartz and plagioclase (An_{25-30}) grains (ranging in size from 0.2 mm in the quartz-rich layers to 0.1 mm in the hornblende-rich layers) with blue-green hornblende (ranging in size from 0.1 mm in quartz-rich layers to 0.5 mm in hornblende-rich layers), elongate grains of which are aligned defining the foliation and lineation. Also present are small amounts of epidote and biotite.

2.3.3 Diopside Rock

West of the Mulga Mine there is a layer about 10 m thick of pale green Diopside Rock which contains thin, fine-grained quartz-feldspar layers. The Diopside Rock is coarse-grained with some diopside crystals up to 20 cm long (Fig. 2.9) and is composed of about 95% poikiloblastic diopside with quartz and plagioclase (A470-017).

2.3.4 Marble

One small outcrop in the east of the area (860275) displays Marble interlayered with Epidote Quartzite. The Marble (A470-018) is composed of recrystallised calcite grains (up to 1 mm across) with randomly oriented grains of talc (up to 0.5 mm) and chlorite (?) (up to 0.1 mm).

2.3.5 Wollastonite-Vesuvianite-Garnet Rock

A bed of calcareous rock about 1 m thick, interlayered with mica schists, occurs south of the Old Boolcoomata Homestead. Compositional layering within this rock is defined by the relative abundances

of various calcsilicate minerals (Fig. 2.10). Some layers consist of a fine-grained matrix of wollastonite with quartz grains (about 0.2 mm across), some epidote and vesuvianite, and porphyroblasts of garnet (up to 5 mm across) (A470-019). Other layers contain a mosaic of quartz grains with garnet and porphyroblasts of vesuvianite up to 10 mm long (A470-020). Accessory minerals in these rocks include fluorite, apatite and scheelite.

2.4 ALBITE ROCKS

Albite-rich rocks occur at a number of places within the mapped area, forming layers within the schists. Three main types of albite-rich rock have been recognised:

(i) Layered Albite Rock;

(ii) Albite Schist;

(iii) Albite Rock Interlayered with Mica Schist

2.4.1 Layered Albite Rock

The Layered Albite Rock is fine-grained and grey, with layering (1 cm - 5 cm thick) defined by variations in grain-size and by variations in content of opaque minerals. In this rock type, a weak foliation is present, oblique to the layering, and is defined by the alignment of scattered actinolite and chlorite. In places, the layering ends abruptly giving rise to a foliated, non-layered albite-rich rock (Fig. 2.11).

Under the microscope, the layered varieties (e.g., A470-021) are seen to consist of a fine-grained mosaic of albite (An_5) and quartz (grain-size 0.05 mm - 0.1 mm) with abundant, small grains of opaque minerals and scattered grains of chlorite, actinolite and epidote. The grain-size of albite is less in layers where opaque

grains are abundant, than in layers where opaque grains are scarce. Microscopically, the non-layered variety (e.g., A470-022) is similar to the layered variety, but differs in the following respects: it has fewer opaque grains; chlorite and actinolite are clustered into aligned lenses; it contains a small amount of calcite.

2.4.2 Albite Schist

The Albite Schist is a dark grey, fine-grained rock, composed almost entirely of albite (e.g., A470-023). The schistosity is defined by the elongation of albite grains and the alignment of small amounts of biotite, chlorite, actinolite and opaques.

2.4.3 Albite Rock Interlayered with Mica Schist

Mica schists adjacent to the Boolcoomata Adamellite are interlayered with fine-grained albite-rich layers 10 cm to 1 m thick. The general appearance of these interlayered rocks is similar to that of the 'Bedded' Schists, and the mica schist interlayers are similar to the Fine-grained Mica Schists.

The albite-rich layers are white, fine-grained and have a saccharoidal texture. Under the microscope, these layers show a granoblastic mosaic of albite (An_5) and quartz, the albite generally being finer grained (0.1 mm - 0.2 mm) than the quartz (0.3 mm - 0.5 mm) (A470-024).

2.5 QUARTZO-FELDSPATHIC ROCKS

Quartzo-feldspathic rocks occur in the core of a major, easterly-plunging synform in the east of the area, and also in a layer south of the Woman-in-White Mine. These rocks can be divided into three main types: Layered Gneiss, migmatite and Granitic Gneiss. The Layered Gneiss geometrically overlies the schists and grades up into migmatite which has a sharp contact with the Granitic Gneiss.

2.5.1 Layered Gneiss

Layered Gneiss, consisting of alternating quartzo-feldspathic and biotite schist layers, occurs at four localities:

(i) the main occurrence is as a layer about 130 m thick below the Granitic Gneiss and Older Migmatite, in the major synform in the east of the area;

(ii) south of the Woman-in-White Mine, the Layered Gneiss forms a distinctive unit about 120 m thick, bounded on the north by Layered Albite Rock and on the south by Medium-grained Mica Schist. The unit crops out over a strike length of 1.5 km and, in the west, is truncated by an amphibolite intrusion, but, in the east, relationships are obscure;

(iii) Layered Gneiss in the Boolcoomata Adamellite is surrounded by migmatite. These areas of Layered Gneiss are represented on the geological map (Fig. 2.1) as Younger Migmatite (see Chapter 2.6.1);

(iv) an outlier consisting of Layered Gneiss and migmatite is surrounded by Adelaidean metasiltstones and crops out 4 km south of the Old Boolcoomata Homestead.

The quartzo-feldspathic layers range in thickness from about 10 cm to 10 m, many having finer layers within them. On the mesoscopic scale, both the fine and thick layers are generally planar and parallel to the macroscopic layering defined by the boundaries with adjacent rock types. The fine layering ranges from 0.5 cm to several centimetres in thickness, and is defined by variations in grain-size and composition (Fig. 2.12).

In several quartz-rich layers south of the Woman-in-White Mine, biotite laminations outline structures which resemble cross-bedding (Fig. 2.13), but which do not give consistent facing directions. In most other rock types in the Layered Gneiss, laminations are parallel to the lithological layering, though some of the laminations lense out. Hence, there are no definite sedimentary structures within the Layered Gneiss.

The quartzo-feldspathic layers range in composition from quartz-rich to feldspar-rich, but in general consist of an equigranular mosaic of quartz, albite and microcline (grain-size about 0.2 mm); biotite and some muscovite are also present (e.g. A470-025).

Some of the feldspar-rich layers consist of a mosaic of interlocking grains of albite (about 0.5 mm across) with biotite (about 0.3 mm long) along many of the albite-albite grain boundaries (e.g., A470-026). Within these layers there are also some large muscovite grains up to 2 mm across.

Other feldspathic layers consist predominantly of microcline which is coarse-grained (up to 2 mm), the larger microcline grains enclosing some small grains of quartz and albite (A470-027). These layers are generally poor in biotite but contain abundant 'porphyroblasts' of muscovite, up to 4 mm across, oriented parallel to the layering. The 'porphroblasts' are ellipsoidal, and generally consist of a single grain of muscovite, though some are aggregates.

In some places, there are 'veins' of coarse microcline with pegmatitic appearance and indistinct contacts with the surrounding gneiss. These 'veins' are generally parallel to the lithological layering in the gneiss (Fig. 2.14). The microcline of these 'veins'

is associated with some quartz, and is in the form of subhedral grains about 1 cm long, but with some up to 2 cm long (A470-028). In general, the large microclines enclose grains of quartz and albite about 0.5 mm across (Fig. 2.15).

The Layered Gneiss contains several distinctive layers: a magnetite-feldspar-quartz layer; a corundum-biotite-plagioclase layer; and a barytes lense.

2.5.1.1 Magnetite-Feldspar-Quartz Rock. The magnetite-feldspar-quartz layer is about 5 m thick, and extends for 3 km around the major synform. In hand specimen, it is a red rock with layering defined by variations in grain-size and mineral content, the most obvious layers being those rich in magnetite.

In thin section, the rock (A470-029) is seen to be composed of an equigranular mosaic of quartz and microcline (grain-size 0.2 mm) with some albite and rare biotite. Magnetite is concentrated in layers 1 mm to 2 mm thick, and occurs as subhedral grains 0.1 mm to 0.3 mm across. These layers also contain quartz, microcline and albite. In some layers rich in microcline the grain-size ranges up to 2 mm.

2.5.1.2 Corundum-Biotite-Plagioclase Gneiss. In the Layered Gneiss south of the Woman-in-White Mine, corundum-biotite-plagioclase gneiss occurs as a layered unit about 15 m thick. It is a medium-grained rock with some layers rich in biotite and other layers rich in albite: porphyroblasts of corundum occur in both layers.

Microscopically, the rock (A470-030) is composed of equi-dimensional albite (An_{0-3}) grains up to 0.5 mm, with biotite (1.0 mm x 0.1 mm). Most of the biotite is aligned defining a mesoscopic foliation,

but some biotites define two weaker orthogonal foliations 30° and 60° from the mesoscopic foliation. Some equidimensional, poikiloblastic grains of muscovite up to 1 mm are scattered through the rock, and some smaller muscovite flakes are parallel to the foliations.

Corundum occurs as porphyroblasts up to 15 mm across. These porphyroblasts include some irregularly shaped muscovite grains, and are surrounded by a corona of coarse-grained muscovite about 2 mm across. The corundum-muscovite boundary is lobate and in the corona some corundum is isolated from the porphyroblast, but is still in optical continuity with the porphyroblast. The muscovite surrounding the corundum porphyroblasts is, in turn, surrounded by a biotite-deficient zone (up to 4 mm wide) in which the albite (An_{0-3}) is slightly coarser grained than in the remainder of the rock (most grains about 0.5 mm - 0.6 mm, see Fig. 216).

2.5.1.3 Barytes Rock At the Mulga Mine, a lense of barytes rock about 20 m thick extends for 500 m along strike, and grades laterally into quartzo-feldspathic gneiss. This rock is composed of coarse-grained barytes with magnetite and chalcopyrite (A470-031).

2.5.2 Older Migmatites

Within the mapped area, there are two discrete occurrences of migmatite: one associated with the Granitic Gneiss and one associated with the Boolcoomata Adamellite. Evidence suggests that the migmatites associated with the Granitic Gneiss are older than those associated with the Boolcoomata Adamellite (see Chapter 7) and so these migmatites have been termed the Older Migmatites and Younger Migmatites respectively.

The Older Migmatites overlie the Layered Gneiss and have a gradational contact with it. In a zone about 30 m wide in the Layered

Gneiss, pegmatitic veins become abundant as the Older Migmatites are approached. The Older Migmatites have a sharp contact with the Granitic Gneiss which overlies them, and which is, in turn, overlain by more migmatite. The features of both these areas of migmatites are similar, but the contact of the upper migmatites with any overlying rocks has not been investigated, as this contact is outside the area studied.

Details of the relationships between the various layers of the Older Migmatites are well exposed on water-worn surfaces in creek beds. Away from the creeks, it is difficult to distinguish the Older Migmatites from the Layered Gneiss.

The Older Migmatites consist of a fine-grained, layered palaeosome and a coarse-grained neosome which occurs as veins and patches, generally cross-cutting the layering of the palaeosome.

2.5.2.1 Palaeosome The palaeosome consists of alternating albite-rich and biotite-rich layers which range in thickness from a few centimetres to a few metres. These layers are generally planar on a mesoscopic scale, and individual layers show only small variations in thickness (Fig. 2.17). These rocks resemble 'banded gneisses' (Deitrich, 1960).

Under the microscope, the leucocratic layers of the palaeosome are seen to be composed of fine-grained albite (An_{5-10}) and quartz, and also a few small grains of muscovite. Albite and quartz form an interlocking mosaic with a grain-size of about 0.2 mm to 0.3 mm. The leucocratic layers have sharp contacts with the melanocratic layers which are composed of a mosaic of albite (An_{10}) and quartz (grain-size of 0.5 mm), together with biotite and muscovite which are generally aligned parallel to the lithological layering, giving the melanocratic layers a weak schistosity. Some of the thicker melanocratic layers contain porphyroblasts of muscovite up to 10 mm across.

2.5.2.2 Neosome The neosome also consists of two parts, the most common one being a quartz-feldspar rock and the less common one being a coarse-grained, biotite-rich rock. The biotite-rich component forms patches and lenses within the quartz-feldspar rock.

Where the quartz-feldspar neosome cuts across the palaeosome the contacts are not sharp (Fig. 2.18). Some layers of the palaeosome protrude into the neosome, and layering in the palaeosome is paralleled by biotite-rich lenses at the edges of the neosome (Fig. 2.19).

In some places the neosome occurs interlayered with the albite-rich layers of the palaeosome (Fig. 2.20) and in these circumstances forms pods around which the palaeosome is curved. Again, biotite-rich lenses occur at the edges of the quartz-feldspar neosome, approximately parallel to the layering in the palaeosome (Fig. 2.21).

The quartz-feldspar neosome is composed of coarse-grained albite (An_{5-10}) and quartz with an average grain-size of 2 mm, though some grains are up to 10 mm across; a small amount of polygonal fine-grained albite and quartz occurs between the large grains. Other minerals present are coarse-grained muscovite up to 20 mm across, and biotite about 5 mm across. The large grains of albite tend to be subhedral with many showing bent twinning, and the coarse-grained quartz shows undulose extinction.

The biotite-rich portions of the neosome are composed of albite (An_5) with grain-size of about 1 mm, a small amount of quartz which is generally finer grained than the albite, and biotite and muscovite (1 mm - 2 mm long) which are aligned to produce a fairly well defined schistosity. The albite grains are also elongate parallel to this schistosity.

2.5.3 Granitic Gneiss

In this area the Granitic Gneiss crops out over a strike length of 4 km and occurs as a layer 650 m thick, bounded above and below by Older Migmatite, with which it has sharp contacts. The Granitic Gneiss is cut by two faults; the southern fault truncates the gneiss, but on the northern fault only slight displacement is apparent and adjacent to this fault the Granitic Gneiss extends eastwards beyond the mapped area (Fig. 2.1).

The Granitic Gneiss is composed of quartz, albite, biotite and magnetite, and shows compositional variation from biotite-rich to biotite-poor. The biotite-rich varieties (e.g., A470-037) have a well defined gneissic foliation and a strong lineation. Both the lineation and foliation are defined by the orientation of biotite and by elongate aggregates of quartz and albite. Those varieties with less biotite (e.g., A470-039) have a strong lineation defined by elongate aggregates of quartz, albite, biotite and magnetite, but have no foliation.

Quartz grains tend to be 'platy' parallel to the foliation in the gneiss and individual grains are up to 10 mm by 2 mm (e.g., A470-038). The quartz grains show strongly developed undulose extinction. Albite grains (An_{10}) are nearly equidimensional and are usually less than 2 mm across, though some are up to 5 mm. Biotite occurs as grains up to 2 mm long generally oriented parallel to the foliation, though scatter is evident. A small percentage of microcline is present as grains up to 2 mm across, and in places where microcline is in contact with albite, myrmekite is developed. Accessory minerals present include zircon, monozite and epidote. Garnet is present in some parts of the Granitic Gneiss.

2.6 BOOLCOOMATA ADAMELLITE

The Boolcoomata Adamellite is a batholith of adamellite with patches of migmatite (hereinafter termed the Younger Migmatite - see Chapter 2.5.2). This batholith intrudes the basement schists in the north of the area mapped, and extends north and northeast beyond the boundary of this area (see Campana and King, 1958, plate 1). The intrusion is eroded to form high rounded hills with typical granitic sheet outcrops and tors.

The adamellite is leucocratic and even-grained throughout most of its outcrop area, but phenocrysts of microcline are present in some areas. The Younger Migmatites within the Boolcoomata Adamellite have gradational contacts with the adamellite and commonly enclose blocks of gneiss. The best exposures of this migmatite and gneiss occur in creek beds.

The contact of the Boolcoomata Adamellite with the Willyama Schists is sharp, but outcrops of the actual contact are rare. The intrusive contact at 710660 is illustrated in Fig. 2.22. Here, coarse-grained adamellite with some microcline phenocrysts is in contact with albite-quartz-muscovite rock. In a zone about 1 cm wide immediately adjacent to the contact, muscovite is particularly abundant.

At 660660, the contact is faulted, and movement has produced a foliated rock with feldspar and quartz augen (A470-042).

Within the adamellite pegmatite dykes are generally parallel to joints in the adamellite. The pegmatite dykes are up to 1 m wide and are composed of perthitic microcline, quartz, albite and muscovite (Fig. 2.23). These pegmatites have a smaller grain size and contain more muscovite than the pegmatites which occur in the schists

(Chapter 2.7). The pegmatites in the adamellite do not extend into the adjacent schists, and within 500 m of the contact there are no microcline-bearing pegmatites in the schists.

In the adamellite there is a weakly developed foliation in a zone about 1 km wide adjacent to the contact. This foliation is defined by lenses of biotite up to 10 cm long and 2 cm wide, and dips 80^{o} towards 150 (Fig. 4.34). These biotite lenses are possibly "sur-micaceous enclaves" (Didier, 1973, p. 303).

The adamellite is composed of quartz, albite, microcline and muscovite with minor amounts of biotite (e.g., A470-040, A470-041). Quartz grains range in size up to 5 mm across but are generally less than 2 mm. They have irregular shapes and show undulose extinction. Albite (An_5) grains occur as elongate laths, but are rarely euhedral, and range in size up to 5 mm, although, in general, are slightly smaller than quartz grains. Microcline grains are not as abundant as quartz and albite, and occur as grains 0.5 mm to 2 mm across some of which are microperthitic. In porphyritic adamellite (e.g., A470-044), microcline forms phenocrysts up to 1 cm long which are commonly poikilitic, enclosing small grains of quartz and albite.

2.6.1 Younger Migmatite

Within the Boolcoomata Adamellite, there are areas predominantly of migmatite, some of which enclose gneiss. These areas have been mapped as Younger Migmatite, but in fact include some adamellite and gneiss. The Younger Migmatite is a layered rock, consisting of quartzo-feldspathic and biotite-rich layers up to 10 cm thick. The layering is usually well defined but is irregular and discontinuous, and in most places is contorted into ptygmatic folds (Figs. 2.24, 2.25).

The quartzo-feldspathic layers are composed of quartz, albite and microcline (some as microperthite) generally with a grain-size of 1 mm to 2 mm, but with some grains up to 5 mm across. Also present are large muscovite grains up to 5 mm across, and scattered biotite 0.5 mm across.

The biotite-rich layers are composed of elongate biotite (up to 7 mm x 1 mm) poorly aligned parallel to the layering, and equant muscovite (up to 10 mm across). Some biotite grains have muscovite interlayered within them; muscovite grains enclose small biotite grains and sillimanite needles.

These migmatites differ from the Older Migmatite (Chapter 2.5.2) in the following respects:

(i) they occur only within the adamellite, commonly surrounding blocks of gneiss;

(ii) the layering is more regular, but is contorted into ptygmatic folds;

(iii) they contain microcline.

2.7 PEGMATITES

Pegmatite pods and veins composed of perthitic microcline and quartz with some muscovite, tourmaline and beryl are common throughout the basement schists. The pegmatites range in size from veins a few centimetres wide, up to pods 10 m wide and 50 m long, generally with their long direction parallel to second generation schistosity in the enclosing schists. Some thin pegmatite pods have been folded and boundinaged by the second period of deformation (see Chapter 4.4.6); other thicker pods have been folded around third generation folds (Chapter 4.5.6). Most pegmatite pods do not appear

to have been deformed by the second period of deformation. These relationships suggest that there have been two periods of pegmatite formation in this area; one before the second period of deformation and one between the second and third periods of deformation.

In one feldspar quarry (690375), both schist and an amphibolite dyke have been intruded by pegmatite, indicating that at least one of these periods of pegmatite formation post-dates the emplacement of the amphibolite dykes in the area mapped.

2.8 AMPHIBOLITES

Amphibolite dykes occur in a number of places in the schists and Granitic Gneiss. Outcrop of the amphibolites is generally poor and so determination of the exact shape of amphibolite bodies is difficult (with the exception of the one south of the Woman-in-White Mine). Most of the amphibolites appear to occur as elongate bodies (up to 25 m long) concordant with the second generation schistosity. Third generation folds have not been seen in the amphibolites.

Generally, the amphibolites are composed of hornblende and plagioclase. In hand specimen, a strong lineation is defined by the alignment of hornblende crystals and aggregates of plagioclase, but no foliation occurs.

Just south of the Woman-in-White Mine, an amphibolite body intruding Layered Albite Rock is well exposed. The intrusion has a subelliptical shape, 1.3 km by 0.3 km, elongate parallel to the strike of the lithological layering in the surrounding Layered Albite Rock, but, in detail, it crosscuts the layering. No contact alteration of the surrounding rocks and no fine-grained margin to the amphibolite have been developed. The amphibolite in this body is fairly uniform, consisting of hornblende and plagioclase, and minor epidote which in

places forms veins and patches. In thin section, the amphibolite is seen to be composed of blue-green hornblende, comprising 40% to 60% of the rock (with grain-size generally between 0.1 mm and 0.5 mm, but some up to 1.0 mm), and plagioclase (An_{35}, with a grain-size of 0.1 mm to 0.5 mm), and minor epidote (e.g., A470-049, A470-050).

At 685380, two small plug-like bodies of felsic amphibolite crop out. Plagioclase (An_{10}) with a grain-size of 0.2 mm to 1.0 mm forms about 80% of the rock, with scattered blue-green hornblende (grain-size generally 0.2 mm to 0.4 mm but ranging up to 1.0 mm) forming the remainder of the rock.

2.9 BRECCIA

Brecciated albite-rock occurs at Cathedral Rock and 1 km west of the Woman-in-White Mine. At Cathedral Rock, the breccia forms a prominent landmark, standing about 25 m above the surrounding schists (Fig. 2.26). The breccia occurs in a subelliptical area 300 m by 200 m, divided into two parts by a layer of Albite Schist about 50 m thick. In the northern part, the breccia has small fragments and a diopside matrix; in the southern part, fragments are larger and the matrix is composed of albite.

2.9.1 Breccia with Diopsidic Matrix

In the northern part, the breccia is composed of fragments of fine-grained, flinty albite rock, usually non-layered. The fragments have irregular shapes and generally range in size from 5 cm to 20 cm (Fig. 2.27, 2.28), though some blocks are larger. The matrix is composed of coarse-grained diopside.

The fragments consist of an interlocking mosaic of albite (An_5) with grains slightly elongate and 0.05 mm to 0.1 mm across. Near

the margins of the fragments grains are distinctly elongate and aligned parallel to these margins, even where quite small irregularities occur in the margins.

The breccia matrix is composed of coarse-grained diopside (which looks like actinolite in hand specimen) with grains up to 10 mm long, many occurring as well formed prisms. In thin section, the diopside has a strong green colour and some grains have anomolous blue interference colours. Also in the matrix there are some grains of quartz, albite and sphene up to 1 mm across.

North of this breccia, veins of diopside about 5 cm thick occur in the adjacent albite rocks (Fig. 2.29). Some of these veins are parallel to the layering in the albite rocks but others are oblique to the layering.

2.9.2 Breccia with Albitic Matrix

In the southern part of Cathedral Rock, the breccia is composed of angular blocks of layered albite rock (ranging up to 1 m across) and an albite-rich matrix (Figs. 2.30, 2.31). In some blocks, the layering is folded and in a few cases the blocks have also been folded (Fig. 2.3.2).

Fragments in this breccia are composed of fine-grained albite with disseminated fine-grained opaques. Layering within the fragments is defined by variations in grain-size and by relative concentrations of the opaques. Grain-size in the finer-grained layers is between 0.01 mm and 0.02 mm, and in the coarser-grained layers is about 0.05 mm. Both have a granoblastic texture.

The breccia matrix is composed, in part, of laths of albite (An_5, up to 0.5 mm long) and quartz grains with undulose extinction (up to 1 mm), and in part of fine-grained (about 0.1 mm) polygonal

quartz and albite. Small amounts of muscovite, apatite and sphene also occur.

2.10 RELATIONSHIPS WITHIN THE SCHISTS OF THE WILLYAMA COMPLEX

One of the aims of this study has been to investigate the sequence within the Willyama Complex. Although a sequence has been previously recognised (Campana and King, 1958), the significance and facing of this sequence has been disputed (Talbot, 1967; Pitt, 1971b; Parker, 1972; and see Chapter 2.11) and so an attempt has been made here to solve this problem. In addition, the sequence in the basement rock types has been used to aid in the interpretation of the macroscopic structure of the area (Chapter 4.7).

Within the schists a sequence of rock types has been recognised which, despite the deformation and metamorphism, is thought to reflect, in part, an original sedimentary sequence. However, some of the sedimentary layers of this sequence have been altered by metasomatism (see Chapter 7.3). Some of the lithological layers within the sequence of schists form continuous, distinctive horizons (e.g., the 'Bedded' Schist), some form discontinuous horizons (e.g., the Calcareous Rocks), whereas others form lenses within other layers (e.g., Chloritoid Schist). The distribution of these various layers is shown on the geological map (Fig. 2.1) and a comparison of the sequences of rock types along various traverses in the schists is shown in Table 2.1.

Evidence that the sequence within the schists represents an original depositional sequence is seen in Traverse 1 where the 'Bedded' Schist contains cross-bedding (see Chapter 2.2). The sequence along Traverse 1 is (from oldest to youngest): Fine-grained Mica Schist, Epidote Schist, Calcareous Rock, Fine-grained Mica Schist and 'Bedded Schist. This sequence of schists is isolated from the remainder of the

basement schists by alluvium and so the units of this sequence cannot be traced to other parts of the area. However, the sequence in Traverse 1 shows similarities to parts of other sequences in the schists elsewhere in the area and especially to parts of the sequences along Traverses 3 and 4.

Along Traverses 3 and 4, the sequence is (from the geometric top): Layered Gneiss, Layered Albite Rock, Medium-grained Mica Schist, Epidote Schist, Calcareous Rock, Layered Schist, 'Bedded' Schist, Layered Schist, Calcareous Rock, Epidote Schist, Medium-grained Mica Schist, Layered Albite Rock, Layered Gneiss. It can be seen that below the 'Bedded' Schist the sequence is repeated in reverse order and this fact, together with the outcrop pattern, suggests that the sequence has been isoclinally folded. (This possible fold is interpreted as a first generation fold - see Chapter 4). The differences between the sequence in Traverse 1 and sequences along Traverses 3 and 4 are:

(i) the Calcareous Rocks in the vicinity of Traverse 1 range from Wollastonite-Vesuvianite-Garnet Rock to Quartz-Plagioclase-Hornblende Rock, whereas those in Traverses 3 and 4 range from Epidote Quartzite to Quartz-Plagioclase-Hornblende Rock to Diopside Rock;

(ii) in Traverse 1, the 'Bedded' Schist consists of fine-grained 'sandy' quartzite with laminations outlining cross-bedding, and interbedded Fine-grained Mica Schist. In Traverses 3 and 4, the quartzite layers are coarse-grained and lack laminations, and the schists are coarse-grained with a strongly developed schistosity similar to that of the Layered Schist;

(iii) other rock types along Traverse 1 are fine-grained schists, whereas Layered Schist and Medium-grained Mica Schist are present in Traverses 3 and 4.

The differences between the Calcareous Rocks of Traverse 1 and Traverses 3 and 4 could be explained by variations in the original rock type. Where the calcareous horizons can be followed with some certainty (e.g., between Traverses 2, 3 and 4) wide mineralogical variations are observed. The differences between the 'Bedded' Schist and other schist horizons of Traverse 1 and Traverses 3 and 4 could be explained by slight differences in metamorphism (see Chapter 7) and degree of deformation.

If the correlation between Traverse 1 and Traverses 3 and 4 is valid, then the schist sequence is younger than the Layered Gneiss although the schist sequence dips under the Layered Gneiss.

The sequences in Traverses 2 to 6 correspond well from Layered Gneiss down to Layered Schist (Table 2.1) and this part of the sequence can be followed almost continuously between these traverses (Fig. 2.1). However, there are some differences between the sequences along these traverses: the mineralogy of the Calcareous Rocks varies widely (see Table 2.1) and in Traverse 5, the Layered Schist contains one layer of Chloritoid Schist and one layer of Epidote Quartzite which extends as far as Traverse 6.

The main difference between the sequences is that in Traverses 2 to 4 below the Layered Schist there is 'Bedded' Schist, whereas in Traverses 5 and 6 below the Layered Schist there is Albite Schist and Interlayered Albite Rock and Mica Schist (see Table 2.1). It is possible that the Interlayered Albite Rock and Mica Schist in Traverses 5 and 6 is the 'albitized' equivalent of the 'Bedded' Mica Schist in Traverses 2 to 4. However, the presence of Albite Schist in Traverses 5 and 6 does not support this theory as it has no equivalent in the sequence of

Traverses 2 to 4. In addition, the observed structures do not support this theory (see Chapter 4) and so the relationships remain obscure.

From the evidence cited in Chapter 2.2 and above, it is thought that the sequence of rock types recognised in the schists of this area reflects, in the greater part, the depositional sequence of these rocks. However, other parts of the sequence have been metasomatised, and although the albite-rich layers appear to be concordant with the lithological layering of the other rock types they cannot be utilized in correlations because the original rock type is unknown. Nevertheless, if albite-rich rocks occur at the same position within similar sequences from different areas, then these albite-rich layers are likely to have been formed from the same original horizon. For example, along Traverse 4 in the Old Boolcoomata Area, two layers of Layered Albite Rock occur; the sequence along Traverse 4 is repeated by folding (see above), and the two layers of Layered Albite Rock occur at the same relative positions in the sequence and so most probably represent the same original horizon.

Before the sequence recognised in the schists can be claimed to be a valid stratigraphic sequence, further evidence of its original sedimentary nature must be found. If sedimentary structures were initially present in the rocks of this area, these structures have been totally obliterated (except in one locality -- see Chapter 2.2) by deformation and metamorphism. The sedimentary origin of the sequence might be supported if a similar sequence can be recognised in schists elsewhere in the Willyama Complex; however, as previous workers have not subdivided the schists of the Willyama Complex (see below), such correlations cannot be made at this time.

2.11 COMPARISONS WITH SEQUENCES ELSEWHERE IN THE OLARY PROVINCE

The Willyama Complex rocks in the Olary Province were first subdivided by Campana and King (1958), who recognised two main units which they termed "Archaean Metasediments" and "Migmatites and Granite-Gneisses". They further subdivided the "Archean Metasediments" into what they considered to be a stratigraphic sequence, which was, from the base up:

Weekeroo-Billeroo Schists - consisting of mica schists, gneisses and quartzites:

Ethiudna Calcsilicate Group - containing calcsilicate horizons separated by "Flaggy sandstones" and schists;

Outalpa Quartzite - composed of feldspathic quartzites and arkoses, grading to granite-gneiss and migmatites.

At Weekeroo 30 km west of this area (see Fig. 1.1), Talbot (1967) recognised a similar sequence of rock types in the Willyama Complex, but considered that it was not a sedimentary sequence because many of the schists show transposition and because parallelism of layering and foliation in the gneisses may have resulted from isoclinal folding (ibid., p. 56). Talbot's sequence based on the geometric order of the rock types is, from the base: layered gneiss, mica schists and "bedded mica schists".

Pitt (1971b) recognised a similar sequence at Weekeroo Hill, but considered that this represented an original depositional sequence. By use of sedimentary structures, he determined the order to be, from the base: layered gneiss, calcsilicate, mica schist, "bedded mica schist".

Parker (1972) recognised a similar sequence near Wiperaminga Hill, also using the facing from sedimentary structures.

A comparison of the sequences observed by the above workers, and the sequence delineated in this study, is shown in Table 2.2.

The oldest group of rocks in the Old Boolcoomata area is the Layered Gneiss, which has features similar to the layered gneisses described by Talbot (1967), Pitt (1971b) and Parker (1972). Campana and King (1958) have mapped these rocks as part of the Outalpa Quartzite. However, at Old Boolcoomata the Layered Gneiss contains no evidence of sedimentary structures and so naming it Outalpa Quartzite may be misleading.

The Calcareous Rocks at Old Boolcoomata show a similar range in mineralogy to the calcsilicates at Ethiudna Mine 45 km west of the area (Campana and King, 1958, pp. 16-17; cf. Chapter 2.3). However, at Ethiunda the calcsilicates form a much thicker sequence and are enclosed in granite. Calcsilicates with similar mineralogy also occur at Weekeroo Hill (Pitt, 1971b), Wiperaminga Hill (Parker, 1972) and Ameroo Hill (Campana and King, 1958, and personal observation). At these three localities, the calcsilicate rocks occur in the sequence in a position similar to the Calcareous Rocks at Old Boolcoomata.

Talbot (1967) considered that the Ethiudna Calcsilicate Group was invalid as a regional unit because:

> "in the type locality . . . the group consists of calc-silicates and dolomites in an isolated gneissic terrain whose 'stratigraphic' position is unknown. The 'stratigraphic' position of the Ethiudna Group as the Middle Group of metasediments is however determined by the position of amphibolites at Weekeroo, Ameroo Hill and Old Boolcoomata. In none of these localities do the rocks resemble the Ethiudna rocks and in fact in two of them the calc-silicates are intrusive igneous rocks. In addition, calc-silicates occur in other parts of the section (e.g., in the migmatitic schist unit at Weekeroo) and it is considered unwise to make long range correlations of this sort in gneissic terrains." (Talbot, 1967, p. 55).

The amphibolites at Weekeroo and at Old Boolcoomata are most certainly igneous in origin, but, at Old Boolcoomata there also exists a distinctive horizon of calcareous rocks which is interlayered with mica schist; the variations in mineralogy within this calcareous horizon (see Chapter 2.3) suggest that it is sedimentary in origin.

Moreover, it can be seen from Campana and King (1958), Pitt (1971b), Parker (1972) and this study, that there is a persistent horizon of calcareous rocks in the sequence within the Willyama Complex. It is perhaps unfortunate that Campana and King (1958B chose the isolated Ethiudna occurrence as the 'type area' for these calcareous rocks.

Other workers in the Olary Province have not subdivided the mica schists, so it is not possible to make detailed comparisons of the sequence in the schists in the Old Boolcoomata Area with sequences in schists elsewhere in the Olary Province. However, the "mica schist" of Talbot (1967), Pitt (1971b) and Parker (1972) is considered to be the equivalent of the schists above the horizon of Calcareous Rocks.

The "bedded mica schist" of Talbot (1967) and Pitt (1971b) are "red brown sandy granofels grading to sandy mica schists" (Pitt, 1971b) and do not correspond to any rocks in the sequence at Old Boolcoomata.

In general in the Olary Province, the sequences recognised in the Willyama Complex have been regarded as sedimentary in origin (e.g., Campana and King, 1958; Pitt, 1971b; Parker, 1972). These sequences are based on broad subdivisions of the Willyama Complex and might represent gross stratigraphic units. Investigations of the sequence in greater detail are required before the detailed depositional sequence can be confidently determined. In some areas (e.g., at Weekeroo, Talbot,

1967, and in the Layered Gneiss in this study) it may not be possible to recognise a depositional sequence because transposition, metasomatism and metamorphic differentiation have obliterated evidence of bedding.

CHAPTER 3

COVER STRATIGRAPHY

3.1 INTRODUCTION

The Adelaidean rocks occupy the western and southern portion of the mapped area and are part of a belt of folded sediments which extends northwest from Olary for about 36 km, to the Bimbowrie Homestead (Fig. 1.1, and Campana and King, 1958, plate 1). The belt of sediments has a synclinal structure with the northeast limb faulted out by the MacDonald Fault, bringing successive members of the Adelaidean sequence into contact with the Willyama Complex. The relationship between the Adelaidean metasediments and the Willyama Complex to the south of this belt is obscured by alluvium (Fig. 1.1).

The Adelaidean succession has a thickness of about 3,300 m, and is composed predominantly of siltstones and interbedded quartzites, with tillite and conglomerate beds and minor dolomite lenses. Five stratigraphic units have been recognized:

Unit 1 conglomerate

Unit 2 interbedded siltstone and quartzite

Unit 3 tillite

Unit 4 interbedded siltstone and quartzite

Unit 5 conglomerate and tillite (?)

Unit 1 rests unconformably on the Boolcoomata Adamellite and is in faulted contact with Unit 5, which is also in faulted contact with Unit 4, and with the Willyama Complex. Units 2, 3 and 4 are exposed in almost continuous outcrop from the Bimbowrie Road, north to the MacDonald Fault, which separates these units from the Willyama Complex and from Units 1 and 5. These relationships, and the proposed correlations of these units, are summarized in Table 3.1.

3.2 UNIT 1

This unit is exposed only in the north of the mapped area, near the Old Boolcoomata Homestead, and can be divided into two subunits.

3.2.1 Subunit 1a

Subunit 1a is a conglomerate which rests unconformably on the Boolcoomata Adamellite (Fig. 3.1). The subunit has a maximum thickness of 300 m, but in places is quite thin due to the relief of the erosional surface on which the conglomerate rests.

The conglomerate is composed mainly of rounded granitic boulders and pebbles, set in a sandy matrix of quartz, feldspar, muscovite and biotite. The granite pebbles and boulders range from about 50 cm to only a few centimetres across, are well rounded and have a high sphericity, with axial ratios generally less than 2. There is a tendency for the more ellipsiodal pebbles to be aligned parallel to bedding (see Chapter 6). There is a small percentage of quartzite and albitites present in the conglomerate, but only as pebbles up to 5 cm diameter.

Bedding is usually not well defined, but is shown in places by variations in the degree of sorting or by variations in the nature of the matrix. Sorting is generally poor, but in some beds, pebbles are of a fairly uniform size, this being more common where the pebbles are small.

Both the grain size and composition of the matrix are variable. The grain size ranges from fine to coarse sand-sized particles. The ratios of the minerals present in the matrix also vary, but quartz and feldspar are always dominant over muscovite and biotite. At one locality (530630) the matrix is dolomitic.

3.2.2. Subunit 1b

Subunit 1b crops out in only a small area about 500 m east-southeast of the Old Boolcoomata Homestead (Fig. 2.1), where it overlies Subunit 1a. The boundary between Subunits 1a and 1b is marked by a change in the degree of rounding of pebbles and a change from predominantly granitic pebbles to abundant metasediment pebbles.

Subunit 1b is a polymictic conglomerate with a fine grained quartz-rich matrix enclosing angular blocks of Willyama Complex rocks and some rounded pebbles. Rock types present are mainly metasediments (quartzite and albitite) and granite pebbles are rare. Pebble size in Subunit 1b ranges from 20 cm to 2 cm, the larger pebbles in particular being angular. Axial ratios are near unity and there is no alignment of pebbles (see Chapter 6). Sorting is poor and bedding indeterminate.

3.3. UNIT 2

This unit is the lowest exposed unit in the sequence between the Bimbowrie Road and the MacDonald Fault. The base of this unit is covered with alluvium and is therefore not exposed.

The unit consists of interbedded siltstones and quartzites and has an exposed thickness of 230 m. The quartzites crop out as prominent hog-back ridges, but the siltstones are exposed only in creek beds.

Quartzite beds are about 3 m thick and are composed almost entirely of quartz with minor feldspar and heavy minerals. Cross-bedding is apparent in some beds.

The siltstones are green, finely laminated and have a weakly developed slaty cleavage.

3.4. UNIT 3

This unit consists of tillite interbedded with some quartzite and slate. The glacial origin of this unit is well established by previous investigators in the Olary Province and elsewhere within the Adelaide System (e.g., Campana and King, 1958; Howchin, 1920; and Thomson, 1969).

The unit crops out along the southern boundary of the area (Fig. 2.1) and develops its maximum thickness in the southeast, where it forms a prominent ridge. The tillite ranges in thickness from 150 m in the west to approximately 2,000 m in the hinge of a tight anticline in the east, but thins rapidly in the limb to the south (Fig. 3.2). These variations in thickness are stratigraphic but may have been modified by folding. The overlying beds (Unit 4) lense out against the tillite and some intertonguing is evident on the northern limb of this anticline (Fig. 2.1 and 3.2).

Most of the pebbles and boulders in the tillite are granitic (granite, gneiss and migmatite) but some are quartzite and biotite schist. Size of the pebbles and boulders ranges from 1 cm up to 2 m in diameter. The pebbles and boulders are generally ellipsoidal with axial ratios in planar faces of up to 4.0 for quartzofeldspathic pebbles, and up to 6.0 for schist pebbles (see Chapter 6).

The matrix of the tillite is composed of quartz, feldspar, biotite and calcite, with a grain size of 0.4 mm to 2 mm. Biotite is aligned to give a weak cleavage in the matrix.

3.5. UNIT 4

This unit consists mainly of siltstones, interbedded with quartzites, tillites, grit beds and dolomites.

The lower contact is not sharply defined, as there are numerous pebble beds above the massive tillite of Unit 3. The base of Unit 4 is taken as the boundary between the massive tillite of Unit 3 and the interbeds of tillite, quartzite and siltstone which overlie, and in places lense into, Unit 3 (Fig. 2.1).

The lower 70 m of Unit 4 consist of interbedded siltstone, quartzite and tillite. The quartzites range from 1 m to 5 m in thickness and generally contain well developed cross-bedding. The tillite interbeds, in general, have a siltstone matrix, and pebbles range in size from 1 cm to 30 cm in diameter.

Overlying these beds are approximately 2,800 m of interbedded siltstone and quartzite, the quartzite beds being thinner and sparser towards the top of the unit. Also towards the top of the unit, some beds of siltstone are calcareous, and there are a few thin dolomite beds.

The siltstone of this unit is grey to dark brown, with some thin (up to 5 mm) quartz-rich laminations. Thickness of individual siltstone beds ranges from a few metres near the base of the unit to tens of metres towards the top. In thin section, the siltstone is seen to consist of biotite, muscovite and quartz, with minor feldspar, chlorite and opaques (mainly magnetite). Grain size is about 0.05 mm and quartz grains are rounded. In most of the siltstones, the micas are aligned to define a cleavage. Where the siltstone is calcareous, calcite is concentrated in small lenses with chlorite and coarse-grained muscovite, the lenses being aligned parallel to crenulation foliation in the siltstone.

Quartzite beds in this unit range in thickness from about 0.2 m to 7 m. They are composed of quartz with minor feldspar and opaques. Festoon cross-bedding occurs in some beds.

The rare dolomite beds crop out poorly, are a buff colour and have a saccharoidal texture.

3.6. UNIT 5

Unit 5 crops out in a small area south of Unit 1, and is apparently in faulted contact with both Units 1 and 4 (see Chapter 6). Unit 5 can be divided into two subunits: 5a, which is a conglomerate with granite pebbles and a minimal amount of slaty matrix, and 5b, which is a strongly foliated tillite (?). The outcrop pattern (Fig. 2.1) suggests that Subunit 5b overlies Subunit 5a, but this relationship is uncertain, as bedding is not preserved in either subunit.

3.6.1. Subunit 5a

Subunit 5a has an irregular outcrop pattern (Fig. 2.1) with thin layers of slate between 'fingers' of conglomerate. Outcrops consist of rounded boulders of granite (to 50 cm in diameter) littering the surface, with only a small amount of grey slate exposed between the granite boulders.

3.6.2. Subunit 5b

Subunit 5b contains pebbles of quartzite, granite, albitite and schist, which range in size from a few millimetres up to 20 cm in diameter, and which are ellipsoidal with long axes subparallel to the cleavage which is developed in the matrix (see Chapter 6). The matrix in the western part of Subunit 5b consists of a fine-grained mosaic of quartz and albite (A470-063), whereas, to the east, the matrix is a biotite, muscovite, quartz schist (A470-064).

3.7. CORRELATIONS AND DISCUSSION

The correlations between the informal units used in this thesis and the formal stratigraphic subdivisions of the Adelaide System are shown in Table 3.1.

From the first detailed mapping of the Old Boolcoomata Area, Whittle (1948) concluded that the granite boulders and pebbles in Units 1 and 5, described in this thesis, were formed by granitisation, related to the formation of the Boolcoomata Adamellite. However, Unit 1 clearly rests unconformably on the Boolcoomata Adamellite, and sedimentary structures in Unit 1 indicate the clastic nature of these granite pebbles and boulders. Campana and King (1958) mapped Units 1 and 5 as part of the Sturt Tillite and concluded that Unit 1 of this thesis represented "land moraine" (ibid, p. 33). However, I agree with Pitt (1971a) that Subunit 1a is a fluvial deposit, derived from the Boolcoomata Adamellite. Subunit 1b is probably also a fluvial deposit, but with a different source area which, because of the angularity of the fragments, must also have been close to the site of deposition.

The age and relationship of Unit 1 to Units 2 to 5 of the Adelaidean succession in this area is uncertain, because Unit 1 is separated from the other units by a fault. However, it is likely that Unit 1 is part of either the Burra or the Umberatana Groups, as it appears to have suffered the same deformational history as these groups.

Campana and King (1958) correlated Unit 2 of this study with the Sturt Tillite, but Pitt (1971a) regarded this unit as part of the Burra Group. This difference of opinion is caused by a change in the definition of the base of the Sturtian Series, which was originally defined as the base of the Belair Group (Mawson and Sprigg, 1950), but has been redefined by Coats (in Thomson, et al., 1964, and Coats, 1967) as the base of the "Lower Glacial Sequence". In the Olary Province, the Umberatana Group unconformably overlies the Burra Group (Talbot, 1967). In the few places where this relationship is evident, tillite directly

overlies this unconformity (Talbot, 1967). There is no evidence of an unconformity between Units 2 and 3 in the area of this study, but if Coats' definition of the base of the Umberatana Group (Thomson et al., 1964) is accepted, then Unit 2 must be correlated with the Burra Group.

Unit 3 correlates with the Appila Tillite, which is an equivalent of the Sturt Tillite (Thomson et al., 1964). Pitt (1971a) has suggested that the Appila Tillite can be divided into three parts, consisting of two tillite units separated by a quartzite bed. Within this area, these three horizons grade into one another, and thus the tillite has been mapped as one unit.

I consider that the great thickness of this unit in the southeast of the area represents a moraine deposit.

Unit 4 correlates with the Benda Siltstones (Forbes, 1970), though Unit 4 is much thicker. However, in the type section (Forbes, 1970) the complete thickness of the Benda Siltstone is not preserved because it is overlain unconformably by the Wilyerpa Quartzite.

The true stratigraphic position of Unit 5 is uncertain, as it is in faulted contact with the other Adelaidean rocks. I agree with the suggestion of Pitt (1971a) that this unit (his "sheared tillite") is part of the Yudnamutana Subgroup.

CHAPTER 4

STRUCTURE OF THE BASEMENT ROCKS

4.1 INTRODUCTION

Three periods of deformation (D_1, D_2, and D_3) can be recognised in the basement rocks, though not all deformations are evident throughout the area. First period folding is obvious in only one outcrop, where tight folds are overprinted by second and third period folds. Second period folds are also tight and have a well developed foliation parallel to their axial planes in most rock types. Third period folds are not as tight and, in schists, have a crenulation foliation parallel to their axial plane. The obvious easterly plunging synform in the area is a third period fold.

Geometric structural analysis has been carried out using the procedures outlined by Turner and Weiss (1963), and interpretation has been aided by comparing the outcrop patterns with interference patterns of superimposed fold systems (Ramsay, 1962). Orientation data of structural elements were collected during mapping; in general, measurements of lithological layering and lineations were made in calcareous rock types and gneiss, whereas schistosity was generally measured in the schists. Measurements were not taken uniformly throughout the area, areas of greater complexity being measured in more detail.

To aid in the interpretation of the macroscopic geometry of the area, sixteen subareas were delineated on the basis of cylindrical folding determined from stereographic projections of poles to bedding (Fig. 4.34). However, some subareas are inhomogeneous, the folds being non-cylindrical even on a small scale. All orientation data have been plotted on lower hemisphere equal-area projections and contoured using the Schmidt method (Turner and Weiss, 1963).

Descriptive terminology of folds follows that of Fleuty (1964). The term 'foliation' is used as a general term in the sense of Turner and Weiss (1963, p. 97) to refer to any planar mesoscopic fabric element of metamorphic (or deformational) origin. In this study, terms used for specific types of foliations are:

cleavage - the ability of rocks to split into thin parallel sheets (cf. Turner and Weiss, 1963, p. 98)

schistosity - a foliation defined by the parallel alignment of mica grains (cf. Turner and Weiss, 1963, p. 100)

crenulation foliation - foliation defined by the axial planes of crenulations (cf. crenulation cleavage of Rickard, 1961).

The characteristics of structural elements observed in the basement rocks are summarised in Table 4.1.

4.2 LITHOLOGICAL LAYERING (S_{OB})

In the area, lithological layering is evident on all scales and in most rock types. The lithological layering here designated S_{OB} is:

(i) gross lithological layering on a macroscopic scale (e.g., as seen on the geological map, Fig. 2.1);

(ii) lithological layering on a mesoscopic scale which is independent of schistosity and which, in general, reflects the orientation of the macroscopic lithological layering.

S_{OB} within the schists is considered to be bedding, whereas in the quartz-feldspathic gneisses, it is possibly metamorphic in origin. In all rock types, S_{OB} is the primary lithological layering observable,

and within subareas it has the same geometry whether it is sedimentary or metamorphic in origin.

4.2.1 Layering (S_{OB}) within the Schists

As already discussed (Chapter 2.2) the major lithological layering within the schists is considered to represent bedding. This is because:

(i) the layering throughout the area is persistent and the composition of the layers (as indicated by the mineral assemblages that they contain) approximates that of sedimentary rocks (cf. Turner and Weiss, 1963, p. 100);

(ii) sedimentary structures are preserved within this layering at one place in the area;

(iii) there is no evidence of structures considered to be characteristic of transposition (e.g., lenticular layering, 'rootless' folds, etc., Bishop, 1972).

Bedding within the schists is observable as thin laminae of muscovite schist in fine-grained biotite schist, and as continuous quartz-rich layers thicker than 5 cm in fine- medium- or coarse-grained schist. In both of these cases, micas are aligned oblique to the layering (e.g., A470-001).

Bedding is not everywhere evident within the schists and possible reasons for this are:

(i) the sedimentary rocks from which the schists originated were initially uniform;

(ii) evidence of bedding has been obliterated by metamorphism and deformation (in general, bedding laminations are only present in fine-grained schists and not in coarse-grained schists).

Within some of the coarse-grained schists (e.g., Layered Schist, Chloritoid Schist) a layering parallel to the schistosity is defined by quartz-rich and mica-rich layers, the layers commonly being lenticular. This layering is not bedding and has been produced during deformation.

Within the Calcareous Rocks, layering is made evident by variations in mineral content. This layering is parallel to the boundary between the calcareous rock unit and the surrounding schists, and so is assumed to be parallel to bedding.

4.2.2 Lithological Layering in Gneisses

Lithological layering in the Layered Gneiss is visible on both macroscopic and mesoscopic scales. Variations in biotite and feldspar content define the lithological layering on the mesoscopic scale. This layering ranges in thickness from a few centimetres up to a few metres, is continuous across outcrops and is parallel to the macroscopic lithological layering. No sedimentary structures have been observed in these rocks and so the origin of this layering remains in doubt (see Chapter 2.5).

The Granite Gneiss has a well developed schistosity, but no mesoscopic lithological layering. No measurements of S_{OB} have therefore been made on the Granitic Gneiss.

4.3 FIRST GENERATION STRUCTURES

Definite first generation folds occur near Hudson's Hut (070045) where they are overprinted by second and third generation folds to give modified type 2 interference patterns (Fig. 4.1, and cf. Ramsay, 1967, p. 525 and fig. 10.8). These folds occur in quartzites within the 'Bedded' Schist and are tight folds with biotite aligned parallel to the axial planes (Fig. 4.2).

At this locality, the first generation folds are easily identified because they are overprinted by second and third generation folds. However, without this overprinting criteria, they would be difficult to distinguish from second generation folds.

4.4 SECOND GENERATION STRUCTURES

Second generation structures are more widely developed than first generation structures and evidence of the second period of deformation can be found in most rock types. In general, the second generation folds are tight with a well developed axial plane foliation.

4.4.1 Schists

The prominent schistosity within the schists is a second generation structure and is parallel to the axial plane of isoclinal folds in bedding within the schists.

Mesoscopic second generation folds are most abundant in the 'Bedded' Schist but are also present in those schists which have laminations parallel to bedding. These folds are tight to isoclinal and show an increase in orthogonal thickness in the hinge area (Fig. 4.3). Thickening is greater in the hinges of schist layers than in quartzite interbeds. Wave lengths of these folds range from a few centimetres (Fig. 4.4) up to macroscopic scale.

Interference patterns produced by the overprinting of second generation folds on first generation folds are restricted to the few outcrops where first generation folds occur (Chapter 4.3). These interference patterns are type 2 of Ramsay (1967) and show the isoclinal nature of both the first and second generation folds (Fig. 4.2).

In the Layered Schist (e.g., A470-066), the schistosity is defined by zones of mica, 1 mm to 5 mm thick which anastomose, enclosing

lenticular quartz-rich domains which range from 2 mm to 10 mm in thickness and 10 mm to 30 mm in length (Fig. 4.5).

The schistosity wraps around some porphyroblasts of garnet and muscovite (Fig. 4.6). However, some fine-grained aggregates of muscovite and quartz (which are thought to represent original porphyroblasts) are ellipsoidal to subellipsoidal with long axes parallel to the schistosity (Fig. 4.7).

In some schists (e.g., A470-009) the schistosity wraps around lenticular aggregates of chlorite and quartz, the chlorite being aligned oblique to the prominent schistosity (Fig. 4.8). The alignment of this chlorite could represent an earlier schistosity, as similar features are observed in some schists which contain third generation crenulations (e.g., A470-067, Fig. 4.9).

In Fine-grained Mica Schist, Medium-grained Mica Schist and Epidote Schist, schistosity is defined by the alignment of micas. In general, no differentiation of mica and quartz occurs in these schists and, although some quartz grains are elongate parallel to the schistosity, elongate aggregates of quartz are absent.

Lineations within the schists are rare. Layering/schistosity intersections are present where layering is evident and in some places faint lineations due to elongate mineral grains are present.

4.4.2 Calcareous Rocks

In the calcareous rocks, mesoscopic folds are lacking and a foliation is present only in the layered variety of the Epidote Quartzite and Quartz-Plagioclase-Hornblende Rock. Lineations due to elongate minerals are present in both these rock types and in the non-layered Epidote Quartzite.

The foliation is defined by the parallel alignment of mineral grains and aggregates of grains of epidote and hornblende (Fig. 4.10), and in those that contain biotite, it too shows parallel alignment. On the microscopic scale, the foliation is non-penetrative, some grains being aligned parallel to layering and others being equidimensional.

Lineations are apparent on the bedding surfaces of the Epidote Quartzite and Quartz-Plagioclase-Hornblende Rock, and in hand specimen, the lineations are defined by elongate grains and aggregates of epidote or hornblende. In many cases, two lineations are present, both defined by elongation of the same mineral species. In such cases, one lineation may be more prominent than the other or the lineations may be equally developed.

The foliation in these calcareous rocks is thought to be a second generation structure as it is folded by macroscopic third generation folds and because first generation foliations are almost entirely obliterated in other rock types. However, the problem of determining the relative ages of lineations, where more than one is present, has not been resolved. Some of the lineations are presumed to be second generation fabric elements.

4.4.3 Granitic Gneiss

No second generation folds occur in the Granitic Gneiss; however the strong foliation and lineation in this rock is thought to be a second generation structure. This well developed fabric is defined by the parallel alignment of biotite grains and by the alignment of elongate aggregates of biotite, magnetite, quartz and plagioclase. The foliation is not uniformly developed throughout the gneiss; it is most strongly developed where biotite is abundant and is absent

where biotite is scarce. Despite the variations in the degree of development of the foliation, the lineation is strongly developed throughout the gneiss.

That the strong fabric in this rock is a second generation structure is evidenced by the parallelism of the foliation in the Granitic Gneiss with the second generation schistosity in nearby schists. This foliation is unlikely to be an original feature of the rock type. As first generation foliations in the schists have been almost obliterated, it seems unlikely that a first generation or earlier structure would have survived the second deformation without any modification. This foliation in the Granitic Gneiss is folded around third generation folds and therefore cannot have been formed during the third deformation.

The relative age of the lineation is also difficult to determine. The lineation is thought to be a second generation structure because it is defined by the elongation of the same minerals which define the foliation.

4.4.4 Layered Gneiss

In general, mesoscopic second generation folds are rare in the Layered Gneiss but everywhere the mica-rich layers contain a well developed schistosity defined by the alignment of biotite grains, and this schistosity is thought to be a second generation structure. Where second generation folds do occur in the Layered Gneiss (e.g., south of Cathedral Rock and south of the Woman-in-White Mine) these folds are tight to isoclinal and show marked thickening in the hinge in both quartz-rich and mica-rich layers (Fig. 4.11). The well developed schistosity in the Layered Gneiss is parallel to the axial plane of these folds.

In other locations, no folds were observed in the Layered Gneiss, but a schistosity generally parallel to the layering in the gneiss is defined by the alignment of biotite in the mica-rich layers. This schistosity is thought to be a second generation structure.

4.4.5 Older Migmatite

Two periods of deformation are apparent in the Older Migmatite, so correlation of these deformations with those in the schists is problematic. It is assumed that the earliest recognisable deformation in the Older Migmatite corresponds to the second deformation in the schists, because the foliation in this migmatite is approximately parallel to the schistosity in adjacent schists and to the foliation in the Granitic Gneiss.

The earliest recognisable folds in the Older Migmatite occur in the neosome, are tight and have an axial plane foliation defined by the alignment of biotite grains in the melanocratic layers (Fig. 4.12). In the palaeosome, no early folds were observed; however, the weak foliation present in the biotite-rich layers is thought to be a second generation structure.

4.4.6 Quartz Veins and Pegmatites

Some quartz veins and pegmatite pods have been deformed during the second period of deformation. The quartz veins have been folded into tight ptygmatically styled folds (Fig. 4.13) with the axial plane foliation in the enclosing schists parallel to the axial plane of the overall fold in these veins (Fig. 4.14).

Some pegmatite pods have been folded into tight folds (Fig. 4.15) and, in the limb areas of these folds, the pegmatite has been boudinaged (Fig. 4.16). Other pegmatites show pinch-and-swell structure (fig. 4.17) indicating extension parallel to the second generation foliation in the enclosing schist.

4.5 THIRD GENERATION STRUCTURES

The third generation of deformation has affected most rock types in the basement. During this period almost the complete layered sequence has been folded into an easterly-plunging synform. The macroscopic geometry of this synform is most obvious in the quartzo-feldspathic rocks but mesoscopic structures are well displayed in the schists.

4.5.1 Schists

Third generation folds in the schists are characterised by the presence of crenulations which fold the prominent second generation schistosity. These folds range from open to close. In schists, the close folds have a similar style, whereas folds in interbedded quartzites and open folds in schists have a concentric style (Fig. 4.3, 4.18). The folds are generally symmetric with upright or steeply dipping axial planes, although minor folds on the limbs of major folds are asymmetric.

In several outcrops, refolded folds are present and attest to the age relationships between the various deformational structures. Near Hudson's Hut, in the 'Bedded' Schist, third generation folds overprint first and second generation folds (Fig. 4.1, 4.3). These third generation folds produce a type 3 interference pattern (Ramsay, 1967, p. 530 and fig. 10.15) with respect to the second generation folds. A similar interference pattern is seen in Albite Schist south of Cathedral Rock, where a third generation warp folds an isoclinal second generation fold (Fig. 4.23). In the Medium-grained Mica Schist at 054045 a modified type 2 interference pattern exists between second and third generation folds (Fig. 4.19).

The third generation crenulations show all gradations, from small corrugations on the second generation schistosity (Fig. 4.21) to a new foliation cutting across the second generation schistosity (Fig. 4.20).

Where the second generation schistosity is predominantly planar, small crenulations cross the schistosity surface in two directions (Fig. 4.21). In thin section, these crenulations can be seen to range in style from open warps of the second generation schistosity (Fig. 4.24) to tight asymmetric folds of the schistosity (Fig. 4.9). Widely spaced narrow zones of micas are oriented parallel to the axial planes of both open and tight third generation crenulations (Fig. 4.25, 4.26).

In the hinge areas of third generation folds, the second generation schistosity is folded into more prominent crenulations which are close and have a chevron style (Fig. 4.20). Individual crenulations have curved hinge lines and extend for only short distances parallel to the hinge (Fig. 4.27). In thin section, these folds are seen to range from sharp crested kinks (Fig. 4.28) to smoothly rounded micro-folds in the schistosity (Fig. 4.29). Throughout the range of styles of third generation crenulations few mica grains show signs of internal deformation.

In some schist layers, micas are oriented parallel to the axial plane of the third generation folds (Fig. 4.18, 4.20) giving rise to a new schistosity, but nowhere in the area is this schistosity well developed.

4.5.2 Calcareous Rocks

No mesoscopic third generation folds and no third generation foliation are present in the Calcareous Rocks, but one of the two

mineral lineations present on some bedding planes (Chapter 4.4.2) is thought to be parallel to third generation fold axes (see Chapter 4.6.3).

4.5.3 Granitic Gneiss

Although the Granitic Gneiss has been folded into a synform during the third period of deformation, no mesoscopic third generation structures have been observed in this rock type.

4.5.4 Layered Gneiss

Third generation folds in the Layered Gneiss range from open flexures to tight folds, which fold both the lithological layering and the second generation foliation (Fig. 4.22). In the closures of the tighter folds, crenulations are developed in some mica-rich layers, but in general no new foliation is developed parallel to the axial planes of these folds.

4.5.5 Older Migmatite

The third generation of deformation in the palaeosome of the Older Migmatite is a brittle deformation. The layering in the palaeosome is cut by numerous, parallel fractures, many of which show small displacement (Fig. 4.30). Spacing between these fractures is about 15 cm and displacement is generally about 5 cm.

The neosome has behaved plastically during both the second and third periods of deformation and so exhibits refolded folds. The third period of deformation has produced folds in both the lithological layering and the second generation schistosity in the neosome (Fig. 4.12).

4.5.6 Pegmatites

At several localities, pegmatites have been folded by the third generation of deformation. In general, these folds are macroscopic with a wave length of approximately 5 m. In the hinge area of

these folds, the pegmatites are cut by numerous, closely spaced fractures parallel to the axial planes, with small displacement along some of the fractures (Fig. 4.31).

Some thin pegmatite veins have been folded by the third generation of folding, these folds having crenulation foliation in the enclosing schists parallel to their axial plane (Fig. 4.32).

4.6 BASEMENT FAULTS

Several faults which only cut basement rock types occur in the mapped area. These faults all strike approximately easterly and have apparently small displacements across them. In the east of the area mapped, gneissic rocks which form the core of the easterly plunging synform are cut by two faults which are approximately parallel to the axial plane of the synform.

The more northerly of these two faults has a single, well defined fault zone 0.5 m wide in which augen schist is developed. This fault is vertical and has a strike slip component of 400 m, but the dip slip movement is indeterminable. The augen schist in the fault zone is composed of lenses (up to 5 cm x 1 cm) of quartz and feldspar surrounded by thin (1 mm in thickness) mica-rich layers (e.g., A470-068). Large quartz grains (2 mm - 5 mm across) show undulose extinction, deformation bands, the development of subgrains (Fig. 4.33) and new grain growth. Small quartz grains are generally strain-free and are thought to have developed by recrystallization of initially larger strained quartz grains. The mica-rich zones are composed of muscovite and minor biotite. The mica grains show a scatter of orientations about the direction of the mica-rich layers.

The southerly fault in fact consists of a zone 300 m wide of parallel faults. Faults in this zone are upright; displacement across the zone is indeterminable.

Faults within the basement schists are parallel to the second generation schistosity and can only be identified where distinctive units (e.g., Calcareous Rocks) are truncated or displaced. These faults are vertical with apparently small displacements.

4.7 MACROSCOPIC GEOMETRY

Macroscopic geometric analysis involves interpretation of three-dimensional structure from the distribution of rock types and from the orientation of the various fabric elements. Limitations on the interpretation in this area are: lack of outcrop in some areas, uncertainty in the stratigraphy, and difficulties in determining the generation of some folds.

4.7.1 Macroscopic First Generation Folds

The presence of a macroscopic first generation fold closure is postulated from the mapped distribution of the rock sequence in the Willyama Complex at 066079 (see Fig. 2.1 and Chapter 2.10) and is supported by the presence of mesoscopic first generation folds which crop out in the creek near Hudson's Hut. However, the macroscopic fold closure does not crop out, and no orientation data are available because of the paucity of first generation structures.

4.7.2 Macroscopic Second Generation Folds

Macroscopic second generation fold closures are exposed in Subareas IV, V, VI and VIII (Fig. 4.34). These subareas contain schists; second generation fold closures are outlined by lithological layering in the schists and Calcareous Rocks.

Orientation data from Subareas IV and VIII reflect the style of the macroscopic second generation folds. Stereographic projections of poles to bedding (π S_{OB}, Fig. 4.34) for these two subareas show point maxima with partial girdles, indicating tight to isoclinal folding which

is in accord with observations of mesoscopic second generation folds (Chapter 4.4.1).

Poles to schistosity (πS_{2B} Fig. 4.34) also plot as point maxima, indicating planar second generation schistosity in Subareas IV and VIII. The average planes of schistosity contain the respective poles to the girdle distributions (β, Fig. 4.31). In Subarea VIII, β also coincides with the point maximum distribution of lineations (L, Fig. 4.34). However, in Subarea IV, Lineations (L) and mesoscopic second generation fold axes ($B^{S_{2B}}_{S_{1B}}$) show a partial girdle distribution coincident with the average plane of schistosity, and β corresponds to the subsidiary concentration within the distribution of lineations.

Because the folds in Subarea IV are isoclinal, it was not possible to take many readings of dips of lithological layering in the hinge areas of folds. Those readings that were taken suggest that folding is cylindrical (πS_{OB}, Fig. 4.34) but the spread of lineations suggests variations in the plunge of folds but no folding of the axial plane (L, Fig. 4.34).

In Subarea VI, outcrop is poor around the second generation fold closure. The orientation data reflect the style and orientation of the macroscopic third generation fold present in this subarea.

4.7.3 Macroscopic Third Generation Folds

Macroscopic third generation folds are evident in Subareas II, III, VI, VII, X, XI, XIII, XIV and XV. Of these, Subareas II and III contain Granitic Gneiss, whereas the others contain schists.

In the Granitic Gneiss, the foliation has been folded into a close fold and this is reflected in the orientation diagrams in which poles of foliation (πS_{2B}, Subareas II and III, Fig. 4.34) have an even distribution around a great circle. As the distribution of

lineations for these two subareas is similar (Fig. 4.34) the data have been combined to give sufficient points for contouring. The distribution is along a great circle representing a plane which dips 45° towards 080, with maxima representing plunges of 45° towards 090 and 45° towards 050.

Stereographic projections for poles to bedding from Subareas VI and VIII show partial girdles with two concentrations approximately 70° apart, indicating open to close folding with an interlimb angle of about 70°. In Subarea XI, the distribution of poles to bedding has two concentrations about 40° apart, indicating tighter folding. Data are not sufficient to indicate the style of macroscopic folding in Subareas X, XIV and XV.

Poles to second generation schistosity for Subareas VI, VII, X and XI are distributed along great circles which, for Subareas X and XI, coincide with the respective distributions of poles to bedding, whereas those for Subareas VI and VII are at a low angle to the respective great circle of distributions of poles to bedding. Fold plunges, determined from great circle distributions of poles to bedding for these subareas, correspond fairly well to the respective measured mesoscopic third generation fold plunges ($B^{S_{3B}}_{S_{0,2B}}$, Fig. 4.34) and all lie close to the average plane of crenulation foliation in the whole area (Total πS_{3B} , Fig. 4.34).

The plunge reversals between Subareas X, XI and XIV, and the range of plunges of crenulations in Subarea X, probably result from inhomogeneous strain during the third generation folding (rather than the folding of a previously folded surface) and reflect the plunge variations observed on the mesoscopic scale (e.g., Fig. 4.27).

Poles to crenulation foliation throughout the area (Total πS_{3B} , Fig. 4.34) show a double maxima representing dips of 88° towards 190 and 80° towards 175. This is interpreted as a conjugate pair of crenulation foliations and this is consistent with observations on the mesoscopic scale (see Chapter 4.5).

The stereographic projection of total plunges of crenulations (other than those from Subareas VIII and IX) and mesoscopic third generation folds (Total $B^{S_{3B}}_{S_{0,2B}}$, Fig. 4.34) show a diffuse girdle distribution with a maximum concentration representing a plunge of 30° towards 097, and a smaller concentration representing a plunge of 50° towards 100. The girdle distribution spreads about the average orientations of the dip of the crenulation foliation.

In Subareas I, IX and XII, no macroscopic fold closures were observed, although mesoscopic second and third generation folds are present. Poles to bedding from Subareas I and XII plot as diffuse point maxima, and poles to second generation schistosity form well defined point maxima (Fig. 4.34), indicating that bedding and second generation schistosity in these subareas are essentially planar on the macroscopic scale.

In Subarea IX, the distribution of poles to second generation schistosity (Fig. 4.34) defines a partial girdle with a single concentration, and poles to bedding show a similar distribution (Fig. 4.34). The concentrations reflect the generally planar attitude of schistosity and bedding, and the partial girdle reflects the presence of mesoscopic folds around which measurements were taken.

Subareas XIII and XVI are inhomogeneous, the folds being non-cylindrical even on a small scale.

In Subarea XIII, the calcareous horizon is folded into a superimposed fold pattern which is similar to a mesoscopic refolded fold in Subarea X (Fig. 4.19). The distribution of poles to bedding in Subarea XIII reflects the westerly plunge of the macroscopic synform outlined by the calcareous layer (see Fig. 4.34); however, one fold in this layer plunges to the east.

Lineations in the calcareous bed in Subarea XIII are all morphologically similar. However, it is obvious that there are two different orientation groups (L, Fig. 4.34): one with a northerwesterly plunge, reflecting the major fold, and one with a southeasterly plunge, reflecting the minor fold. The minor, southeasterly plunging fold is interpreted as a second generation fold which has been refolded during the third generation deformation.

4.8 STRUCTURAL SYNTHESIS

An interpretation of the structural geometry of the basement rocks in this area is presented in Fig. 4.35.

The first generation structure is interpreted as an isoclinal syncline with 'Bedded' Schist in the core, and this fold is thought to be responsible for the repetition of the sequence of rock types in the basement schists (see Chapter 2.10).

The second generation structure is interpreted as an antiform-synform pair with the antiform to the east of the synform. The only outcrop of the two fold closures is west of the Mulga Mine (070032). At Hudson's Hut (070050), the closure of the antiform is exposed, and it is postulated that the closure of the first generation syncline accounts for the absence of the second generation synform here (Fig. 4.35). Other fold closures, which should occur along the extensions of these second generation axial traces to the northeast, have not been observed.

Explanations for this may be that:

(i) the folds die out along the axial plane;

(ii) the folds are truncated by a fault;

(iii) the folds were not detected because of modification by third generation folding.

The macroscopic third generation structure is dominated by an easterly-plunging synform with gneissic rocks in the core. This fold is readily identified as a third generation fold by the fact that the second generation cleavage in the Granitic Gneiss and adjacent schists is folded around it. In the Granitic Gneiss, Older Migmatite and Layered Gneiss, this fold is a simple close synform, though the plunge does vary from Subarea II to Subarea III.

In the schists the overall synform is present but is obscured by first and second generation folds, and by the presence of many smaller wave-length third generation synforms and antiforms (see Figs. 4.34, 4.35).

In the eastern part of Subarea VI adjacent to the Layered Gneiss, schistosity in schists follows around the major synform, but further west the schistosity has been folded into tighter folds with shorter wave lengths; these folds extend for only short distances parallel to their axes (e.g., in Subareas X, XI and XIV).

CHAPTER 5

STRUCTURE OF THE COVER ROCKS

5.1 INTRODUCTION

The cover rocks have been folded into a syncline plunging 35^{o} towards 100, of which the northern limb has been faulted out by the MacDonald Fault. Adjacent to this fault two periods of deformation are evident but the later deformation does not appear to have affected the macroscopic structure of the cover rocks.

The major syncline in the cover rocks corresponds in style and orientation to the third generation synform in the basement rocks, and so these two structures are thought to have developed during the same period of deformation (D3). Hence, the first generation structures recognisable in the cover correspond to third generation structures in the basement (see Chapter 8.2).

The terminology used in describing the structure of the cover rocks is the same as that used in Chapter 4, and the shorthand notation is summarized in Table 5.1.

5.2 BEDDING (S_{OC})

Bedding is the primary layering within the cover rocks. The abundance of sedimentary structures, distinctive beds (e.g., tillites and conglomerates) and the presence of only a weak to moderately developed cleavage, all indicate that this layering is, in fact, bedding and that it still retains its stratigraphic significance.

However, bedding is not easily detected in all outcrops and, particularly in the slates of Unit 4, bedding is difficult to find. In addition, the cleavage in Unit 4 is prominent both on mesoscopic and macroscopic scale, so that interpretation of the structure in this unit is difficult. Similarly in Unit 5 slaty cleavage is prominent in the matrix, and no bedding was observed, making macroscopic interpretation difficult.

5.3 FIRST GENERATION STRUCTURES

Throughout most of the cover rocks, only first generation structures are visible. Mesoscopic $B_{S_{0C}}^{S_{1C}}$ folds are rare but cleavage is developed in the finer-grained rock types and in the matrix of Units 3 and 5.

In Unit 4 mesoscopic $B_{S_{0C}}^{S_{1C}}$ folds occur mainly as sinistral minor folds but some minor synclines and anticlines are present. These mesoscopic folds are close, show some thickening in the hinge and have a slaty cleavage (Fig. 5.1) which shows slight fanning about the axial plane which is almost upright. As mesoscopic folds occur only in this unit, it has not been possible to determine variations in style of folds with variations in rock type.

Macroscopic $B_{S_{0C}}^{S_{1C}}$ folds have been recognised in Units 3 and 4 and these are slightly more open than the mesoscopic folds. Interlimb angles range from 40° to 110° and thus the folds range from close to open (Fleuty, 1964) and fold shapes as seen in profile (Fig. 3.2) range from class 1B to class 3 (Ramsay, 1967).

Slaty cleavage is developed in the fine-grained rocks and is seen as a regular, though not well developed, parting in the rocks.

Refraction of cleavage was not observed. The lack of refraction of cleavage may be due to the lack of mesoscopic folds in which to observe refraction and the lack of cleavage in the coarser-grained rock types.

The slaty cleavage is defined by the subparallel alignment of biotite grains and, in some rocks, this is paralleled by thin veins of calcite (Fig. 5.1). Some grains of quartz and feldspar are aligned parallel to the cleavage whereas others are at a high angle to cleavage.

In the matrix of the tillite of Unit 3, biotite grains are aligned to define a weak foliation but the tillite does not break along

this direction. Schist pebbles in the tillite have been deformed and are now elongate parallel to the foliation in the matrix; quartzo-feldspathic pebbles have been only slightly deformed but also show a tendency towards alignment in the foliation (see Chapter 6.3).

The strongly developed cleavage in the tillite of Unit 5 is defined by the alignment of biotite and the tillite splits parallel to this cleavage. In this tillite, both schist and quartzo-feldspathic pebbles have been strongly deformed and are elongate in the cleavage plane (see Chapter 6.4).

Within this area, the Adelaidean quartzites show no evidence of foliation, and sedimentary structures in these rocks are preserved even in the hinges of tight folds (Fig. 5.2).

5.4 SECOND GENERATION STRUCTURES

Mesoscopic second generation folds occur only adjacent to the MacDonald Fault. In general, second generation structures are apparent only as faint crenulations in the slaty cleavage of Unit 4, but at a few localities (e.g., 029056) mesoscopic folds of bedding and cleavage have developed. These folds have a chevron style (Fig. 5.4) and have small crenulations (wave length and amplitude approximately 0.5 mm) parallel to their fold axes. Where the siltstones of Unit 4 are calcareous, lenses of calcite (from 5 mm to 30 mm long and up to 5 mm across) with randomly oriented muscovite flakes, are parallel to the axial plane of the crenulations (Fig. 5.3).

The second generation of deformation has had no effect on the macroscopic geometry of the cover.

5.5 MACROSCOPIC STRUCTURE

On a macroscopic scale, the structure of the cover rocks is the southerly limb of a first generation syncline which plunges 35°

towards 100 (πS_{0C}, Fig. 4.34) and with the axial plane dipping 80° towards 194 (πS_{1C}, Fig. 4.34). As only one limb is exposed it is not possible to determine fully the style of the major syncline but, from the dip of the limb and the dip of the axial plane, the fold probably has an interlimb angle of between 60° and 70°, making it a close fold. This corresponds to the style of the macroscopic minor folds and the mesoscopic folds within the area.

From the geological map of the Olary Province (Campana and King, 1958, plate 1), it appears that the syncline (of which the structure in this area is a part of one limb) is tighter than the adjacent anticline which occurs near MacDonald Hill.

Within the area mapped, there is some disharmonic folding and quite large variations in the tightness of first generation folds (see Fig. 2.1 and 3.2). These variations are probably the result of inhomogeneous deformation.

The contoured diagram of poles of bedding (πS_{0C}, Fig. 4.34) shows a great circle distribution with two approximately equal concentrations and one subsidiary concentration, the equal concentrations indicating a close fold with interlimb angle of 60°. In addition, the pole to the great circle distribution (β for πS_{0C}, Fig. 4.34) does not coincide with the maximum concentration of bedding/cleavage intersections (L_{1C}, Fig. 4.34 - though β does lie well within the scatter of L_{1C}), neither does it lie on the great circle defined by the maximum concentration of poles to cleavage (πS_{1C}, Fig. 4.34). A possible explanation for these discrepancies is that the cleavage is not parallel to the axial plane of the fold (cf. Bell, 1969, who has described folds with slaty cleavage oblique to the axial plane in the Tapley Hill Formation - a part of the Umberatana Group - near Oodla Wirra, 140 km southwest

of this area). However, no evidence of cleavage oblique to the axial plane of folds was observed in the field; mesoscopic folds in which these relationships could be observed are rare in this area.

Poles to cleavage (πS_{1C}, Fig. 4.34) define a fairly sharp point maximum, indicating that the cleavage is planar with little fanning except in areas where there are mesoscopic second generation folds in the cleavage.

As mentioned previously (Chapter 5.4) the second generation structures have no effect on the macroscopic structure, and the only observed occurrences are close to the MacDonald Fault, suggesting that the formation of the second generation structures could be related to the faulting; however, the crenulation cleavage is, in places, shallowly dipping (e.g., at 068030) whereas the MacDonald Fault is thought to be nearly vertical (see Chapter 5.8). In the Whey Whey Creek area, crenulations are developed in the cover rocks close to a fault with the basement; Talbot (1962) has suggested that these crenulations might be related to the faulting.

5.6 STRUCTURE AROUND THE BASEMENT INLIER

An inlier of basement rocks crops out in a valley 4 km south of the Old Boolcoomata Homestead (Fig. 5.8). The inlier has an elliptical outcrop shape (Fig. 5.6) 500 m long by 200 m wide and is composed predominantly of migmatites and Layered Gneiss, with minor amphibolite dykes and pegmatites.

In places around the inlier, conglomerate is exposed resting unconformably on the basement migmatites (Fig. 5.9) and in faulted contact with the slates of Unit 4 which surround the inlier.

Southeast of the inlier, a continuous, north-facing section of Unit 4 is exposed. At the eastern end of the inlier, beds of Unit 4 are folded and diverge around the inlier (Fig. 5.6). At the western end of the inlier, exposure is not good and therefore it is not possible to confirm the continuity of the Adelaidean sequence.

At the eastern end of the inlier, folds in Unit 4 plunge at approximately 30° towards 100 (Fig. 5.6), whereas at the western end, folds plunge at approximately 60° towards 100 (Fig. 5.6). The folds around the inlier have a similar orientation to the major first generation structure in the cover rocks (Chapter 5.6).

The orientations and extent of the faults separating the inlier from the cover rocks are difficult to determine. Even where outcrop is good (e.g., 044025, see Fig. 5.9), the fault can only be identified by the change in facing across it.

A series of subparallel quartz reefs at the northwestern end of the inlier have displacments across them of the order of 1 m. These reefs do not appear to be related to the faulting which was responsible for the emplacement of the inlier, as the displacement across these is too small.

5.6.1 Emplacement of the Inlier

Three possible explanations can be offered for the origin of the inlier:

(i) it is an ice rafted block deposited in the Adelaidean sequence;

(ii) it is a klippe (assuming that the MacDonald Fault is a low angle thrust);

(iii) it is a 'slice' of basement which has been faulted into the Adelaidean sequence.

The first explanation can be discounted because the Adelaidean sequence diverges around the inlier and does not lap onto it or lense into the conglomerate which overlies the inlier. In addition, the reversal of facing between Unit 4 and the conglomerate overlying the inlier at locality 044024 indicates the presence of a fault at that locality.

The second possible explanation is unsatisfactory because the deformation of Unit 4 surrounding the inlier is not consistent with the inlier being a klippe; also, evidence indicates that the MacDonald Fault is almost vertical (Chapter 5.7).

Campana and King (1958) have explained a similar inlier near the Bimbowrie Homestead as being a basement 'slice' that has been faulted into the Adelaidean sequence (ibid, fig. 30a). However, contrary to the claim of Campana and King (1958, p. 41) that the major structure is overturned to the west (i.e., with axial plane dipping to the east), the axial plane dips at 80^{o} towards 195 (πS_{1C}, Fig. 4.34) indicating that the major structure is almost upright. The evidence seen in this investigation suggests that the inlier in the Old Boolcoomata area has been faulted through the Adelaidean sequence, probably at the time of development of the MacDonald Fault.

5.7 THE MACDONALD FAULT

In the mapped area, the basement and cover are separated by the MacDonald Fault which extends northwesterly from Radium Hill to the Bimbowrie Homestead (Fig. 1.1 and Sprigg, 1954). Although the fault has an overall northwesterly trend, locally it diverges from this trend (see Campana and King, 1958, plate II): Pitt (1971a) has suggested that some of these divergences are due to cross-faulting.

In the Old Boolcoomata area, the MacDonald Fault follows the general shape of the major synform in the basement and the major syncline in the cover (Fig. 2.1).

The nature of the fault zone varies according to the rock types that the fault cuts. Where the fault separates basement schist from cover slates, the fault is a single plane (Fig. 5.10) but where the fault separates basement pegmatites from cover tillites, a mylonite zone 5 m wide is developed. The mylonite (A470-069) is a strongly foliated and lineated quartzo-feldspathic rock. In thin section, plagioclase grains (up to 3.0 mm) show bent twinning and micro-faulting (Fig. 5.11) and quartz grains are generally small and segregated into narrow zones parallel to the foliation (Fig. 5.12). Muscovite is also present and this is aligned parallel to the foliation. Where the mylonite crops out (075013), the mylonite foliation is vertical and the lineation in this foliation has a steep plunge. At other localities where the MacDonald Fault is exposed it is also vertically dipping (e.g., at 051060, Fig. 5.10).

Vertical displacement on the MacDonald Fault is possibly of the order of 3 km: the Adelaidean sequence in this area is approximately 3,300 m thick and the structure in this area is a part of one limb of a syncline.

5.7.1 Curvature of the MacDonald Fault

In the Old Boolcoomata area, the MacDonald Fault diverges markedly from its average trend, but, unfortunately, outcrop along the fault is not good. Some of these divergences may be due to cross-faults; if such cross-faults exist they do not extend far into the cover or basement. At 029056 where the MacDonald Fault changes direction sharply, chevron folds are developed in the bedding and slaty

cleavage of Unit 4 (Fig. 5.4), but the layering and schistosity of the adjacent basement schists are not folded. The chevron folds in the cover rocks have crenulations developed parallel to their fold axes which plunge steeply.

Possible explanations for the curvature of the MacDonald Fault are:

(i) the fault is a low angle thrust;

(ii) the fault has been off-set by cross-faults;

(iii) the fault was originally curved;

(iv) the fault has been folded along with the basement and cover.

If the MacDonald Fault Zone was a low angle thrust, the shape of the fault trace could be explained by slight variations in the dip of the fault plane and by topography, and the basement inlier (see Chapter 5.7) could be explained as a klippe. However, detailed field evidence does not support this hypothesis. Firstly, where it is exposed, the MacDonald Fault has a vertical dip and secondly, the basement inlier cannot be explained as a klippe because the sediments of Unit 4 have been folded around the inlier (see Chapter 5.7).

There is little evidence for the presence of cross-faults, and they cannot account for all the changes in direction of the MacDonald Fault.

The presence of mesoscopic folds in the cover rocks closely following the shape of the fault (Fig. 4.34) suggests that the fault has in fact been folded (Berry, 1973 considered that the Springs Fault which is tectonically equivalent to the MacDonald Fault, see Fig. 1.1, has been folded). However, these folds deform both bedding

and slaty cleavage in the cover rocks. In addition, the MacDonald Fault cuts both the north and south limbs of macroscopic folds in the cover (see Fig. 2.1) and so the MacDonald Fault must post-date the development of folds and cleavage in the cover rocks. However, the general shape and position of the fault suggest that the curvature of the fault is due to folding during the main period of deformation of the cover (D_3); it is possible that faulting occurred at a late stage during the third period of deformation (D_3) and continued deformation may have caused folding of the fault.

5.7.2 Relationship of the MacDonald Fault to Folding in the Cover

If, as suggested above (5.7.1), the MacDonald Fault is related to folding in the cover, then it should have some relationship to the symmetry of deformation in the cover (Turner and Weiss, 1963, pp. 385-386).

From strain analysis, it was determined that the cleavage in the cover rocks is approximately parallel to the principal plane of the strain ellipsoid for the major deformation of the cover (Chapter 6; c.f. Cloos, 1947; Ramsay, 1967, p. 180; Siddans, 1972). In the profile plane of the major cover folds, the cleavage trace pitches 90° and the fault trace (assuming the fault to be vertical with an average strike over its whole length of 305) pitches 70°N. The cleavage trace represents the direction of maximum finite elongation in the profile plane, and the maximum finite shortening is perpendicular to this direction. The sense of movement on the MacDonald Fault is such that it leads to shortening parallel to the direction of maximum finite shortening indicated by the cleavage (Fig. 5.7; c.f. Chapter 6.3.1); this is consistent with the hypothesis that folding and faulting were parts of the same deformational episode.

If the faulting has actually taken place in the southerly-dipping limb of this syncline, then the above observations and interpretations are in agreement with the predictions of Dieterich (1969, p. 163 and fig. 7) regarding faults developed during folding.

Curvature of the MacDonald Fault has probably resulted from folding in response to continuing deformation during D_3.

CHAPTER 6

STRAIN IN THE COVER ROCKS

6.1 INTRODUCTION

Conglomerate and tillites in the cover rocks provide ellipsoidal markers from which the strain in these rocks can be estimated. Dunnet (1969), Dunnet and Siddans (1971) and Elliott (1970) have derived methods using ellipsoidal particles for the analysis of strain in rocks. The methods are based on the theory that shape and orientation of an ellipsoidal particle after deformation are dependent upon its initial shape and orientation, the axial ratio and orientation of the strain ellipsoid, and the viscosity contrast between the particle and the matrix (Dunnet, 1969, p. 117, fig. 1; and Elliott, 1970, pp. 2234-2235 and fig. 6). All these methods require the measurement of the axial ratios and orientations of long axes of elliptical markers from one or more surfaces in the rock. If three surfaces parallel to the principal planes of the strain ellipsoid are chosen, calculation of the three dimensional strain ratios is simplified (Ramsay, 1967, pp. 142-148).

The methods devised by Dunnet (1969) and Dunnet and Siddans (1971) make use of R_f/ϕ diagrams which are plots of the logarithm of axial ratios (R_f) against orientation of long axes (ϕ). Elliott (1970) utilizes polar graphs of these quantities with logarithmic radius scale and plotting of 2ϕ.

The advantage of Elliott's method is that, in general, the initial (pre-strain) fabric of the elliptical particles can be recognised from a contoured distribution of points on the polar graph, although some ambiguities arise (Elliott, 1970, pp. 2229-2230).

Estimations of strain were attempted in Adelaidean rocks from Units 1a, 1b, 3 and 5b, and from a specimen of porphyroblastic schist from the Willyama Complex. Data were collected in two ways: at certain locations measurements were taken in the field from one or two

outcrop surfaces; at other localities, specimens about 50 cm x 50 cm x 50 cm were collected and measurements made on mutually perpendicular, serially cut faces. On each face, 30 to 60 measurements were made of those quartzo-feldspathic pebbles with long axes between 1 cm and 10 cm. Where sufficient schist pebbles were present on a face, measurements of these were also taken and the results recorded separately.

In general, data were plotted on polar graphs and contoured using the Mellis method (Elliott, 1970); however, some results are presented on R_f/ϕ diagrams (Dunnet, 1969).

6.2 UNIT 1

In Subunits 1a and 1b, pebbles and boulders do not show evidence of deformation and no foliation is developed in the matrix. Axial ratios of pebbles in Unit 1 are generally less than two and long axes are randomly oriented (Fig. 6.1), suggesting that strain is extremely low.

Data for these two subunits have been measured in the field and results have been plotted in R_f/ϕ diagrams (Dunnett, 1969) as these readily show the low axial ratios and the wide spread of axial orientations.

The lack of cleavage in the matrix and the apparent lack of strain suggest that Unit 1, together with the Boolcoomata Adamellite on which it rests unconformably, behaved as an almost rigid body during the third deformation (D_3).

6.3 UNIT 3

Evidence of deformation is more abundant in Unit 3 than in Unit 1. In the matrix a weakly developed cleavage is defined mainly by the alignment of micas (predominantly biotite). The degree of development of cleavage varies with composition of the matrix: where

the matrix is rich in quartz and feldspar, cleavage is barely discernable (Fig. 6.2) but where biotite or schist pebbles are abundant, the cleavage is more obvious (Fig. 6.3). The cleavage is curved around pebbles and does not cut across matrix/pebble boundaries. Pebbles rarely touch each other and there is no evidence of pitting.

6.3.1 Quartzo-feldspathic Pebbles

Evidence of plastic deformation of the quartzo-feldspathic pebbles in Unit 3 is rarely observed in outcrop but evidence of a change in shape of the pebbles is seen in the plots (Fig. 6.15). In rare cases, this cohesive change in shape is obvious from the shape of the pebbles (Fig. 6.4) but brittle deformation of the pebbles is more common.

Some quartzo-feldspathic pebbles are cut by parallel fractures with small displacements subparallel to the cleavage in the matrix (Fig. 6.5). In some pebbles with layering subparallel to the cleavage in the matrix, deformation has taken place by slip on the layering (Figs. 6.6 and 6.7). Other pebbles have been deformed by slip on both layering and cross-cutting fractures (Fig. 6.8). In all pebbles which show brittle deformation, fractures are at a low angle to cleavage, and movement on all fractures within any one pebble is in the same direction to give shortening perpendicular to the cleavage. In rare cases, fractures in the pebbles have been infilled by matrix (Fig. 6.9).

6.3.2 Schist Pebbles

Most schist pebbles have obviously been deformed and are now ellipsoidal with long axes nearly parallel to cleavage in the matrix (Fig. 6.10). Evidence that these pebbles have been deformed plastically

(rather than changing shape by other processes such as 'pressure solution' - Dearney, 1972) is that:

(i) schistosity in these pebbles is parallel to the length of the pebbles (Fig. 6.11);

(ii) where schist pebbles curve around other pebbles, the schistosity in the schist pebbles is also curved (Figs. 6.12 and 6.13).

Few schist pebbles show evidence of brittle deformation; however, one pebble observed is cut by numerous curved fractures which have been infilled by quartz (Fig. 6.14).

6.3.3 Strain Estimations

Strain estimations were carried out on six specimens of tillite; at two localities, measurements were taken in the field and at the other four localities, oriented specimens were collected. Polar graphs of the measurements are shown in Fig. 6.15 and the results are summarized in Table 6.1.

The two-dimensional strain ratios for the quartzo-feldspathic pebbles are consistently low (ranging from 1.0 to 2.0 - See Table 6.1). As measurements have, in most cases, been made on three mutually perpendicular faces, the three dimensional strain ratios must also be low. Where the direction of the cleavage trace can be measured, it is found to be approximately parallel to the principal extension in that face. In many cases, the exact orientation of cleavage is difficult to measure because the cleavage curves around pebbles and because the cleavage is generally only weakly developed. Thus the discrepancy between cleavage and the principal extension direction may be due to errors in measurement of the cleavage.

In the unstrained state most quartzo-feldspathic pebbles would have had axial ratios less than 2:1, with long axes having a bimodal distribution of orientation.

Strain estimations for schist pebbles could only be made on faces approximately perpendicular to cleavage because the flattened shape of these pebbles resulted in few being found on sections parallel to cleavage. Two-dimensional strain ratios for the schist pebbles are generally higher (4.0 to 6.5) than for the quartzo-feldspathic pebbles on the same face, and consequently the three-dimensional strain ratios of the schist pebbles are higher than the strain ratios of the quartzo-feldspathic pebbles.

Before strain, the schist pebbles would have had axial ratios up to 4.0 and the orientation of long axes, most commonly, had a unimodal distribution.

The strain in the tillite body cannot be directly estimated from the strain in the component pebbles. However, an estimate of strain in the tillite can be obtained by use of equations derived by Gay (1968a, 1968b and 1969) which relate pebble-to-pebble and pebble-to-matrix viscosity ratios in conglomerates. The applicability of these equations to the deformation of conglomerates is doubtful as rocks probably do not behave as Newtonian fluids during deformation (Hobbs, 1972; Bayly, 1974). However, these equations may give some indication of the relationship between strain in the pebbles and the strain in the rock as a whole.

The equation which gives pebble-pebble viscosity ratios can be written as:

$$\frac{\mu_B}{\mu_A} = \frac{\ln R_{SB}}{\ln R_{SA}} - \frac{3}{2R_A}\left(1 - \frac{\ln R_{SB}}{\ln R_{SA}}\right) \quad \text{(Gay, 1969, equation 4)}$$

where:

μ_A, μ_B are the viscosities of pebble types A and B respectively;

R_{SA}, R_{SB} are the strain ratios for pebble types A and B respectively;

$R_A = \frac{\mu_A}{\mu_M}$ where μ_M is the viscosity of the matrix.

To use this equation, a value of the pebble-to-matrix viscosity ratio (R_A) must be assumed (Gay, 1968a, p. 299) although an approximate value can be determined by comparing $\frac{\mu_A}{\mu_B}$ with the reciprocal of the calculated value of $\frac{\mu_B}{\mu_A}$. Having obtained approximate values of R_A and R_B, estimates of R_{MA} and R_{MB}*/ can be made from fig. 10 of Gay (1968a) which can then be used in an equation of the form:

$$\ln R_S = \frac{2R_{MA} + 3}{5} \ln R_{SA} \quad \text{(Gay, 1969, equation 3a)}$$

to give an estimate of the strain in the rock (R_S being the strain ratio of the rock).

The value of the viscosity ratio for schist pebbles relative to matrix (R_{schist}) is assumed to be less than 1. That is, the schist pebbles are assumed to be less viscous than the matrix. This assumption is supported by the fact that schist pebbles have small 'tails' which merge into the matrix (these 'tails' are visible only in thin section, e.g., A470-070). Also, from a visual estimate of strain in the tillite using the 'centre-to-centre method' (Ramsay, 1967, pp. 195-197), strain ratios appear to be low and so are likely to fall between the measured strain ratios for schist and quartzo-feldspathic pebbles.

Calculations and results of strain ratio estimates for the tillite are shown in Table 6.2.

---

*/ Viscosity ratios of pebble to pebble-matrix system.

The results of estimates of strain ratio in the tillite using schist pebbles are not in very close agreement with the results using quartzo-feldspathic pebbles; however, the quartzo-feldspathic pebbles give consistently lower strain ratios. These estimates suggest that the strain ratios of these specimens of tillite are in the range of 2:1 to 4:1.

6.4 UNIT 5

In Subunit 5b, schistosity is strongly developed and all pebbles show evidence of a cohesive change in shape, being elongate in the plane of the schistosity.

Strain estimates were made at two localities in this subunit: at one locality, measurements were made in the field and at the other, a block was collected and three plane surfaces cut from it. Polar graphs for these measurements are shown in Fig. 6.16 and results are summarised in Table 6.1.

In this unit, estimates of two-dimentional strain ratios for quartzo-feldspathic pebbles on faces perpendicular to cleavage range from 2.5 to 4.5, whereas an estimate of strain in the plane of the cleavage gave a strain ratio of 1.6 (one specimen only). These results indicate that strain ratios for the quartzo-feldspathic pebbles in this unit are considerably higher than strain ratios for quartzo-feldspathic pebbles from Unit 3. However, strain in Subunit 5b does not appear to be very much greater than the strain recorded in its component pebbles. Thus the strain in Subunit 5b might not be very much higher than strain in Unit 3.

6.5 BASEMENT SCHIST

Strain estimation was carried out on a specimen of basement schist (A470-071) for comparison with the strain measurements in the cover metasediments. The rock chosen is a fine-grained biotite schist which is interbedded with albite rock. The schist contains ellipsoidal aggregates of white mica, elongate approximately parallel to schistosity and these ellipsoidal markers were used in the estimation of strain. Measurements of axial ratios and orientation of long axes of their elliptical traces were made on three mutually perpendicular faces. Contoured polar plots of these measurements are shown in Fig. 6.12a, b and c and the results summarised in Table 6.1.

For comparison, the 'centre-to-centre' method (Ramsay, 1967, pp. 195-197) was used to estimate strain on one face. This method assumes that particles were originally evenly distributed in the rock and that, after strain, the distance between the centres of adjacent particles reflects the longitudinal strain in the direction between the centres. Fig. 6.17f shows a graph of distance and direction between centres of adjacent 'porphyroblasts' on face 1. The graph has a maximum value 15^{o} from the cleavage and a minimum 80^{o} from the maximum (the minimum should in fact be 90^{o} from the maximum - Ramsay, 1967, p. 197- the discrepancy is probably due to the fact that few readings could be taken in the direction of shortening). The strain ratio estimated by this method is 3.2 with the principal elongation 15^{o} from the cleavage.

These results are at variance with those obtained using the method of Elliott (1970). Possible explanations are that the 'porphyroblasts' and enclosing schist have not been deformed homogeneously, or that the 'porphyroblasts' had an unusual initial fabric. Using an R_f/ϕ graph (Dunnet, 1969) and assuming an initially random fabric, the

strain in the 'porphyroblasts' (Fig. 6.17d) corresponds very closely to that obtained by the 'centre-to-centre' method (Ramsay, 1967) for the schist, i.e., $R_S = 3$, with principal extension 15° from the cleavage. This would suggest that strain in the 'porphyroblasts' is almost the same as that in the schist, and that the discrepancy between the Elliott method and the 'centre-to-centre' method is due to an unusual initial fabric.

The schistosity in the schist is curved around the ends of all 'porphyroblasts' in the same sense. This curvature could have been produced by rotation of the 'porphyroblasts' during deformation or could have been produced by inhomogeneous strain around the 'porphyroblasts'.

The schistosity in this schist is a second generation fabric element (S_{2B}) and the fact that the 'porphyroblasts' have been deformed during this deformation implies that the 'porphyroblasts' grew prior to the second deformation (D_2). The initial fabric of these 'porphyroblasts' (suggested by their orientation - see above) may have been due to alignment parallel to a first generation foliation.

6.6 CONCLUSIONS

Strain estimates in the cover rocks vary from almost zero in Unit 1 to low strain ratios in Units 3 and 5. These variations in strain may indicate either:

(i) the varying response of the different rock types to a fairly uniform stress field; or

(ii) variations in bulk strain throughout the area;

(cf. Cloos, 1947).

The units in which strain estimates were made all have different pebble sizes, pebble concentrations and matrix compositions. These

differences could influence the relative amounts of strain that would be produced in these rocks in response to the same total deformation. Unit 1, which has the lowest strain, is composed of boulders and pebbles of granite set in a matrix of quartz, feldspar and biotite; the pebble to matrix ratio is high, thus the viscosity of the conglomerate would have approached that of the pebbles. In Unit 3, average pebble size is smaller than for Unit 1 and pebbles are not quite as abundant. Estimated strain ratios for Unit 3 show that the strain is higher where quartzo-feldspathic pebbles are rarer and the matrix is richer in biotite (cf. A470-055 and A470-056). Subunit 5b apparently has the highest strain and also has fewer and smaller pebbles than either Unit 1 or Unit 3. The matrix of Subunit 5b is schistose.

Unfortunately, no single strain marker is continuous across the whole area and so there is no check on variations in the bulk strain throughout the area. A possible clue to these variations is given by the degree of development of cleavage; in Subunit 5b cleavage is strongly developed and, in places, rocks of this subunit are schistose; in Unit 4 the cleavage is moderately developed and in Unit 3 the cleavage is weakly developed. The matrix in Subunit 5b appears to have been initially similar to the siltstones of Unit 4, thus the strain in Subunit 5b may be higher than that in Unit 4 (there are no suitable markers from which to estimate the strain in Unit 4) the difference being due to a higher bulk strain in the slice of cover rocks faulted between the Boolcoomata Adamellite and the basement schists.

The estimated strains in the cover rocks are low (strain ratios perpendicular to foliation being in the range of 2:1 to 4:1) in comparison to strain estimates from many other slates (e.g., Cloos, 1947; Borradaile, 1974; Wood, 1973; Ramsay and Wood, 1973). However,

the strain ratio estimates in this study represent at least 30% shortening perpendicular to the foliation, this amount of shortening generally being considered the minimum necessary for the production of slaty cleavage (e.g., Cloos, 1947; Ramsay, 1967, p. 180; Ramsay and Wood, 1973).

The foliation in the cover rocks is subparallel to the principal plane of the finite strain ellipsoid and thus approximately perpendicular to the direction of maximum finite shortening (see Table 6.1). Cleavage is generally considered to form perpendicular to the direction of maximum finite shortening (e.g., Cloos, 1947; Ramsay, 1967, p. 180; Siddans, 1972; Borradaile, 1974), but this may be true only for a coaxial strain history (Hobbs, et al., 1974). In this study it was not possible to determine whether the discrepancy between foliation and the principal plane of the strain ellipsoid is due to inaccuracies of measurement (see Chapter 6.3.3), inhomogeneous strain on the scale of specimens studied, or a non-coaxial strain history.

CHAPTER 7

METAMORPHISM

7.1 INTRODUCTION

The schists of the Willyama Complex in this area have been metamorphosed at least three times. The first two recognisable events (M_1 and M_2) correlate with events in the Willyama Complex at Broken Hill which have been dated at about 1700 m.y. and 1550 m.y. respectively (see Chapter 7.6.4). It is suggested that these two high-grade events have taken place with temperatures in the range of about 500°C to 650°C and pressures between 0.4 GPa and 0.6 GPa (1 kb = 01. GPa). Metamorphic assemblages characteristic of the amphibolite facies were produced and partial melting produced migmatites and intrusive granitic bodies. The third metamorphic event (M_3) which correlates with the so-called Delamerian Orogeny (dated at about 500 m.y. - see Thomson, 1969) took place after the deposition of the cover rocks and affected both the basement and cover. During this episode of metamorphism, temperature was probably of the order of 400°C and pressure about 0.4 GPa. This resulted in retrogression of the high grade assemblages in the basement rocks and produced greenschist facies assemblages in the cover rocks. No zonal arrangement of mineral assemblages of any of the different episodes was observed (see Fig. 7.3).

7.2 HIGH GRADE METAMORPHIC EVENTS

It is difficult to distinguish between the products of the first and second episodes of metamorphism and so the effects of these two episodes are considered together. The relationship between the Granitic Gneiss and amphibolites provides evidence that in fact two episodes of high grade metamorphism have affected the basement rocks of this area. The Granitic Gneiss, which is presumed to be a product of the first high grade metamorphism (M_1), is intruded by basic dykes

which have been metamorphosed to the amphibolite facies by a later episode of metamorphism (presumably M_2).

Mineral assemblages thought to have been produced during these episodes of metamorphism are listed in Table 7.1 as high grade mineral assemblages and are characteristic of the amphibolite facies of metamorphism. However, few rocks in the area contain only these assemblages; most rock contain both high and low grade assemblages with textures suggesting disequilibrium between minerals of the different episodes.

7.2.1 Mineral Assemblages

In many schists aggregates of fine-grained muscovite and quartz appear to have replaced original porphyroblasts. In one specimen (A470-007) remnants of andalusite occur within some of these aggregates (see Chapter 2.2.3) and possibly the original porphyroblasts in other schists were also andalusite.

In the Layered Schist, muscovite porphyroblasts commonly contain sillimanite needles which in rare cases outline small folds (Fig. 7.1). Garnet porphyroblasts are mainly confined to the mica-rich layers in this schist. Schistosity bends around some of these porphyroblasts but abuts against others.

In other rock types, high grade mineral assemblages generally show granoblastic textures with only biotite, where present, aligned subparallel to the weak schistosity in these rocks (see Chapters 2 and 4).

7.2.2 Formation of the Older Migmatite and Granitic Gneiss

The neosome of the Older Migmatite forms veins and isolated patches within the Layered Gneiss (see Chapter 2.5.2) suggesting that

this migmatite has formed by partial melting of the Layered Gneiss and that the mobilized components have moved only a very small amount after melting.

Experimental work relevant to the formation of migmatites by partial melting (e.g., von Platen, 1965; von Platen and Holler, 1966) suggests that the composition of the initial melt is dependent upon the temperature and pressure at the beginning of melting and also upon the composition of the original rock types (Kilinc, 1972).

In comparison with experimentally produced melts (e.g., von Platten, 1965; von Platten and Holler, 1966) the composition of the neosome of the older Migmatite (albite and quartz with minor muscovite) is unusual. It could possibly have been produced by the partial melting of albite-rich rocks (cf. Kilinc, 1972): the palaeosome of this migmatite is in fact albite-rich (see Chapter 2.5.2.1). Because of the unusual composition of the neosome it is not possible to determine from the experimental work cited above the likely conditions of temperature and pressure prevailing at the time of formation of this migmatite, although the presence of muscovite suggests that the temperature was of the order of 650^{o}C and pressure was greater than 0.4 GPa (with $P_{H_2O} = P_{total}$, see Fig. 7.2).

The close field association of the Older Migmatite and Granitic Gneiss (see Chapter 2.5.2) suggests that the two rock types are genetically related. The mineralogy of the Granitic Gneiss (albite, quartz, microcline and biotite) is granodioritic and textures reflect deformation and recrystallization. These facts suggest that the Granitic Gneiss was formed by crystallization from an anatectic melt of granodioritic composition and was subsequently deformed during the

second period of deformation (D_2). The absence of muscovite from the Granitic Gneiss suggests that P - T conditions during crystallization were not appropriate for the formation of muscovite. However, the associated migmatites contain muscovite, suggesting that the water content of the Granitic Gneiss was lower than that of the surrounding migmatites, or alternatively that the temperature within the Granitic Gneiss was slightly higher than in the surrounding rocks.

An alternate hypothesis for the origin of the Granitic Gneiss and Older Migmatite is that they represent a "mantled gneiss dome" (Eskola, 1948). This hypothesis is supported by the facing of the schist sequence which is thought to young away from the Layered Gneiss (Chapter 2.10). The Layered Gneiss and sequence of schists could represent a sequence of rocks deposited on to an older granitic basement (represented by the Granitic Gneiss). However, to the southeast of the Old Boolcoomata area, calcsilicates (thought to be equivalent to the horizon of Calcareous Rocks mapped in this area) are incorporated within the migmatite and granite gneiss (Campana and King, 1958, plate 1). In addition, in many areas in the Olary Province the boundary between the migmatites and the metasediments is quite irregular and transgressive to the trend of the schists (e.g., at Outalpa Hill and south of Triangle Hill, Campana and King, 1958, plate 1) suggesting that this boundary is metamorphically rather than stratigraphically controlled. Furthermore, the metamorphic history of the schists as determined in this study is consistent with an anatectic origin for the Granitic Gneiss.

7.2.3 Origin of the Boolcoomata Adamellite and Younger Migmatite

The Boolcoomata Adamellite has definite intrusive contacts with the schists of the Willyama Complex (see Chapter 2.6) and blocks

of gneiss in the adamellite are surrounded by Younger Migmatite. These field relationships suggest that the adamellite has crystallized from a magma which was formed by the melting of metamorphic rocks and which was intruded into the rocks of this area. In this model, the enclosed gneisses represent unmelted fragments of the metamorphic rocks from which the magma was formed and the migmatites represent a stage of partial melting of these gneisses.

The approximately equal amounts of albite and microcline in the Younger Migmatite suggest that partial melting took place at relatively low water pressure (Winkler, 1967, p. 206) whereas the presence of muscovite suggests high water pressure (Hyndman, 1972, p. 137) and possibly also high load pressure. The Boolcoomata Adamellite has very similar mineralogy to these migmatites and contains approximately equal amounts of albite and microcline with subordinate quartz and muscovite. It is therefore assumed that these migmatites and the Boolcoomata Adamellite are genetically related and that they formed at a temperature of about 650^{o}C with a load pressure of at least 0.4 GPa (Fig. 7.2). These conditions are consistent with those prevailing during the second episode of metamorphism (Chapter 7.2.5).

7.2.4 Origin of Pegmatites

In the Old Boolcoomata area two generations of pegmatites can be recognised. The earlier pegmatites have been folded during the second period of deformation, suggesting that they were formed during the first metamorphic episode (M_1). The later pegmatites intrude amphibolite which has been metamorphosed during the second metamorphic event (M_2 - see Chapter 7.2) suggesting that these pegmatites were produced during the second metamorphic event (M_2). Both generations of pegmatite are thought to have formed by differentiation during metamorphism.

Pegmatites also occur within the Boolcoomata Adamellite (Chapter 2.6). Although these pegmatites occur near the border of the intrusion they do not extend out from the adamellite into the country rocks. It is thought that these pegmatites were produced by late stage crystallization of the intrusive magma.

7.2.5 Temperature and Pressure Conditions during High Grade Metamorphism

Much of the evidence for the conditions of temperature and pressure prevailing during the first period of high grade metamorphism (M_1) has been obscured by the later periods of metamorphism. The presence of the Granitic Gneiss and Older Migmatite provide the only clues to the temperature and pressure conditions during this metamorphic event. These conditions were probably similar to those which prevailed during the second metamorphic event (see below) though the absence of muscovite from the Granitic Gneiss suggests that the water pressure was lower or the temperature higher in this gneiss than in the surrounding rocks.

Evidence for the conditions of temperature and pressure prevailing during the second high grade metamorphic episode (M_2) is available from two independent sources:

(i) the stability fields of the minerals present in the metamorphic rocks (i.e., by use of the petrogenetic grid); and

(ii) the relative abundances of quartz, albite and potassium feldspar in the Younger Migmatite.

The presence of sillimanite and primary muscovite and the absence of kyanite and orthoclase in the schists and the presence of wollastonite in the Calcareous Rocks give some indication of the temperature and pressure that prevailed during this metamorphism. A possible

further indicator of the temperature-pressure environment is the absence of cordierite, though this may be due to the lack of rocks of suitable composition.

The stability fields of these minerals are shown on a petrogenetic grid (Fig. 7.2) and from this it can be seen that the possible range of temperatures and pressures is bounded by the kyanite-sillimanite equilibrium curve and the upper temperature limit for the stability of muscovite in the presence of quartz. The field outlined by these equilibrium curves intersects the minimum melting curve for granitic rocks at a temperature of about 650^{o}C and pressure between 0.4 GPa and 0.6 GPa.

The Younger Migmatite contains coarse-grained muscovite with fine sillimanite needles: similar muscovite grains occur in the Layered Schist (Chapter 2.2.3) suggesting that these migmatites may have formed under conditions similar to those responsible for the metamorphism of these schists.

The presence of wollastonite in calcareous rocks subjected to these metamorphic conditions suggests that the partial pressure of carbon dioxide (X_{CO_2}) must have been less than 0.25 (see Fig. 7.2). The partial pressure of carbon dioxide can be reduced below total fluid pressure either by the escape of carbon dioxide or by dilution of carbon dioxide with other fluid phases (Harker and Tuttle, 1956).

It seems unnecessary to postulate thermal metamorphism by the Boolcoomata Adamellite to account for the skarn-like mineral assemblages in the Calcareous Rocks because:

(i) wollastonite can be formed under conditions of regional metamorphism provided the partial pressure

of carbon dioxide is low (Harker and Tuttle, 1956; Misch, 1964; Sharma and Narayan, 1974);

(ii) the distribution of amphibolite facies mineral assemblages in the Calcareous Rocks in the east of this area shows no relationship in space to the Boolcoomata Adamellite (see Fig. 7.3);

(iii) the wollastonite-bearing rocks in this area (which occur south of the Old Boolcoomata Homestead) are separated from the Boolcoomata Adamellite by a fault and so the original disposition of this calcareous unit with respect to the Boolcoomata Adamellite is unknown.

The minerals present in the micaceous schists indicate that the second metamorphic episode occurred with temperatures in the range of 500°C to 650°C and pressures between 0.4 GPa and 0.6 GPa. The presence of sillimanite in these rocks indicates that temperatures could have been sufficiently high to allow for partial melting of some of the rocks to form the Boolcoomata Adamellite. The presence of muscovite in association with sillimanite in the Younger Migmatite suggests that the partial pressure of water was high (see Fig. 7.2). The high partial pressure of water could have caused dilution of carbon dioxide in the fluid phase and so have provided conditions suitable for the formation of wollastonite in some of the Calcareous Rocks.

7.3 METASOMATISM

Albite-rich rocks in this area are thought to have formed by sodium metasomatism. Field evidence suggests that one or more of three

rock types in the area could possibly have provided the sodium or have been associated with its distribution, these rock types being:

(i) the Granitic Gneiss;

(ii) the amphibolites;

(iii) the Boolcoomata Adamellite.

7.3.1 Metasomatism Related to the Granitic Gneiss

The Albite Schist and Layered Albite Rock both contain a foliation which is parallel to the second generation schistosity (S_{2B}) in adjacent micaceous schists. In the case of the Albite Schist, the foliation is defined by the elongation of albite grains; this suggests that albitization of these rock types occurred before or during the second deformation (D_2).

Layered Albite Rock surrounds the amphibolite body near the Woman-in-White Mine and also occurs as a layer adjacent to the Layered Gneiss which surrounds the Granitic Gneiss (Fig. 2.1). Albite Schist occurs in a northeasterly-trending zone between the Boolcoomata Adamellite and the Granitic Gneiss, and at Cathedral Rock surrounds (and is included in) the breccia.

Thus, the Layered Albite Rock and Albite Schist have no unique relationship to any of the three rock types which are possible sources of sodium. However, the fact that these albite-rich rocks are thought to pre-date the second period of deformation suggests that these albite rocks may have been metasomatised by sodium-rich solutions migrating away from the Granitic Gneiss during the first metamorphic episode, as this body was probably at a slightly higher temperature than the surrounding rocks (see Chapter 7.2.2).

One objection to this hypothesis is that the mineral assemblages in the albite-rich rocks are indicative of the greenschist facies (Table 7.1)

whereas the Older Migmatite and Granitic Gneiss are thought to have been formed during amphibolite facies metamorphism (Mehnert, 1968, p. 282, has suggested that mineral assemblages in rocks associated with migmatites should reflect the same metamorphic conditions as the migmatites).

Two possible explanations for this anomaly in the area concerned can be offered. Firstly, the albite-rich rocks may have suffered retrograde metamorphism during the last metamorphic episode (M_3) and so may have adjusted to these conditions. However, this would require mimetic growth of the retrograde products, chlorite and actinolite. Secondly, if the albite-rich rocks were formed at a late stage of the first metamorphic episode, metamorphic conditions may have been waning so that greenschist facies assemblages could have been stable.

Hoeve (1974) has suggested that albite-rich rocks in the Vastervik region of Sweden were formed during regional metamorphism by leaching of potassium, iron and magnesium from the country rocks and by the deposition of sodium. Solutions responsible for these processes migrated upwards away from areas where anatectic granites were forming, i.e., where metamorphic temperatures were highest (Hoeve, 1974, pp. 112-115). Vernon (1961) has suggested that banded albite-rich rocks in the Broken Hill district were formed by metasomatism, the source of the sodium being "a 'by-product' of the regional metamorphism" (ibid., p. 55). A similar origin is envisaged for the Layered Albite Rock of this area.

7.3.2 Metasomatism Associated with Amphibolite Intrusions

In the Willyama Complex some amphibolite bodies are closely associated with albite-rich rocks. For example, at Whey Whey Creek

the main amphibolite body is surrounded by albite-rich rocks which may have been produced by the addition of sodium expelled from the amphibolite during metamorphism (Cobb and Morris, 1970).

In the Old Boolcoomata area, the amphibolite body at the Woman-in-White Mine is surrounded by albite-rich rocks. However, the fact that these albite-rich rocks are more extensive than the amphibolite and that similar albite-rich rocks occur at a comparable position in the basement sequence elsewhere in the area (see Chapter 2.10) suggests that these albite-rich rocks have been formed by the metasomatism of a favourable horizon, rather than by the addition of sodium from the amphibolite body (cf. Cobb and Morris, 1970).

The breccia at Cathedral Rock is divided into two parts: one with albitic matrix and one with diopsidic matrix (Chapter 2.9). The origin of the albite in the matrix appears to be related to both the origin of the diopside and the breccia. The breccia is thought to be part of a diatreme, the formation of which might be related to the emplacement of the amphibolites (which are probably metamorphosed basic intrusive bodies).

7.3.3 Metasomatism Associated with the Boolcoomata Adamellite

Albite Rock Interlayered with Mica Schist occurs in a zone about 500 m wide, adjacent and parallel to the contact of the Boolcoomata Adamellite (Chapter 2.6). Within this zone, the fact that the albite concentration increases towards the contact suggests that these albite-rich layers have been formed by sodium metasomatism, the source of the sodium being the Boolcoomata Adamellite.

On the other hand, late-stage crystallization within the Boolcoomata Adamellite has produced microcline-rich pegmatites, thus suggesting that the Boolcoomata Adamellite is an unlikely source of the sodium.

Thus, the origin of the albite-rich rocks in this area remains an enigma which can only be solved by more detailed work beyond the scope of the present investigation.

7.4 LOW GRADE METAMORPHISM

Low grade metamorphism has affected both the basement and cover rocks, though not all the basement rocks show evidence of this metamorphism.

Mineral assemblages in the cover rocks are characteristic of the greenschist facies (Table 7.1) and metamorphism of this grade has also affected the basement. There is evidence of retrograde metamorphism in many of the basement schists and calcareous rocks though retrograde effects are not apparent in the gneissic rocks (with the exception of the corundum-bearing gneiss).

7.4.1 Low Grade Mineral Assemblages in the Basement

Some basement schists and Calcareous Rocks show greenschist facies mineral assemblages without mineral relics of a higher metamorphic grade. These rocks are thought to have completely readjusted to the conditions of the last metamorphism (M_3). Interlayered with these rocks are others, some with stable amphibolite facies assemblages and others with disequilibrium assemblages.

Examples of basement rocks which show apparently stable greenschist facies assemblages include Piemontite Schist, Chloritoid Schist and parts of the Epidote Quartzite (see Table 7.1 and Fig. 7.4).

In some places the Epidote Quartzite contains the mineral assemblage calcite-epidote-chlorite. This is an unusual assemblage (cf. Winkler, 1967, figs. 24, 25 and 31; Miyashiro, 1973, figs. 11.1(a) and 11.2(a)) and possibly indicates high carbon dioxide pressure (Miyashiro, 1973, p. 304).

Some basement schists contain only muscovite, biotite and quartz. This assemblage is stable under both high grade and low grade metamorphic conditions (see Fig. 7.4) and may have formed during the earliest metamorphic event and remained stable during subsequent metamorphisms.

7.4.2 Retrograde Reactions

Some of the retrograde reactions are displayed by porphyroblasts which have been partially replaced during the low grade metamorphism (M_3). For example, both andalusite and corundum porphyroblasts have been altered to muscovite.

A possible reaction for the breakdown of andalusite has been suggested by Carmichael (1969, equation 1):

$$3Al_2SiO_5 + 2K^+ + 3SiO_2 + 3H_2O = 2KAl_3(AlSi_3O_{10})(OH)_2 + 2H^+$$

andalusite quartz muscovite

This reaction is dependent upon f_{H_2O}, a_{K^+}, pH and temperature (Eugster, 1970, p. 118). Carmichael (1969, p. 251) suggests that this reaction will proceed only at interfaces between quartz and aluminosilicate. In the specimen containing remnants of andalusite (A470-007) the andalusite poikiloblastically encloses small quartz grains. Some of these quartz grains have been replaced by fine-grained muscovite, suggesting that breakdown of the andalusite has occurred by reaction between the andalusite and quartz with the introduction of H_2O and K^+. However, other quartz grains remain intact and in places reaction appears to have proceeded along fractures in the porphyroblast, suggesting that silica has been added to the porphyroblasts, perhaps by the reaction:

$$3Al_2SiO_5 + 3Si(OH)_4 + 2K^+ = KAl_3(AlSi_3O_{10})(OH)_2 + 2H^+ + 3H_2O$$

(Carmichael, 1969, equation 3).

In some of the 'porphyroblastic' schists, chlorite is associated with the alteration of the porphyroblasts (thought to have been andalusite - e.g., A470-072) and has possibly been produced by a reaction involving the breakdown of biotite present in these schists:

$$4Al_2SiO_5 + 2K(Mg, Fe)_3 AlSi_3O_{10}(OH)_2 + 3H_2O = 2KAl_3(AlSi_3O_{10})(OH)_2 +$$

andalusite biotite muscovite

$$(Mg, Fe)_5 Al(AlSi_3O_{10})(OH)_8 + (Mg, Fe)^{2+} + SiO_2$$

chlorite quartz

However, during this episode of metamorphism (M_3) biotite has grown in the cover rocks (see Chapter 7.4.3) and biotite appears to be a stable phase in many of the basement schists. In the sillimanite-bearing schists, chlorite is ubiquitous but biotite is scarce. These features are probably a consequence of the variations in the composition of the schists, the more aluminous schists containing chlorite and relics of aluminosilicates, whereas the less aluminous schists contain biotite (see Fig. 7.4).

Corundum porphyroblasts in the Corundum-Biotite-Plagioclase Gneiss (A470-030) are surrounded by a corona of muscovite which in turn is surrounded by a biotite-deficient, albite-rich zone. An examination of the coronas around the corundum shows that the corundum is embayed by the muscovite and that the muscovite has also developed at the expense of the albite (Fig. 2.16 and Chapter 2.5.1.2), suggesting that the ionic reaction for the development of the muscovite might be:

$$3Al_2O_3 + 2NaAlSi_3O_8 + 2K^+ + 6H^+ = 2KAl_3(AlSi_3O_{10})(OH)_2 + 2Na^+$$

corundum albite muscovite

The absence of biotite in a zone surrounding these coronas suggests that the K^+ for the formation of the muscovite might have been derived from the breakdown of biotite by the reaction:

$$K(Mg,Fe)_3 AlSi_3O_{10}(OH)_2 + Na^+ + 6H^+ = NaAlSi_3O_8 + K^+ + 3(Mg,Fe)^{2+} + 4H_2O$$

biotite albite

(Carmichael, 1969, equation 7.)

The above two reactions allow for the breakdown of the corundum porphyroblasts without the migration of aluminium (which Carmichael, 1969, considers to be an immobile element) and also without the addition of silica.

7.4.3 Prograde Metamorphism of the Cover Rocks

Metamorphism of the cover rocks has produced only a limited number of metamorphic assemblages (see Table 7.1), namely:

quartz-muscovite-biotite ($\pm$ chlorite);

quartz-albite-muscovite-biotite;

quartz-muscovite-biotite-dolomite.

These reflect the limited compositional range of the original sediments and the uniformity of the metamorphic conditions affecting the cover rocks.

The above assemblages appear to correspond to the biotite grade but they are slightly unusual in lacking chlorite (present in only minor amounts in one specimen) and containing dolomite. In the Whey Whey Creek area, Talbot (1962) has found mineral assemblages characteristic of the biotite grade in some of which tremolite is present rather than dolomite plus quartz, though at Doughboy Well, Berry (1973) found assemblages similar to those described here.

Most workers (e.g., Winkler, 1967, pp. 100 and 118; Turner, 1968, p. 280; Hyndman, 1972, p. 346) have found that, in general, in

the biotite zone, dolomite plus quartz is replaced by tremolite, but under conditions of high carbon dioxide pressure, dolomite and quartz may be stable to higher temperatures (Billings and White, 1950; Winkler, 1967, p. 100; Miyashiro, 1973, p. 304). It would seem, therefore, that somewhat higher pressure of carbon dioxide (P_{CO_2}) pertained in the Old Boolcoomata and Doughboy Well areas than at Whey Whey Creek.

7.4.4 Conditions During Low Grade Metamorphism

From the low grade mineral assemblages in the Calcareous Rocks of the basement and from the co-existence of quartz and dolomite in the cover rocks, it is concluded that carbon dioxide pressure during the low grade metamorphism was relatively high. Experimental work has not yet delineated accurately the temperature and pressure conditions for the formation of biotite (see Lambert, 1972) and so it is not possible to use the presence of this mineral as an indicator of metamorphic conditions.

If the high pressures indicated by the coexistence of quartz, biotite and dolomite are found only in Barrovian facies series (Winkler, 1967, p. 100) then, from data in Hietanen (1967, fig. 1), temperature would have been in the range of 300°C to 350°C with a pressure of about 0.45 GPa, or from data in Lambert (1972, fig. 1) the temperature could have been as high as 450°C with a pressure of about 0.55 GPa.

7.5 COMPARISON OF THE HIGH AND LOW GRADE METAMORPHIC EVENTS

The high grade metamorphic events (M_1 and M_2) have taken place with a temperature range of about 500°C to 650°C and pressure between 0.4 GPa and 0.6 GPa. This suggests that the geothermal gradient at the time of metamorphism was about 35° C/km which is slightly higher than the normal range of geothermal gradients

(Richardson, 1970). Radioactive decay of uranium, which is an abundant element in the Willyama Complex of the Olary Province (see Campana and King, 1958) may have contributed to the heat flow causing the higher than 'normal' geothermal gradient.

Conditions of temperature and pressure during the low grade metamorphism appear to have been of the order of 400^{o}C and 0.4 GPa, suggesting a geothermal gradient of about 27^{o}C/km (which is within the range of normal geothermal gradients) and a depth of burial of about 15 km.

If it is assumed that the pressure acting during this metamorphism was due to the weight of overlying rocks, then a calculation can be made of the depth of burial by determining the thickness of Adelaidean sediments in the Olary region. The Umberatana Group has a thickness of approximately 7,000 m to 8,000 m in the Olary district (Thomson, 1969, fig. 22) and is overlain by the Wilpena Group, the thickness of which ranges from about 7,000 m east of the Barrier Ranges (in which the Willyama Complex is exposed in New South Wales) to about 3,000 m in the Orrorro area (which is west of Olary district) (Thomson, 1969, p. 73). Thus the thickness of the Wilpena Group in the Olary district was probably between 3,000 m and 7,000 m and the total thickness of Adelaidean metasediments overlying this area was probably between 10,000 m and 15,000 m. This is in fair agreement with depth of burial indicated by the metamorphic mineral assemblages.

That the geothermal gradient was 'normal' during this metamorphic episode is not surprising. The basement rocks had been stabilized as continental crust for about 700 m.y. (see Chapter 8) and sedimentation rate of the Adelaidean System was low. Thus, the Adelaidean rocks would have had time to adjust to the heat flow conditions from the basement rocks (see Richardson, 1970).

7.6 TIMING OF THE METAMORPHIC EVENTS

Timing of the metamorphic events relative to the periods of deformation can be determined by examining the field relationships between various rock types and by investigating the relationship between the growth of the various mineral phases relative to each other and relative to foliations in the rocks.

From field evidence, the following sequence of deformational and metamorphic events can be recognised:

(i) deformation (D_1) and metamorphism (M_1) producing pegmatites, Granitic Gneiss and Older Migmatite;

(ii) intrusion of basic dykes;

(iii) deformation (D_2) and metamorphism (M_2) producing Boolcoomata Ademellite, Younger Migmatite and pegmatites;

(iv) deposition of cover rocks;

(v) deformation (D_3) and metamorphism (M_3) of all the above rock types.

The Albite Schist and Layered Albite Rock appear to pre-date the second period of deformation but the exact timing of the metasomatism relative to the formation of the Granitic Gneiss and the intrusion of the amphibolites is not certain.

It is thus suggested that the area has been affected by three periods of deformation which have been associated with metamorphic events; the first two metamorphic events were apparently high grade and the last event was low grade.

Correlation of these events with growth of the metamorphic minerals is attempted below.

7.6.1 Time of the First Metamorphic Event

The paucity of first generation structures (see Chapter 4.3) makes it difficult to determine the relationship of mineral growth to the first deformation. However, what is thought to be first generation schistosity is seen in some of the Layered Schists (see Chapter 4.4.1). This schistosity is defined by an alignment of chlorite, which is thought to mimic earlier biotite.

Lenticular aggregates of fine-grained mica, which are thought to represent porphyroblasts, are flattened in the second generation schistosity, suggesting that the original porphyroblastic minerals may have grown prior to the second deformation. Evidence of this early growth of porphyroblasts is also indicated from the strain analysis of a basement schist specimen (Chapter 6.5) which shows that the porphyroblasts in this rock had a pre-D_2 fabric. This evidence is consistent with the field evidence and suggests that the first metamorphic event was probably a high grade event.

7.6.2 Time of the Second Metamorphic Event

There are abundant indications of mineral growth coincident with the second period of metamorphism, but again there are some anomalies.

The well developed second generation schistosity is defined by the alignment of muscovite and biotite. Lenticular aggregates of fine-grained muscovite are elongate parallel to this schistosity, suggesting that the original porphyroblastic minerals were retrograded before or during the second period of deformation. However, it is possible that the porphyroblastic minerals changed shape (e.g., by slip or by 'pressure solution') during deformation and were retrograded by a later metamorphic event.

Muscovite porphyroblasts in the Layered Schist contain fine needles of sillimanite which in some cases outline folds (e.g., Fig. 7.1) though the enclosing muscovite shows no evidence of deformation. This suggests that the muscovite has grown later than the sillimanite, or that both have grown simultaneously, with the sillimanite growing mimetically after some early mineral.

The relics of andalusite porphyroblasts in A470-007 show curved trails of inclusions. The porphyroblasts are aligned in the second generation schistosity and show euhedral and subhedral shapes. This evidence suggests that these porphyroblasts grew during the second metamorphic episode.

7.6.3 Time of the Third Metamorphic Event

The age of the third metamorphic event relative to other geological events can be easily determined. The similarity in metamorphic conditions indicated by the retrograde assemblages in the basement and the metamorphic assemblages in the cover rocks suggests that these assemblages were produced during the same metamorphic episode.

In the cover rocks, the alignment of the biotite grains parallel to the cleavage in the metasiltstones suggests that this episode of metamorphism was active during the deformation of the cover rocks (D_3).

7.6.4 Absolute Ages of the Metamorphic Episodes

The absolute ages of the second and third metamorphic events can be estimated from published isotopic age dates of Willyama Complex and Adelaide System rocks (e.g., Compston, et al., 1966; Compston and Arriens, 1968) and from the dating of the Boolcoomata Adamellite (Compston, et al., 1966).

The age of the Boolcoomata Adamellite is 1580 m.y. (Compston, et al., 1966, specimen Ga 388) which is close to the age of the Mundi Mundi Granite (1520±40 m.y. Compston and Arriens, 1968, p. 578) which intrudes the Willyama Complex at Broken Hill. These ages are younger than the age of the high grade metamorphism in the Broken Hill region which has been dated at 1650 m.y. to 1700 m.y. (ibid., p. 578). This suggests that the first metamorphism in this area corresponds to the high grade metamorphism at Broken Hill (dated at about 1700 m.y.) and that the second metamorphism took place about 1550 m.y. ago.

The age of the third metamorphism possibly corresponds to the age of 'young' pegmatites and biotites in the Broken Hill area which have ages in the range of 495 m.y. to 530 m.y. (Compston and Arriens, 1968, p. 578). This is in fairly close agreement with the age of metamorphism of the Adelaide System of 465 m.y. (Compston, et al., 1966).

CHAPTER 8

BASEMENT-COVER RELATIONSHIPS

8.1 INTRODUCTION

This study was undertaken to investigate the geology of the Old Boolcoomata area and, in particular, to investigate:

(i) the sequence of rock types in the Willyama Complex; and

(ii) the structural relationships between the basement and cover sequences.

The sequence of rock types in the Willyama Complex has been described in Chapter 2, and comparisons of that sequence with sequences recognised by previous workers, are made in that chapter.

The deformation and metamorphism of the basement and cover rocks have been considered in Chapters 4 to 7. In this chapter an interpretation of these data is made and a synthesis of the geological history of the rocks of this area is presented.

Prior to the deposition of the cover rocks, the basement rocks had been deformed and metamorphosed during two tectonothermal events (D_1/M_1 and D_2/M_2). The deformations produced tight folds in the basement schists and the metamorphic events produced amphibolite facies assemblages, pegmatites and granitic bodies with associated migmatites.

After the deposition of the Adelaidean sediments in the Olary district, both the cover and basement rocks were deformed and metamorphosed, the two events apparently happening simultaneously. The deformation produced folding in both the basement and cover and also produced differential movement between the basement and cover as evidenced by the MacDonald Fault (Chapter 5.7).

The presence of tight synclines and broad anticlines in the cover rocks suggests that during this deformation the cover behaved

as a body with lesser competency than the basement (see Ramsay, 1967, p. 383). The tight synclines in the cover became areas with strain greater than the adjacent anticlines (cf. Coward and James, 1974), and so were the most likely sites for the development of faults.

8.2 COMPARISON BETWEEN BASEMENT AND COVER STRUCTURES

The macroscopic structure of the basement consists of a complex superimposed fold pattern produced by the interference of first, second and third generation folds. The first generation fold is thought to be an isoclinal syncline that has been refolded by an isoclinal synform-antiform pair during the second period of deformation; both of these structures were refolded to produce a close, easterly plunging synform during the third period of deformation (see Chapter 4.8). The general shape of the third generation synform is best seen in the Granitic Gneiss where it is a close fold with an interlimb angle of about 60° and a plunge of about 50 towards 085 (πS_{2B} Subareas II and III, Fig. 4.34) and axial plane dipping 85° towards 185 (Total πS_{3B}, Fig. 4.34).

The macroscopic structure of the cover is the limb of a syncline. From the stereographic projection of poles to bedding (πS_{OC}, Fig. 4.34) this fold is interpreted as a close fold with an interlimb angle of 60°, a plunge of 35° towards 100, and an axial plane dipping 80° towards 195.

Thus, it can be seen that the third generation structures in the basement are similar in style and orientation to first generation structures in the cover. It is therefore concluded that these structures developed in response to the same deformational event (D_3).

8.2.1 Parallelism between Basement and Cover Folds

In many areas of basement and cover deformation, foliation in the basement is parallel to the unconformity between basement and cover and hence parallel to bedding in the cover (e.g., Ramsay, 1967, pp. 514-516; Reece, 1959). At Old Boolcoomata, the similarity of plunges of third generation folds in the basement to those of first generation folds in the cover indicates that bedding in the cover was sub-parallel to both the lithological layering (S_{OB}) and schistosity (S_{2B})* in the basement where they are folded around the third generation synform. This parallelism may have been produced by either:

(i) the initial angle between the layering (and schistosity) in the basement and bedding in the cover being reduced by deformation (Ramsay, 1967, p. 129; Watson, 1967, p. 217); or

(ii) rotation of the Adelaidean rocks by movement on the MacDonald Fault; or

(iii) lithological layering and schistosity in the basement being sub-horizontal at the time of deposition of the cover sediments.

The change in the angle between two lines in a plane during deformation can be estimated if both the strain ratio in that plane and the orientation of the lines with respect to the principal elongation

---

* Lithological layering (S_{OB}) and schistosity (S_{2B}) are sub-parallel in the limbs of second generation folds which are tight to isoclinal in this area (see Chapter 4.4).

are known (see Ramsay, 1967, pp. 129-132). In areas of intense deformation, the strain may be sufficiently high to cause almost total obliteration of original angular discordances (e.g., Ramsay, 1967, pp. 514-516). However, at Old Boolcoomata the low strain ratios estimated for sections parallel to cleavage in the cover rocks (all less than 1.5 - Chapter 6.3, 6.4) would be too low to cause significant changes in the angles between lines in the axial plane (see Ramsay, 1967, fig. 4.6) and hence could not greatly reduce an initially large angle between bedding in the cover and foliation in the basement.

The plunge of folds in the cover in this area is similar to plunges of folds in the cover elsewhere in the Olary Province (e.g., Talbot, 1962; Berry, 1973) and so it seems unlikely that the folds in the cover rocks have been rotated into parallelism with third generation folds in the basement by movement on the MacDonald Fault.

In this area evidence is lacking to indicate the orientation of the second generation schistosity in the basement before deposition of the cover rocks because the MacDonald Fault separates the basement from the cover (except where conglomerate of Unit 1 unconformably overlies the Boolcoomata Adamellite). At Whey Whey Creek, Talbot (1962) has shown that much of the main foliation in the basement was approximately vertical at the time of deposition of the Burra Group. However, in places the basement foliation at Whey Whey Creek appears to have been sub-horizontal at that time (e.g., north of the main amphibolite body - personal observation).

Of the above three possible explanations for the parallelism of folds in the cover with those in the basement, only the last explanation satisfies the observations in this area. Thus, the lithological

layering and foliation in the basement were probably sub-horizontal or shallowly dipping at the time of deposition of the cover rocks, suggesting that the second generation folds in the basement were recumbent or gently inclined.

8.3 MODEL FOR THE BASEMENT AND COVER DEFORMATION

Sprigg (1954) has attributed most of the deformation in both the basement and the cover rocks in the Olary region to movement on faults, in particular the MacDonald Fault. However, Campana (in Campana and King, 1958) considered that folding has affected both the cover and basement simultaneously, and that faulting was of minor importance. In fact, faults are not shown on Campana's geological map or main cross-sections (ibid., plates I and III), though they are shown on some sketch cross-sections (e.g., ibid., fig. 30a and plate II).

In the basement rocks of the Whey Whey Creek area (Talbot, 1962), the pre-Adelaidean schistosity is, in general, parallel to the axial planes of folds in the cover rocks. Talbot (ibid., p. 170) suggested that folding in the cover may have been produced by the concentration of basement deformation in zones parallel to the main (pre-Adelaidean) foliation in the basement. This relationship is quite different from the general pattern of basement-cover interaction in the Old Boolcoomata area where both basement and cover have been folded simultaneously (see Chapter 8.2). However, the type of relationship described by Talbot may explain some of the minor structures. For example at 029056, second generation folds in the cover occur adjacent to basement in which schistosity and lithological layering are not folded (Chapter 5.7.1). These folds could be accounted for by Talbot's

model of basement/cover deformation. On the other hand, most evidence suggests that chevron folds form by shortening parallel to layering (e.g., Ramsay, 1974; Patterson and Weiss, 1968) rather than by slip on axial planar structures (see Ramsay, 1967, pp. 431-432). If the direction of shortening was perpendicular to layering in the basement but almost parallel to bedding and cleavage in the cover, then folds would be formed in the cover rocks but not in the basement.

The model of basement and cover deformation which best fits the structures in the Old Boolcoomata area and also explains some aspects of the basement-cover relationships in other parts of the Olary Province is that proposed by Ramsay (1967, pp. 382-386). In this model, basement and cover were folded together but, due to differences in competence between basement and cover, the cover was folded into a series of tight synclines and broad anticlines.

In the Olary Province, tight synclines in the Adelaidean rocks are seen in Old Boolcoomata area (see Chapter 5), east of Outalpa Homestead (Campana and King, 1958, plate I) and the Whey Whey Creek area (Talbot, 1967, fig. 2), and separating these synclines are broad anticlines in the cores of which the Willyama Complex is exposed. All of these synclines are associated with faults (e.g., the MacDonald Fault at Old Boolcoomata and the north trending faults at Whey Whey Creek - Talbot, 1967, fig. 2). Crenulations are developed adjacent to the eastern-most fault at Whey Whey Creek (Talbot, 1962) and adjacent to the MacDonald Fault (Chapter 5.7), suggesting that these faults post date folding and the development of cleavage in the cover rocks. On the other hand the MacDonald Fault appears to have been folded. Therefore, it is proposed that movement on the MacDonald Fault commenced

after the initiation of folding, and that folding continued after the development of the fault.

It seems unlikely that the MacDonald Fault pre-dates the deposition of the cover and that renewed movement on this fault has caused folding in the cover, as suggested by Sprigg (1954).

Thus, the third period of deformation (D_3) in the Old Boolcoomata area caused folding of both the basement and the cover producing tight synclines and more open anticlines in the cover (see Fig. 8.1). Strain in the synclines was probably higher than in adjacent anticlines (see Coward and James, 1974), making the synclines favourable sites for the development of faults. The MacDonald fault is interpreted as having developed in response to the same deformational event (D_3) as the cover folding, but with movement on the fault occurring after the initiation of folding and the development of cleavage. After development of the fault, continued deformation caused local folding of the fault plane.

The model for basement-cover deformation proposed here is based on observations in the Old Boolcoomata area. The model is probably applicable to other areas in the Olary Province which show similar structures (e.g., in the zones of tight synclines and associated north trending faults in the Outalpa and Weekeroo areas - see Fig. 1.1) but studies of the structure of the cover rocks in areas of synclinal depressions (e.g., north-west of the Outalpa Homestead - see Campana and King, 1958, plate I) are needed before the structure of the cover rocks can be completely understood.

8.4 TECTONIC SYNTHESIS

The sequence of geological events in this area as elucidated in this study is summarized in Table 8.1.

The oldest recognisable sediments in this area are the interbedded schists, quartzites and calcareous rocks of the Willyama Complex which overlie layered quartzo-feldspathic gneisses (Chapter 2). The similarity of these gneisses to rock types elsewhere in the Olary Province which contain sedimentary structures (e.g., at Wipareminga Hill, Parker, 1972) suggests that these gneisses also had a sedimentary origin.

It is difficult to interpret the environment in which these sediments were deposited, but the sequence represents clastic deposits grading from coarse-grained feldspathic sediments to finer-grained sediments with some chemically precipitated calcareous horizons.

These sediments have since been deformed and metamorphosed at least three times and have been intruded by basic dykes, pegmatite veins and granitic bodies with associated migmatites.

Evidence of the earliest deformation (D_1) is obscure (see Chapter 4.3); this deformation appears to have produced isoclinal folding and to have been accompanied by high-grade metamorphism (M_1), during which temperatures reached approximately 650^{o}C causing partial melting of some of the rocks to produce migmatites and a granodiorite body (the granodiorite was later deformed to produce the Granitic Gneiss). Metasomatic alteration of some of the metasediments was produced by the movement of sodium-rich solutions away from the granodiorite body as this body was probably at a slightly higher temperature than the surrounding rocks. A similar origin is envisaged for albite-rich rocks in the Broken Hill district (Vernon, 1961) and in the Vastervik area of Sweden (Hoeve, 1974).

Dating of this deformational and metamorphic event (D_1/M_1) is uncertain but, by comparison with the isotopic dating of rocks from

the Broken Hill district, it seems likely that this event took place about 1700 m.y. ago (see Chapter 7.6).

Basic dykes (later metamorphosed to amphibolites) were probably intruded in the fairly short interval between the first and second deformations.

The second period of deformation and metamorphism (D_2/M_2) occurred about 1580 m.y. ago (see Chapter 7.6). This deformation was responsible for the production of the prominent schistosity and isoclinal folds in the basement schists, and also produced the strongly developed fabric in the Granitic Gneiss. This metamorphism produced amphibolite facies mineral assemblages under conditions of temperature in the range of 500°C to 650°C and pressure in the range of 0.4 GPa to 0.6 GPa. The high heat flow, possibly augmented by radiogenic heat, caused partial melting of rocks at a level slightly deeper in the crust than the present area represents; the magma so formed intruded the rocks of this area and subsequently crystallized as the Boolcoomata Adamellite.

This deformational event (D_2) caused crustal thickening, producing continental crust which was stable for a period of about 1000 m.y. During the first 700 m.y. of this time, erosion and uplift brought the rocks of the study area close to the surface. Transgression of the sea about 900 m.y. ago resulted in deposition of the Burra Group sediments; a regression of the sea concluding this deposition. About 750 m.y. ago (see Thomson, 1969), a cold climate resulted in glacial erosion and deposition to produce rocks of the Appilla Tillite. Subsequent warmer conditions brought an end to glaciation; melting of the ice sheet possibly accounted for the transgression of the sea which followed, resulting in deposition of sediments on the continental shelf to produce rocks of the lower Umberatana Group. Deposition continued for a period

of about 100 m.y. to produce rocks of the Upper Umberatana Group and Wilpena Group, these rocks not being represented in this area.

Sedimentation was brought to a close by the onset of the Delamerian Orogeny (D_3) the beginning of which is dated at 520-530 m.y. by Milnes, 1973. During this orogeny both basement and cover rocks were folded in response to crustal shortening, the cover being folded into tight synclines and broad anticlines as it was less competent than the basement. The tight synclines formed areas where strain was concentrated: further shortening led to the development of faults which closely follow the trace of the synclines.

Metamorphism (M_3) at this time occurred with temperature between 300^{o}C and 400^{o}C and pressure of approximately 0.5 GPa, indicating a fairly 'normal' geothermal gradient (for stable crust) of about 27^{o}C/km and a depth of burial of about 15 km. This metamorphism produced greenschist facies assemblages in the cover rocks and caused retrogression of some of the mineral assemblages in the basement rocks.

Since the close of the Delamerian Orogeny about 490 m.y. ago (Thompson, 1969), the crust in this area has remained stable, only being affected by uplift and erosion which have produced the present topography.

REFERENCES

ANDERSON, D.E., 1965: The structural and metamorphic petrology of the Mt. Robe district, Broken Hill, N.S.W. Unpubl. Ph.D. thesis, Univ. Sydney.

BAYLY, M.B., 1974: An energy calculation concerning the roundness of folds. Tectonophysics, 24, 291-316.

BELL, T.H., 1969: The stages in development of slaty cleavage across the Nacara Arc of the Adelaide Geosyncline. Unpubl. B.Sc.(Hons) thesis, Univ. Adelaide.

BERRY, R.F., 1973: Geology of the Doughboy Creek Area, Outalpa Station, Olary Province, South Australia. Unpubl. B.Sc.(Hons) thesis, Flinders Univ. S. Aust.

BILLINGS, M.P. and WHITE, W.S., 1950: Metamorphosed mafic dykes of the Woodsville Quadrangle, Vermont and New Hampshire. Am. Miner., 35, 629-643.

BINNS, R.A., 1964: Zones of progressive regional metamorphism in the Willyama Complex, Broken Hill district, N.S.W. J. geol. Soc. Aust., 11, 283-330.

BISHOP, D.G., 1972: Transposition structures associated with cleavage formation in the Otago Schists. N.Z. Jl Geol. Geophys., 15, 360-371.

BORRADAILE, G.J., 1974: Bulk finite tectonic strain estimates from the deformation of neptunian dykes. Tectonophysics, 22, 127-140.

BORRADAILE, G.J. and JOHNSON, H.D., 1973: Finite strain estimates from the Dalradian Dolomitic Formation, Islay, Argyll, Scotland. Tectonophysics, 18, 249-259.

CAMPANA, B., 1952: Geological Atlas of South Australia, Sheet Kalabity, 1:63,360 series. Geol. Surv. S. Aust., Adelaide.

CAMPANA, B., 1955: The structure of the Eastern South Australian Ranges - The Mt. Lofty-Olary Arc. J. geol. Soc. Aust., 2, 47-61.

CAMPANA, B., 1956a: Geological Atlas of South Australia, Sheet Glenorchy, 1:63,360 series. Geol. Surv. S. Aust., Adelaide.

CAMPANA, B., 1956b: Geological Atlas of South Australia, Sheet Plumbago, 1:63,360 series. Geol. Surv. S. Aust., Adelaide.

CAMPANA, B. and KING, D., 1958: Regional geology and mineral resources of the Olary Province. Bull. geol. Surv. S. Aust., 34.

CARMICHAEL, D.M., 1969: On the mechanism of prograde metamorphic reactions in quartz-bearing pelitic rocks. Contr. Mineral. and Petrol., 20: 244-267.

COATS, R.P., 1967: The "Lower Glacial Sequence" - Sturtian type area. Q. geol. Notes, geol. Surv. S. Aust., 23, 1-3.

COBB, M.A. and MORRIS, B.J., 1970: The Weekeroo Amphibolite, Olary Province, South Australia. Unpubl. B.Sc.(Hons) thesis, Univ. Adelaide.

COMPSTON, W. and ARRIENS, P.A., 1968: The Precambrian geochronology of Australia. Can. J. Earth Sci., 5, 561-583.

COMPSTON, W., CRAWFORD, A.R., and BOFINGER, V.M., 1966: A radiometric estimate of the duration of sedimentation in the Adelaide Geosyncline, South Australia. J. geol. Soc. Aust., 13, 229-276.

COWARD, M.P. and JAMES, P.R., 1974: The deformation patterns of two Archaean greenstone belts in Rhodesia and Botswana. Precambrian Res., 1, 235-258.

DEARNEY, D.W., 1972: Solution-transfer, an important geological deformation mechanism. Nature, 235, 315-316.

DIDIER, J., 1973: Granites and Their Enclaves: The Bearing of Enclaves on the Origin of Granites. Elsevier Scientific Publishing Co., Amsterdam.

DIETERICH, J.H., 1969: Origin of cleavage in folded rocks. Am. J. Sci., 267, 155-165.

DIETRICH, R.V., 1960: Banded gneisses. J. Petrol., 1, 99-120.

DUNNET, D., 1969: A technique of finite strain analysis using elliptical particles. Tectonophysics, 7, 117-136.

DUNNET, D. and SIDDANS, A.W.B., 1971: Non-random sedimentary fabrics and their modification by strain. Tectonophysics, 12, 307-326.

ELLIOTT, D., 1970: Determination of finite strain and initial shape from deformed elliptical objects. Bull. geol. Soc. Am., 81, 2221-2236.

ESKOLA, P.E., 1948: The problem of mantled gneiss domes. Q. Jl geol. Soc. Lond., 104, 461-476.

EUGSTER, H.P., 1970: Thermal and ionic equilibria among muscovite, K-feldspar and alumino-silicate assemblages. Fortschr. Miner., 47, 106-123.

FLEUTY, M.J., 1964: The description of folds. Proc. Geol. Assoc., 75, 461-492.

FLINT, R.B., 1974: A petrological and structural study of a portion of the Olary Province east of Whey Whey Creek, South Australia. Unpubl. B.Sc(Hons) thesis, Flinders Univ. S. Aust.

FORBES, B.G., 1970: Benda Siltstones. Q. geol. Notes, geol. Surv. S. Aust., 33, 1-2.

GAY, N.C., 1968a: Pure shear and simple shear deformation of inhomogeneous viscous fluids. I Theory. Tectonophysics, 5, 211-234.

GAY, N.C., 1968b: Pure shear and simple shear deformation of inhomogeneous viscous fluids. II The determination of the total finite strain in a rock from objects such as deformed pebbles. Tectonophysics, 5, 295-302.

GAY, N.C., 1969: The analysis of strain in the Barberton Mountain Land, Eastern Transvaal, using deformed pebbles. J. Geol., 77, 377-396.

HARKER, R.I. and TUTTLE, O.F., 1956: Experimental data on the P_{CO_2}-T curve for the reaction: calcite + quartz = wollastonite + carbon dioxide. Am. J. Sci., 254, 239-256.

HIETANEN, A., 1967: On the facies series in various types of metamorphism. J. Geol., 75, 187-214.

HOBBS, B.E., 1966: The structural environment of the northern part of the Broken Hill orebody. J. geol. Soc. Aust., 13, 315-338.

HOBBS, B.E., 1972: Deformation of non-Newtonian materials in simple shear. In, Heard, H.C., Borg, I.Y., Carter, N.L. and Raleigh, C.B. (Eds.): Flow and fracture of rocks. Geophys. Monogr., 16, 243-258.

HOBBS, B.E., MEANS, W.D. and WILLIAMS, P.F., 1974: Experimental production of axial plane foliation and the relationship to strain. (Abstr.) Geol. Soc. Aust. Tectonics and Structural Newsletter, 3, 19.

HOEVE, J., 1974: Soda metasomatism and radio-active mineralization in the Vastervik area, southeastern Sweden. Unpubl. Ph.D. thesis, Vrije Univ. Amsterdam.

HOWCHIN, W., 1920: Past glacial action in Australia. Off. Yb. Commonw. Aust., 13, 1133-1146.

HYNDMAN, D.W., 1972: Petrology of Igneous and Metamorphic Rocks. McGraw-Hill, New York.

KILINC, I.A., 1972: Experimental study of partial melting of crustal rocks and formation of migmatites. Int. geol. Congr., 24(2), 109-113.

LAMBERT, R. St.J., 1972: The metamorphic facies concept - continued. Int. geol. Congr. 24(2), 100-108.

MAWSON, D., 1912: Geological investigations in the Broken Hill Area. Mem. R. Soc. S. Aust., 2, 211-319.

MAWSON, D. and SPRIGG, R.C., 1950: Subdivision of the Adelaide System. Aust. J. Sci., 13, 69-72.

MEHNERT, K.R., 1968: Migmatites and the Origin of Granitic Rocks. Elsevier Scientific Publishing Co., Amsterdam.

MICHELMORE, T.R., 1971: The geology of copper mineralized areas in the Olary Province. Unpubl. B.Sc.(Hons) thesis, Univ. Adelaide.

MILNES, A.R., 1973: The Encounter Bay Granites, South Australia, and their environment. Unpubl. Ph.D. thesis, Univ. Adelaide.

MISCH, P., 1964: Stable association wollastonite-anorthite, and other calc-silicate assemblages in amphibolite-facies crystalline schists of Nanga Parbat, northwest Himalayas. Contr. Mineral. and Petrol., 10, 315-356.

MIYASHIRO, A., 1973: Metamorphism and Metamorphic Belts. George, Allen and Unwin, London.

PARKER, A.J., 1972: A petrological and structural study of a portion of the Olary Province west of Wiperaminga Hill, South Australia. Unpubl. B.Sc.(Hons) thesis, Univ. Adelaide.

PATTERSON, M.S. and WEISS, L.E., 1966: Experimental deformation and folding in phyllite. Bull. geol. Soc. Am., 77, 343-374.

PITT, G.M., 1971a: Geology of the MacDonald Corridor, Olary Province. Q. geol. Notes geol. Surv. S. Aust., 39, 3-7.

PITT, G.M., 1971b: Progress report of geology of the Plumbago 1:63,360 map area. Rept. Bk No. 71/63, Dept. Mines, S. Aust. (Unpubl.)

RAMSAY, J.G., 1962: Interference patterns produced by the superposition of folds of 'similar' type. J. Geol., 70, 466-481.

RAMSAY, J.G., 1967: Folding and Fracturing of Rocks. McGraw-Hill, New York.

RAMSAY, J.G., 1974: Development of chevron folds. Bull. geol. Soc. Am., 85, 1741-1754.

RAMSAY, J.G. and WOOD, D.S., 1973: The geometric effects of volume change during deformation processes. Tectonophysics, 16, 263-278.

REECE, A., 1959: The stratigraphy, structure and metamorphism of the Pre-Cambrian rocks of North-West Ankole, Uganda. Q. Jl. geol. Soc. Lond., 115, 389-420.

RICHARDSON, S.W., 1970: Petrogenetic grid, facies series and the geothermal gradient. Fortschr. Miner., 47, 65-76.

RICKARD, M.J., 1961: A note on cleavages in crenulated rocks. Geol. Mag., 98, 324-332.

ROBERTSON, R.S., 1972: Petrological and structural investigation of Willyama Complex rocks, Wiperaminga Hill area, South Australia. Unpubl. B.Sc.(Hons) thesis, Univ. Adelaide.

SHARMA, R.S. and NARAYAN, B., 1974: Wollastonite paragenesis in a regional metamorphic terrain southeast of Beawar, Rajasthan, India. Neues Jb. Miner. Mh., (12), 561-569.

SIDDANS, A.W.B., 1972: Slaty cleavage - a review of research since 1815. Earth-Sci. Rev. 8, 205-232.

SPRIGG, R.C., 1954: Geology of the Radium Hill mining field. Bull. geol. Surv. S. Aust., 30, 7-50.

TALBOT, J.L., 1962: A study of the structural and metamorphic relationships between older and younger Precambrian rocks in the Mount Lofty-Olary Arc, South Australia. Unpubl. Ph.D. thesis, Univ. Adelaide.

TALBOT, J.L., 1967: Subdivision and structure of the Precambrian (Willyama Complex and Adelaide System), Weekeroo, South Australia. Trans. R. Soc. S. Aust., 91, 45-58.

THOMSON, B.P., 1969: The Precambrian basement cover - the Adelaide System. In, Parkin, L.W. (Ed.): Handbook of South Australian Geology. Geol. Surv. S. Aust., Adelaide.

THOMSON, B.P., COATS, R.P., MIRAMS, R.C., FORBES, B.G., and DALGARNO, C.R., 1964: Precambrian rock groups in the Adelaide Geosyncline. A new subdivision. Q. geol. Notes geol. Surv. S. Aust., 9, 1-19,

TURNER, F.J., 1968: Metamorphic Petrology: Mineralogical and Field Aspects. McGraw-Hill, New York.

TURNER, F.J. and WEISS, L.E., 1963: Structural Analysis of Metamorphic Tectonites. McGraw-Hill, New York.

VERNON, R.H., 1961: Banded albite rich rocks of the Broken Hill district, New South Wales. Mineragr. Invest. tech. Pap. C.S.I.R.O. Aust., 3.

von PLATEN, H., 1965: Kristallisation granitischer Schmelzen. Contr. Mineral. and Petrol., 11, 334-381.

von PLATEN, H. and HOLLER, H., 1966: Experimentelle Anatexis des Stainzer Plattengneises von der Koralpe, Steiermark, bei 2, 4, 7 und 10 Kb H_2O - Druck. Neues Jb. Miner. Abh., 106, 106-130.

WATERHOUSE, J.D., 1971: The geology of the Ethiudna and Walparuta Mine areas, Olary Province, South Australia. Unpubl. B.Sc.(Hons) thesis, Univ. Adelaide.

WATSON, J., 1967: Evidence of mobility in reactivated basement complexes. Proc. Geol. Assoc., 78, 211-235.

WHITTLE, A.W.G., 1949: The geology of the Boolcoomata Granite. Trans. R. Soc. S. Aust., 72, 228-243.

WILLIAMS, P.F., 1967: Structural analysis of the Little Broken Hill area, New South Wales. J. geol. Soc. Aust., 14, 317-331.

WINKLER, H.G.F., 1967: Petrogenesis of Metamorphic Rocks. Revised Second Edition. Springer-Verlag, New York.

WOOD, D.S., 1973: Patterns and magnitudes of natural strain in rocks. Phil. Trans. R. Soc. Lond., Ser. A., 274, 373-382.

TABLES

TABLE 2.1

Sequences in the Willyama Complex Schists in the Old Boolcoomata Area

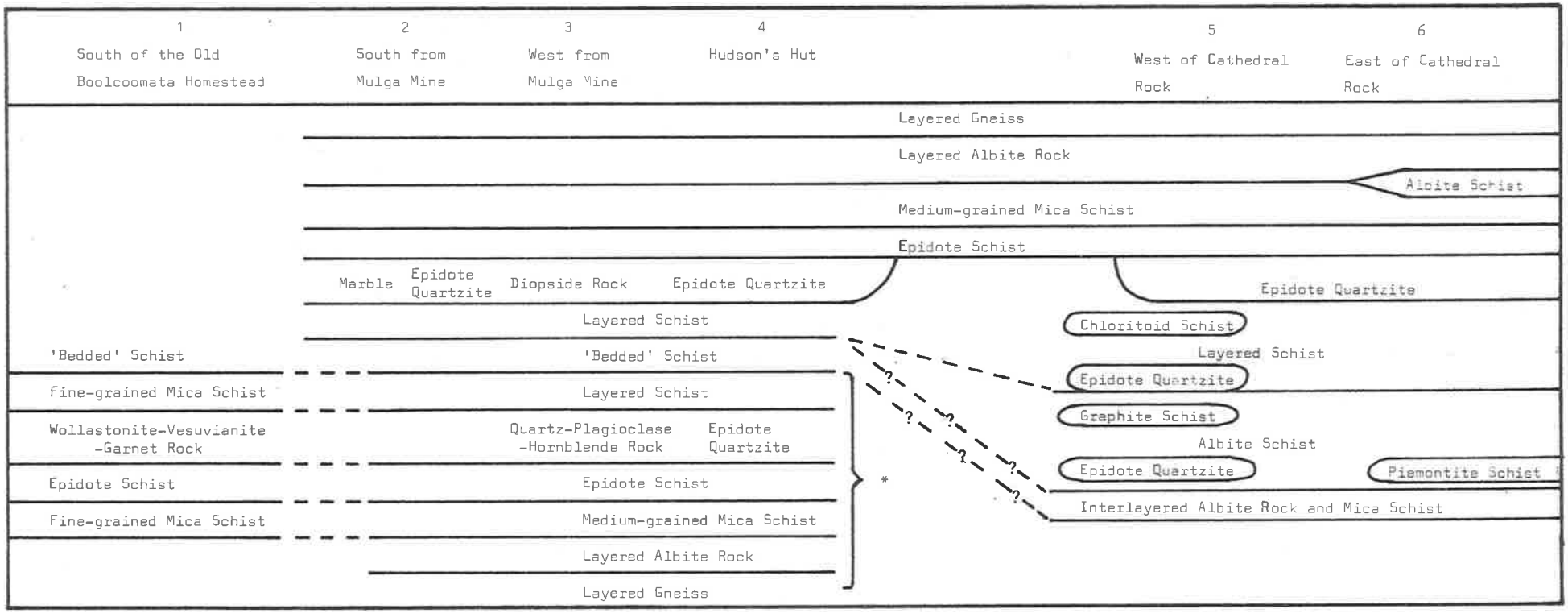

* Repetition due to first generation folding

See Fig. 2.1 for location of traverses 1 to 6

TABLE 2.2

Campana and King, (1958) (sequence inverted)	Talbot, (1967)	Pitt, (1971)	Parker, (1972)	Rock Names in this Study
Weekeroo-Billeroo Schists	Bedded mica schist	Bedded mica schist	Not present	Not present
				'Bedded' Schist Interlayered Albite Rock and Mica Schist Albite Schist Graphite Schist
	mica schist	mica schist	mica schist	Layered Schist including Chloritoid Schist
Ethiudna Calcsilicate Group	Not present	Ethiudna Calcsilicates	Ethiudna Calcsilicates	Calcareous Rocks
				Epidote Schist Medium-grained Mica Schist Layered Albite Rock
Qutalpa Quartzites	layered gneiss	layered gneiss and schists	layered gneiss and schists (with migmatite and quartzite)	Layered gneiss

TABLE 2.3

COMPARISON OF FEATURES OF BASEMENT SCHISTS AND COVER SLATES

	Basement Schists adjacent to the MacDonald Fault	Cover Slates
Rock type	schist - but some are fine-grained	mainly slate, cut grade into schists in places
Bedding	generally not easily discernable	generally present but not easily discernable where cleavage is strongly developed
Pebbles	absent	present in some beds
Metamorphism	middle amphibolite facies retrograde to greenschist facies	biotite grade
Minerals present	muscovite-biotite-quartz ±chlorite ±garnet	muscovite-biotite-quartz ±carbonate
Grain size	generally medium to coarse, but may be fine-grained	generally fine-grained but may be medium-grained
Foliation	usually well-developed, but not strong in fine-grained schists	present, but only strongly developed where micas are coarse-grained
Pegmatites	present, but not pervasive	absent

TABLE 3.1

CORRELATION OF COVER UNITS

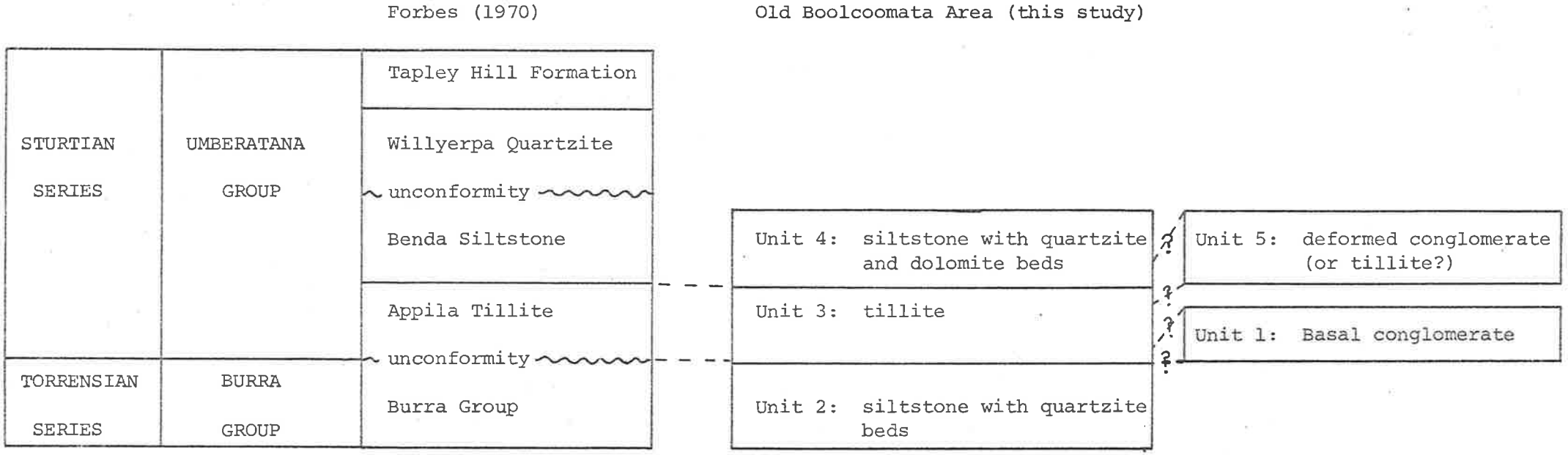

TABLE 4.1

STRUCTURAL ELEMENTS IN THE BASEMENT ROCKS

S_{OB}	Lithological layering in basement rocks defined by compositional layerings which are independent of the orientation of foliation.
S_{1B}	First generation foliation defined by the alignment of biotite grains parallel to the axial plane of first generation folds.
S_{2B}	Second generation foliation parallel to the axial plane of second generation folds. This is generally the most prominent foliation in the area and is defined by the alignment of micas in schists and gneisses.
S_{3B}	Third generation foliation parallel to the axial plane of third generation folds. This foliation is defined by the axial plane of crenulations in S_{2B}.
$B^{S_{2B}}_{S_{0B}}$	Second generation folds in which lithological layering (S_{OB}) is folded and second generation schistosity (S_{2B}) is parallel to the axial plane.
$B^{S_{3B}}_{S_{0,2B}}$	Third generation folds in which both lithological layering (S_{OB}) and second generation schistosity (S_{2B}) are folded and third generation crenulation foliation (S_{3B}) is parallel to the axial plane.
$B^{S_{3B}}_{S_{2B}}$	Crenulations of second generation schistosity (S_{2B}).

TABLE 5.1

STRUCTURAL ELEMENTS IN THE COVER ROCKS

S_{OC}	Bedding in cover rocks.
S_{1C}	Slaty cleavage and schistosity defined by the alignment of micas parallel to the axial plane of first generation folds in cover rocks.
S_{2C}	Crenulation foliation parallel to the axial plane of second generation folds in cover rocks.
$B^{S_{1C}}_{S_{0C}}$	First generation folds in the cover which fold bedding (S_{OC}) and have slaty cleavage (S_{1C}) parallel to the axial plane.
$B^{S_{2C}}_{S_{1C}}$	Crenulations of slaty cleavage in cover rocks.

TABLE 6.1

STRAIN ESTIMATIONS

Specimen	Fig.	Face	Pebble Type	Number	Initial Fabric	Angle between principal extension & foliation	R_s
Unit 1a							
loc. 050065	6.1a	horizontal	granite	19			1
	6.1b	10°-120	granite	20			1
Unit 1b							
054065	6.1c	90°-135	quartzo-feldspathic	21			1
Unit 3							
033020	6.15a	18°-186	quartzo-feldspathic	50	Unimodal	0	2.0
	6.15b	87°-080	"	28	Unimodal	10°	2.0
035018	6.15c	58°-250	quartzo-feldspathic	50	Unimodal		1.7
A470-055	6.15d	⊥ foliation	"	40	bimodal, 90° between maxima	5°	1.2
	6.15e	// foliation	"	52	bimodal		1.4
	6.15f	⊥ foliation	"	50	bimodal, 60° between maxima	0°	1.2
	6.15g	⊥ foliation	schist	30	Unimodal	10°	4.0
	6.15h	⊥ foliation	schist	33	Unimodal	0	4.5
A470-056	6.15i	⊥ foliation	quartzo-feldspathic	58	bimodal	0	2.0
	6.15j	// foliation	"	60	bimodal		1.75
	6.15k	⊥ foliation	"	50	bimodal, 80° between maxima		1.8
A470-057	6.15l	⊥ foliation	"	65	bimodal	5°	
	6.15m	// foliation	"	50	bimodal		
	6.15n	⊥ foliation	"	54	bimodal	0°	
A470-578	6.15o	// foliation	quartzo-feldspathic	60	bimodal		1
	6.15p	⊥ foliation	"	48	bimodal	10°	1.2
	6.15q	⊥ foliation	schist	43	bimodal	12°	4.5
	6.15r	⊥ foliation	schist	34	unimodal	10°	6.5
Unit 5							
A470-065	6.16a	⊥ foliation	quartzo-feldspathic	68	Unimodal	0°	3.3
	6.16b	⊥ foliation	"	70	Unimodal	5°	3.3
	6.16c	// foliation	"	50	Unimodal		1.6
loc. 055061	6.16d	horizontal	"	50	bimodal		2.5
	6.16e	55°-085	"	57	Unimodal	5°	4.5
Basement							
A470-071	6.17a	⊥ foliation	porphyroblasts	68	bimodal	25	2.7
	6.17b	⊥ foliation	"	73	random	15	2.0
	6.17c	// foliation	"	76	modified by later deformation		

TABLE 6.2

Estimates of strain ratios for tillite (Unit 3) from strain ratios of component pebbles

	A470-055 face 1	A470-055 face 3	A470-058 face 3
R_{SCH} =	$\frac{0.9}{\frac{\mu_{QF}}{\mu_{SCH}} - 7.6}$	$\frac{10.8}{\frac{\mu_{QF}}{\mu_{SCH}} - 8.2}$	$\frac{13.8}{\frac{\mu_{QF}}{\mu_{SCH}} - 10.3}$
R_{QF} =	$\frac{1.2}{0.14 - \frac{\mu_{SCH}}{\mu_{QF}}}$	$\frac{1.2}{0.12 - \frac{\mu_{SCH}}{\mu_{QF}}}$	$\frac{1.4}{0.1 - \frac{\mu_{SCH}}{\mu_{QF}}}$
Assuming $\frac{\mu_{SCH}}{\mu_{QF}} = \frac{1}{\mu_{QF}/\mu_{SCH}}$, R_{QF} =	$\frac{1.2(\mu_{QF}/\mu_{SCH})}{0.14(\mu_{QF}/\mu_{SCH})-1}$	$\frac{1.2(\mu_{QF}/\mu_{SCH})}{0.12(\mu_{QF}/\mu_{SCH})-1}$	$\frac{1.4(\mu_{QF}/\mu_{SCH})}{0.1(\mu_{QF}/\mu_{SCH})-1}$
Assuming $R_{SCH} < 1$, R_{QF} =	10-14	12-18	15-24
From Gay, 1968, fig. 10, R_{MQF} =	3.5-7.0	4.0-6.0	10-20
R_S from quartzofeldspathic pebbles ≃	1.6	2.5	3.6
Assuming $R_{SCH}<1$, R_{MSCH} ≃	1	1	0.6
R_S from schist pebbles ≃	3.0	3.3	4.5

TABLE 7.1

MINERAL ASSEMBLAGES

ROCK TYPE	HIGH GRADE	INDETERMINABLE	LOW GRADE
Fine-grained Mica Schist A470-001		quartz-muscovite-biotite ±albite	
Medium-grained Mica Schist A470-003		quartz-muscovite-biotite-microcline	
A470-004		quartz-muscovite-biotite-albite	
Layered Schist A470-007	adalusite-biotite-muscovite-quartz		
A470-006	sillimanite-muscovite-garnet-quartz		chlorite-muscovite-quartz
Chloritoid Schist A470-009			chlorite-chloritoid-muscovite-quartz ±almandine?
Epidote Schist A470-010		muscovite-biotite-quartz-epidote ±garnet	chlorite
Piemontite Schist A470-013			quartz-piemontite-biotite-garnet
Epidote Quartzite A470-014		quartz-epidote-biotite	quartz-epidote-chlorite-calcite
Quartz-Plagioclase-Hornblende Rock A470-016	plagioclase-hornblende-quartz		
Diopside Rock A470-017	diopside-quartz		
Wollastonite-Vesuvianite-Garnet Rock A470-019	wollastonite-quartz-epidote-vesuvianite-garnet ±diopside		
Marble A470-018			calcite-chlorite-talc
Albite rocks A470-018			albite-actinolite-chlorite-calcite-quartz
Layered Gneiss A470-026	plagioclase-biotite-quartz		
A470-027	microcline-biotite-quartz-muscovite		
Corundum-Biotite-Plagioclase Rock A470-030	corundum-biotite-albite-muscovite		
Amphibolite A470-049	hornblende-plagioclase ±epidote		
Cover A470-081			quartz-biotite-muscovite-dolomite
A470-082			quartz-albite-muscovite-biotite
A470-083			quartz-muscovite-biotite-±chlorite

TABLE 8.1

Summary of geological events in the Old Boolcoomata Area

Approximate Absolute Age		Basement	Cover
		Deposition of sediments	
1700 m.y.	D_1/M_1	Deformation and metamorphism of above sedimentary rocks, production of pegmatites, Granitic Gneiss and Older Migmatites and metasomatism to form albite-rich rocks.	
		intrusion of basic dykes	
1580 m.y.	D_2/M_2	Deformation and metamorphism: production of Boolcoomata Adamellite, Younger Migmatites and pegmatites.	
		uplift and erosion	
1000 m.y.			deposition
500 m.y.	D_3/M_3	Deformation and retrograde metamorphism.	Deformation and prograde metamorphism. Faulting.

FIGURES

Fig. 1.1a Regional geological map of the Olary Province compiled from mapping by Campana and King (1958), Talbot (1967), Berry (1973) and the present study.

Willyama Complex - red; Adelaide system - brown.

Areas outlined:

1. The Old Boolcoomata Area examined in this study.
2. Doughboy Well area mapped by Berry (1973) and Flint (1974).
3. Whey Whey Creek or Weekeroo Area investigated by Talbot (1962, 1967).

Fig. 1.1b Locality map of the Olary Province of South Australia.

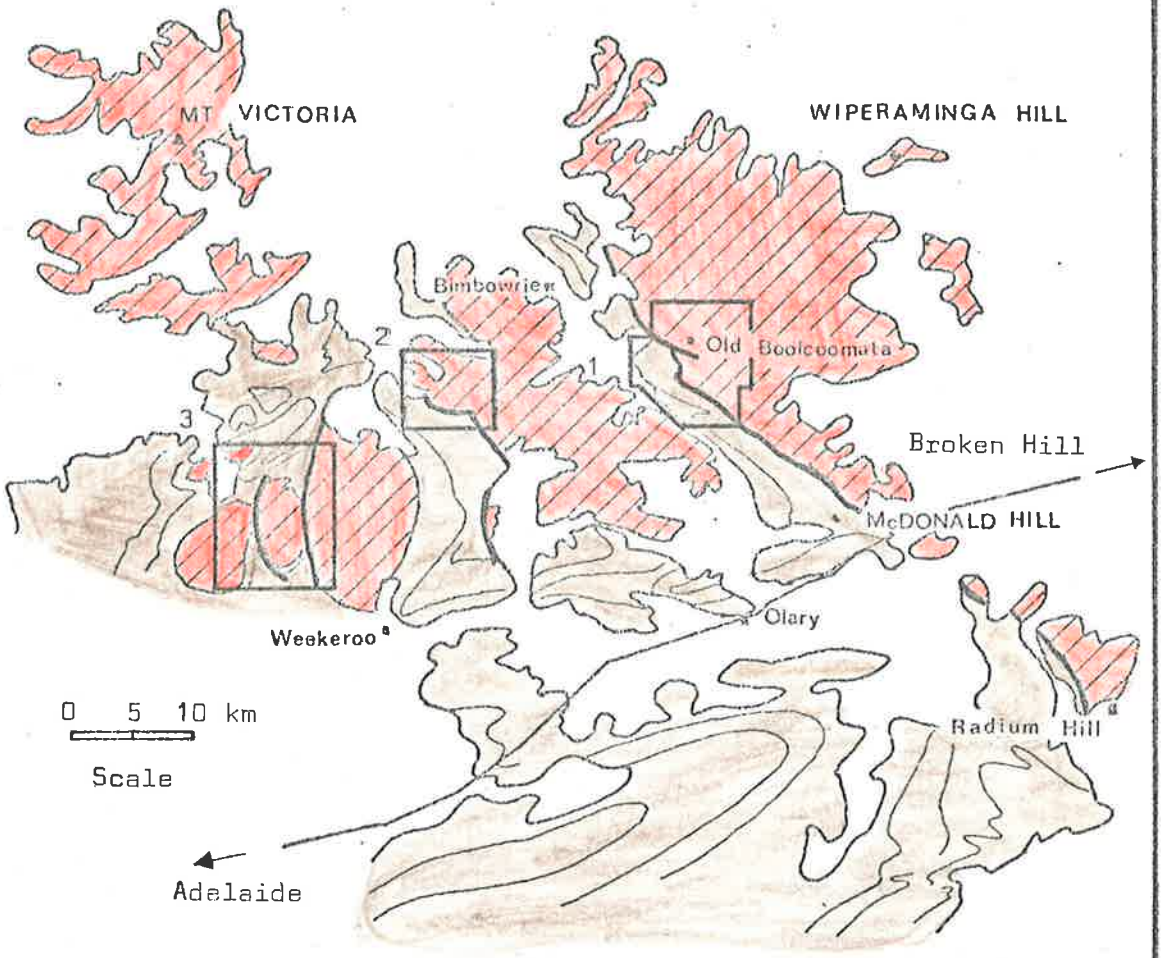

Fig. 1.1a

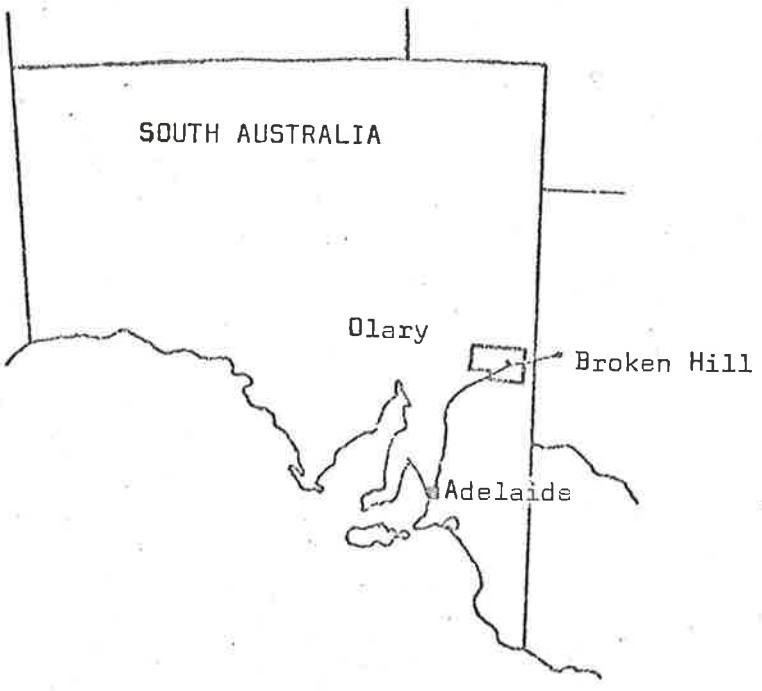

Fig. 1.1b

Fig. 2.1 Geological Map of the Old Boolcoomata Area, South Australia.

(In back pocket)

Fig. 2.2 Cross bedding in quartzite layers in "Bedded" Schist, south of the Old Boolcoomata Homestead.

Lens cap 50 mm in diameter.

Fig. 2.3 Layered Schist showing strongly developed schistosity (S_{2B}) with mica-rich layers bifurcating around quartz-rich lenses.

(A470-005)

Field of view, 12 cm.

Fig. 2.4 Remnants of andalusite (dary grey) poikiloblastically enclosing quartz in porphyroblast which has been almost completely replaced by fine-grained muscovite (light grey). The inclusions of quartz outline curved trails in the poikiloblast which is aligned parallel to the second generation schistosity.

(A470-007)

Field of view 9 mm; crossed polars.

Fig. 2.5 Muscovite porphyroblast in Layered Schist. Schistosity (S_{2B}) is curved around the muscovite porphyroblast which has basal cleavage oblique to the schistosity.

(A470-006)

Field of view 8 mm; plane polarised light.

Fig. 2.2

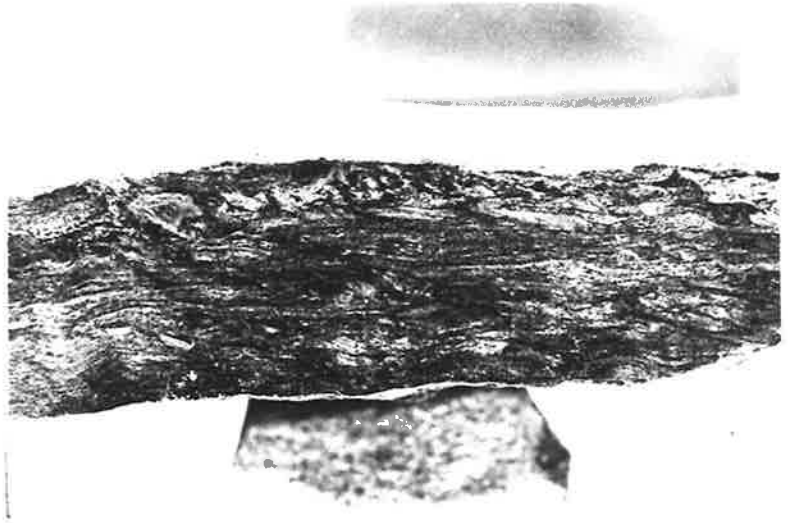

Fig. 2.3

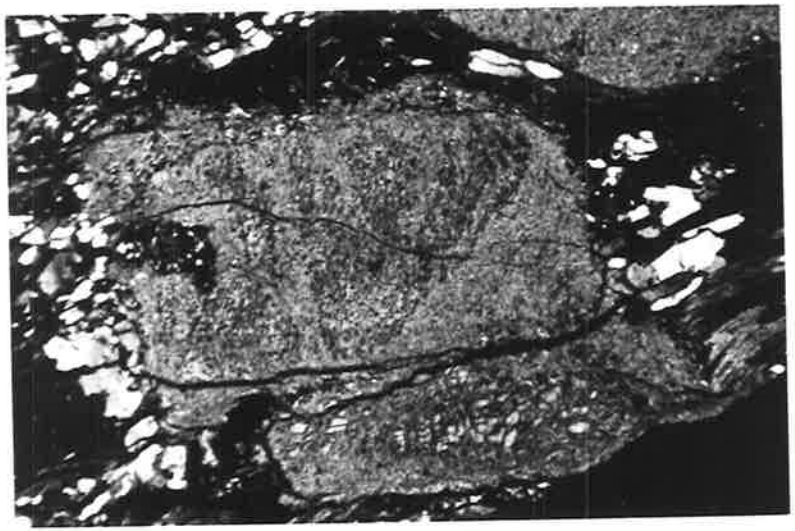

Fig. 2.4

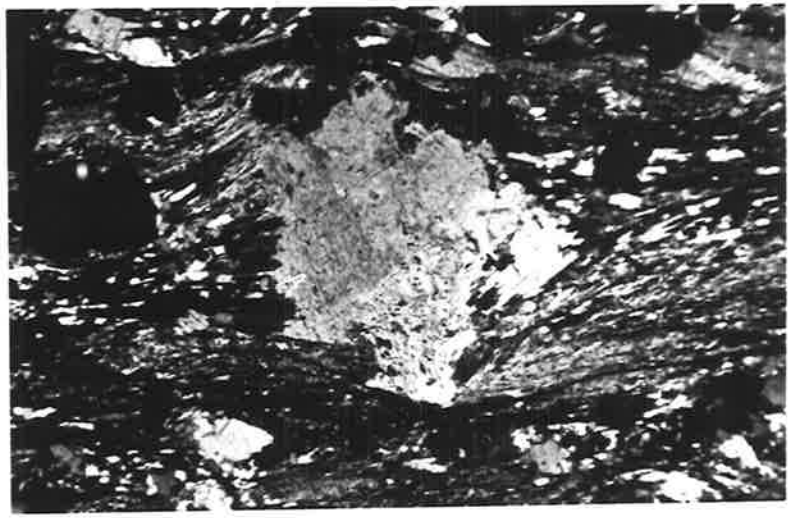

Fig. 2.5

Fig. 2.6 Sillimanite needles in muscovite porphyroblast in Layered Schist.

(A470-073)

Field of view 0.7 mm; plane polarised light.

Fig. 2.7 Chlorite grains oblique to schistosity in a lense elongate parallel to schistosity (S_{2B}) in Layered Schist.

(A470-066)

Field of view 15 mm; crossed polars.

Fig. 2.8 Chloritoid (showing multiple twinning) cross cutting schistosity, S_{2B} in Chloritoid Schist.

(A470-009)

Field of view 4 x 2.5 mm; crossed polars.

Fig. 2.9 Diopside crystals in Diopside Rock, west of Mulga Mine.

Pen 130 mm long.

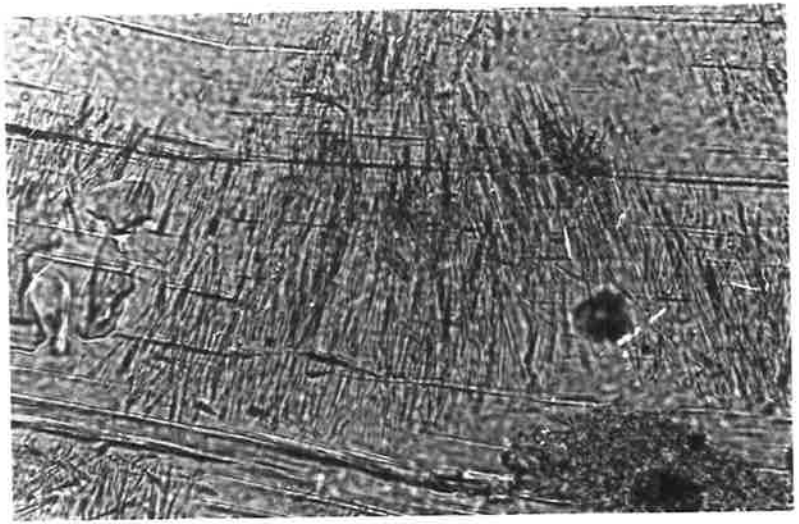

Fig. 2.6

Fig. 2.7

Fig. 2.8

Fig. 2.9

Fig. 2.10 Typical outcrop of Wollastonite-Vesuvianite-Garnet Rock showing layers with garnet porphyroblasts (standing out on weathered surfaces) and layers containing vesuvianite and wollastonite (smooth surfaces).

Hammer 30 cm long.

Fig. 2.11 Layered Albite Rock (foreground) with 'spots' of actinolite passing to non-layered, foliated albite rock with foliation oblique to the layering in the adjacent Layered Albite Rock.

Field of view 1 m wide.

Fig. 2.12 Layered Gneiss showing layers rich in biotite (dark) and quartzo-feldspathic layers (light).

(A470-075)

Field of view 5 cm.

Fig. 2.13 Biotite laminations in quartz-rich layer of Layered Gneiss showing 'pseudo-cross bedding'.

(A470-076)

Field of view 10 cm.

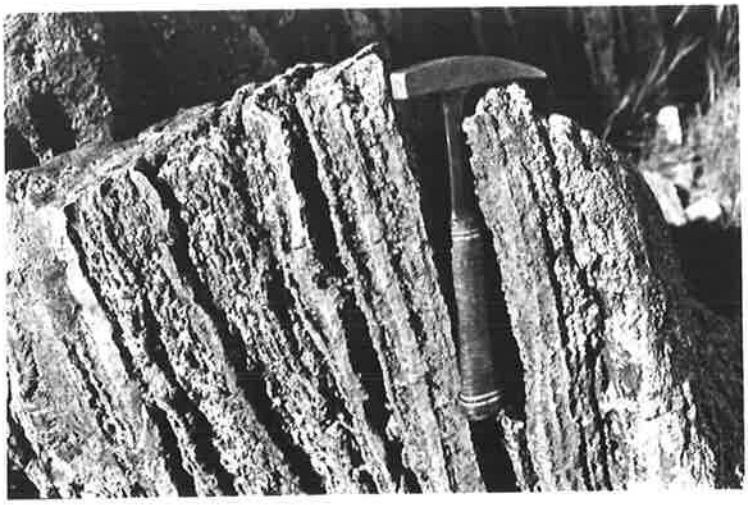

Fig. 2.10

Fig. 2.11

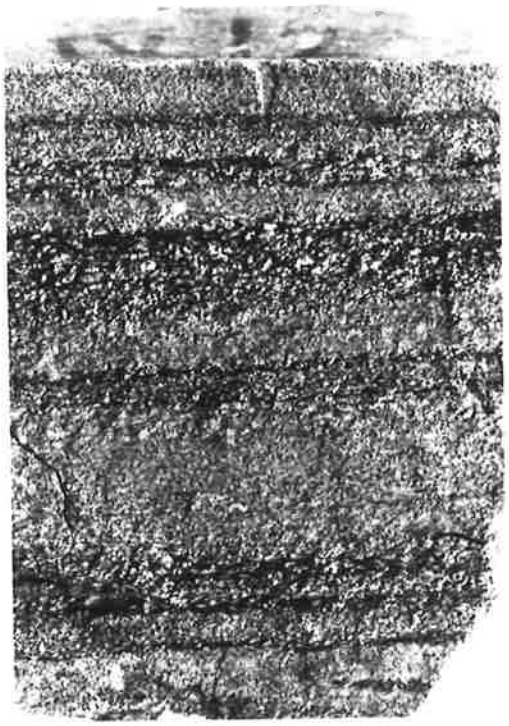

Fig. 2.12

Fig. 2.13

Fig. 2.14 Pegmatitic vein parallel to lithological layering in Layered Gneiss.

Hammer handle 15 cm long.

Fig. 2.15 Microcline poikiloblast enclosing small grains of quartz and albite.

(A470-028)

Field of view 1 mm; crossed polars.

Fig. 2.16 Corona of muscovite (single large grain showing basal cleavage) surrounding corundum (high relief) and surrounded by albite (showing multiple twinning).

(A470-029)

Field of view 3 mm; crossed polars.

Fig. 2.17 Regularly layered neosome of the Older Migmatite showing albite-rich (light) and biotite-rich (dark) layers.

Hammer 30 cm long.

Fig. 2.14

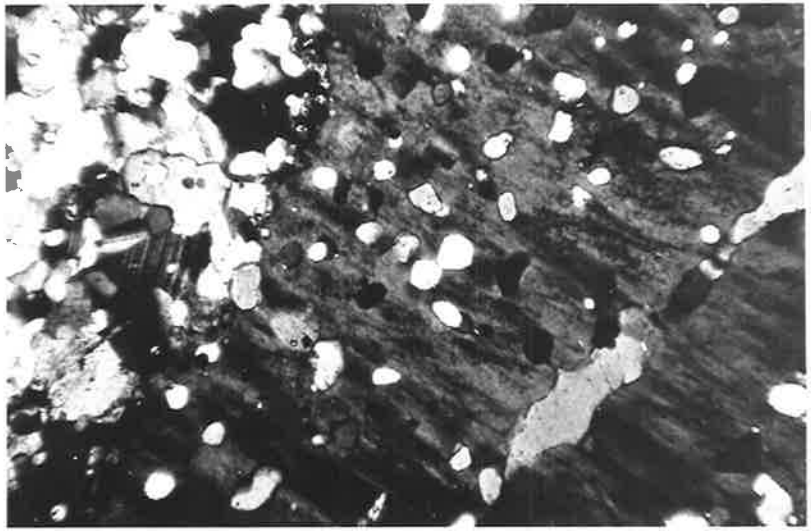

Fig. 2.15

Fig. 2.16

Fig. 2.17

Fig. 2.18 Contact between palaeosome and neosome in Older Migmatite. The palaeosome (below hammer head) has regular layering. In the neosome the layering is irregular.

Hammer 30 cm long.

Fig. 2.19 Regularly layered palaeosome (lower left and centre right) passing into 'chaotic' neosome (centre). Adjacent to the palaeosome, regular layering can be seen in the neosome.

Field of view 2 m.

Fig. 2.20 Coarse-grained neosome interlayered with fine-grained albite-rich palaeosome.

Hammer 30 cm long.

Fig. 2.21 Biotite-rich layers in coarse-grained neosome parallel to layering in palaeosome.

Hammer 30 cm long.

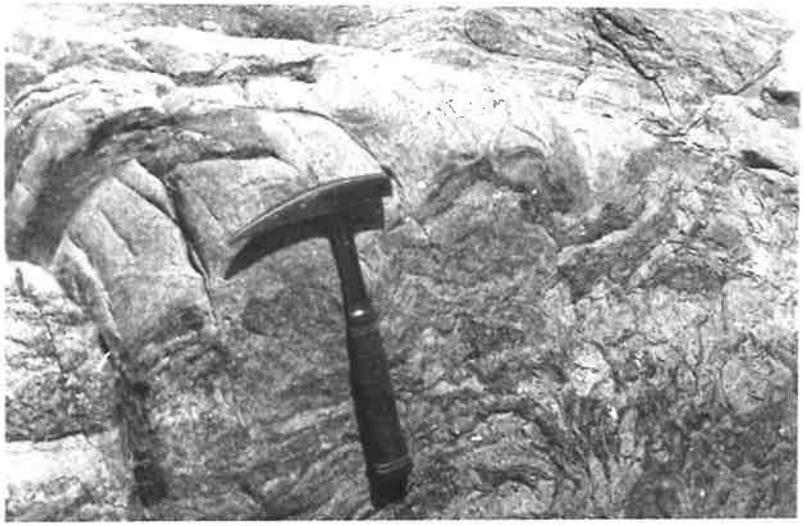

Fig. 2.18

Fig. 2.19

Fig. 2.20

Fig. 2.21

Fig. 2.22 Contact between Boolcoomata Adamellite (coarse-grained) and albite-quartz-muscovite rock (fine-grained).

Match 4.5 cm long.

Fig. 2.23 Veins of pegmatite consisting of quartz and microcline in Boolcoomata Adamellite.

Hammer 30 cm long.

Fig. 2.24 Ptygmatic folding in Younger Migmatite.

Hammer 30 cm long.

Fig. 2.25 Detail of portion of Fig. 2.24 showing folding of quartzo-feldspathic layer (light) and biotite-rich layers (dark) of Younger Migmatite.

Lens cap 50 mm diameter.

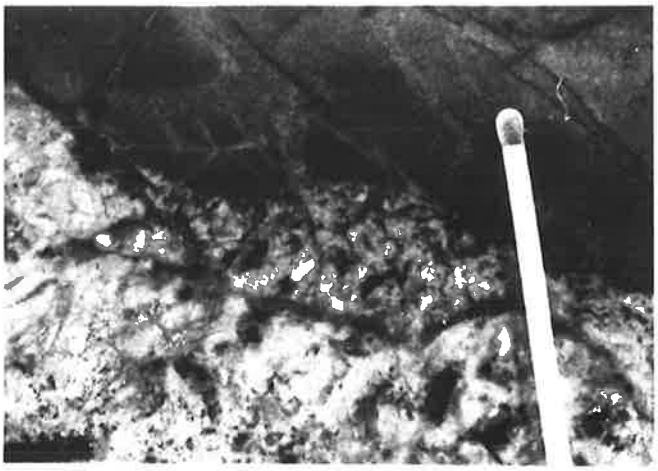

Fig. 2.22

Fig. 2.23

Fig. 2.24

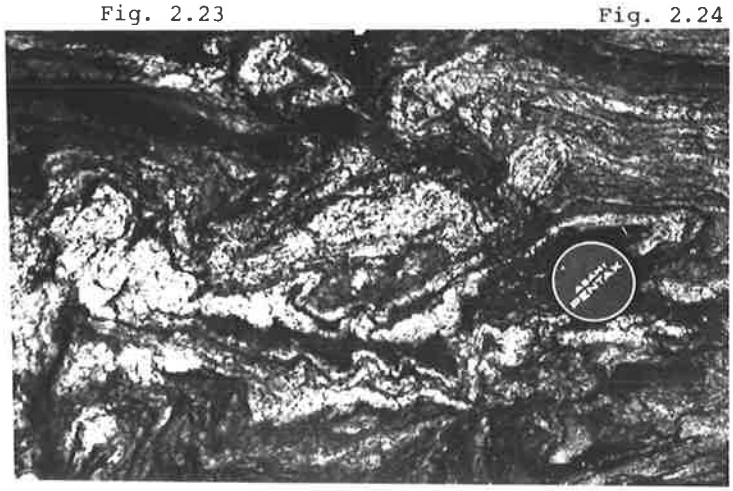

Fig. 2.25

Fig. 2.26 Cathedral Rock looking west. Right peak is composed of breccia with diopsidic matrix and left peak is composed of breccia with albitic matrix.

Fig. 2.27 Breccia with diopsidic matrix - fragments are composed of fine-grained albite rock.

Lens cap 50 mm diameter.

Fig. 2.28 Breccia with diopsidic matric (dark) showing irregular nature of the fragments.

(A470-052)

Field of view 50 mm.

Fig. 2.29 Albite Schist (light) with veins of diopside (dark), some veins parallel and others oblique to schistosity in the Albite Schist.

Lens cap 50 mm in diameter.

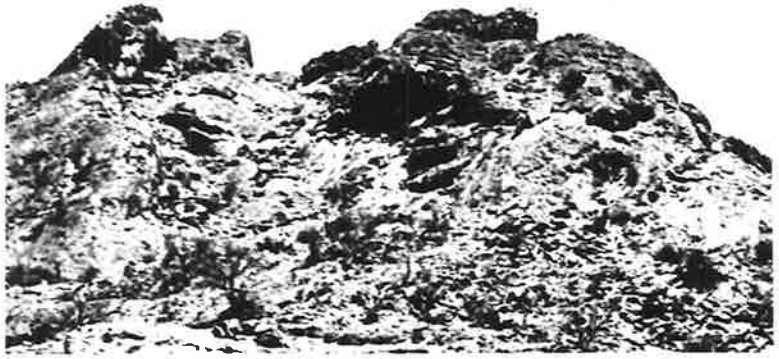

Fig. 2.26

Fig. 2.27

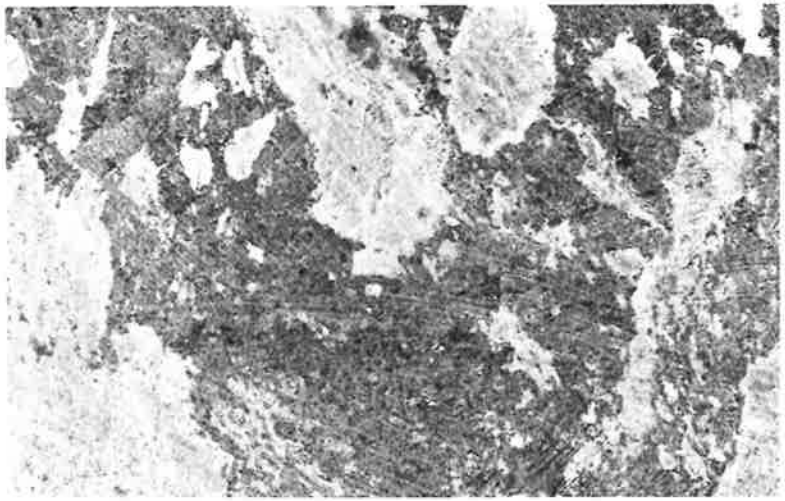

Fig. 2.28

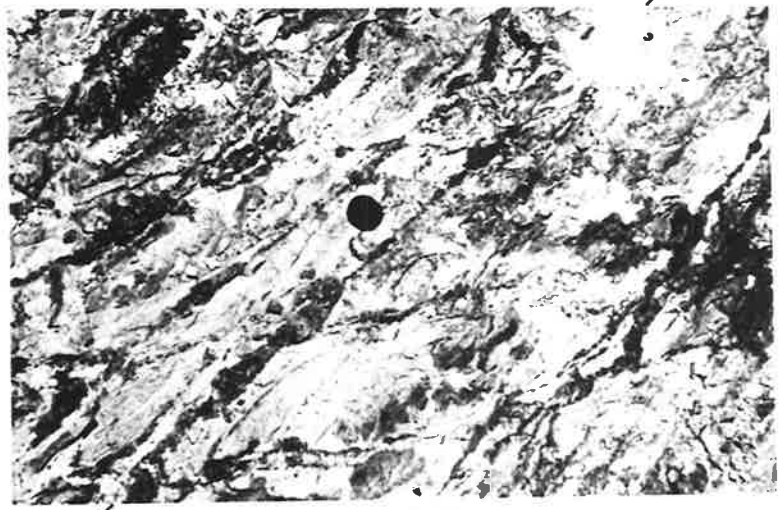

Fig. 2.29

Fig. 2.30 Blocks of layered albite rock in breccia with albitic matrix.

Hammer 30 cm long.

Fig. 2.31 Details of layered albite rock in breccia with albitic matrix showing slight folding of layering in some blocks.

Hammer 30 cm long.

Fig. 2.32 Folded block of layered albite rock in breccia with albitic matrix.

Hammer 30 cm long.

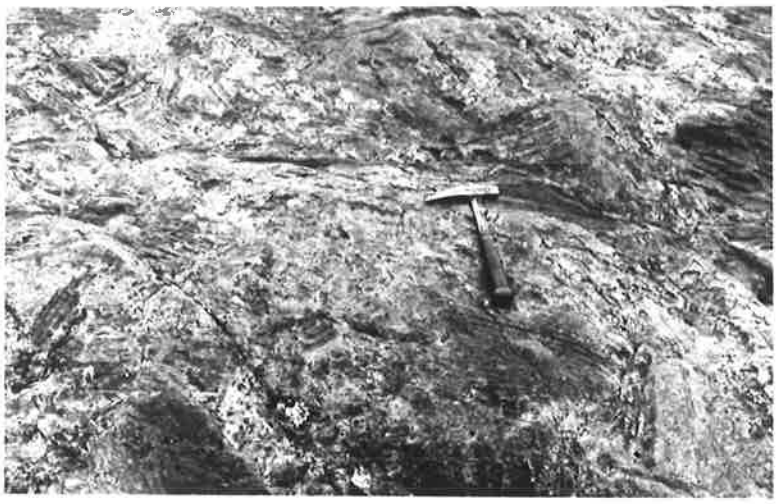

Fig. 2.30

Fig. 2.31

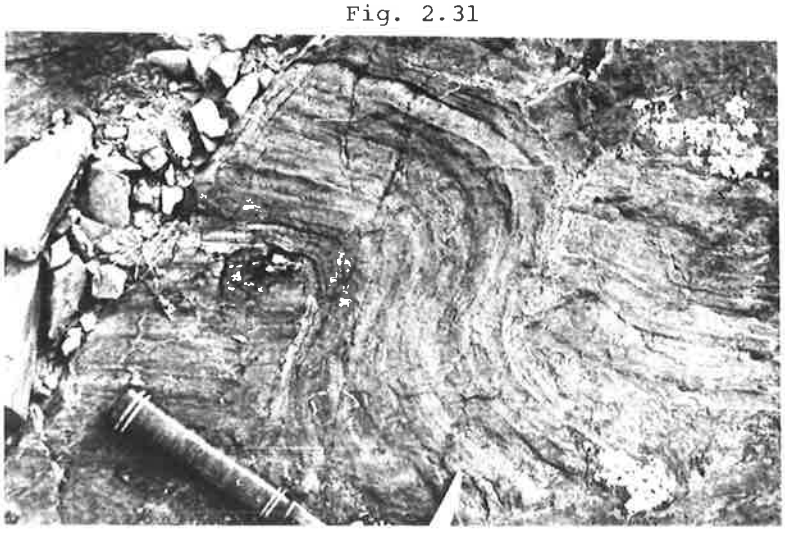

Fig. 2.32

Fig. 3.1 Conglomerate of Subunit 1a unconformably overlying Boolcoomata Adamellite. Bedding in the conglomerate is indicated by layers containing pebbles of similar sizes.

Hammer 75 cm long.

Fig. 3.2 Profile of folds in Units 3 and 4 in the southeast of the mapped area. Unit 3 is 2000 m thick in the hinge of the anticline, but is much thinner in the limbs.

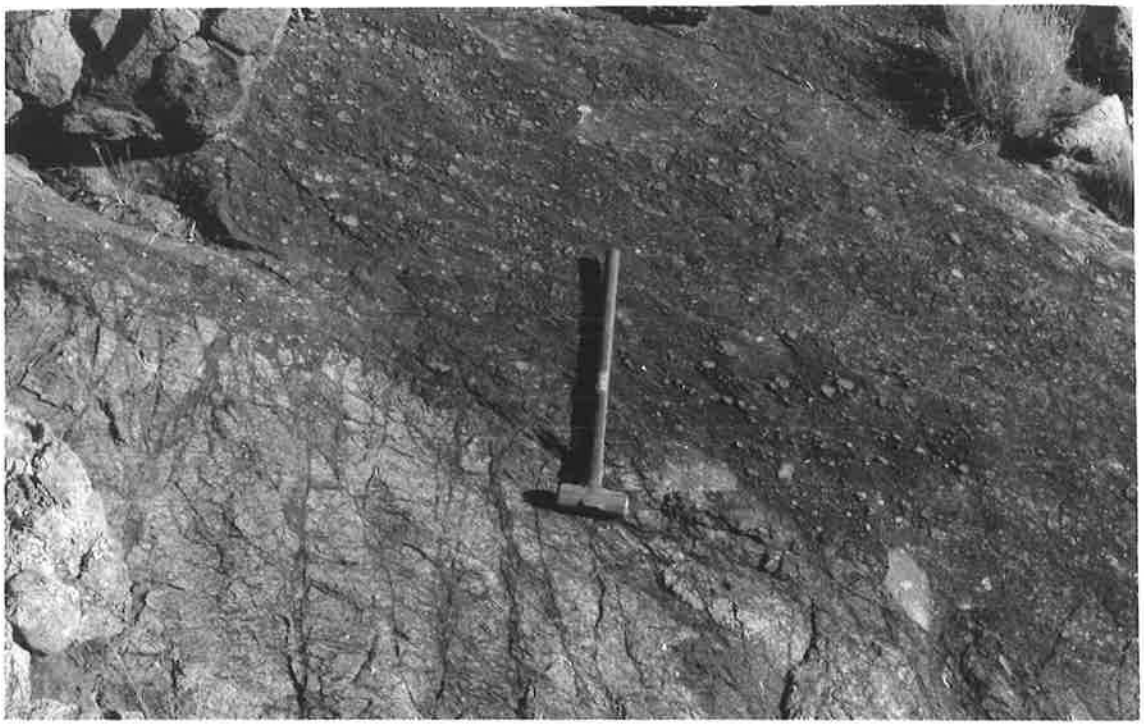

Fig. 3.1

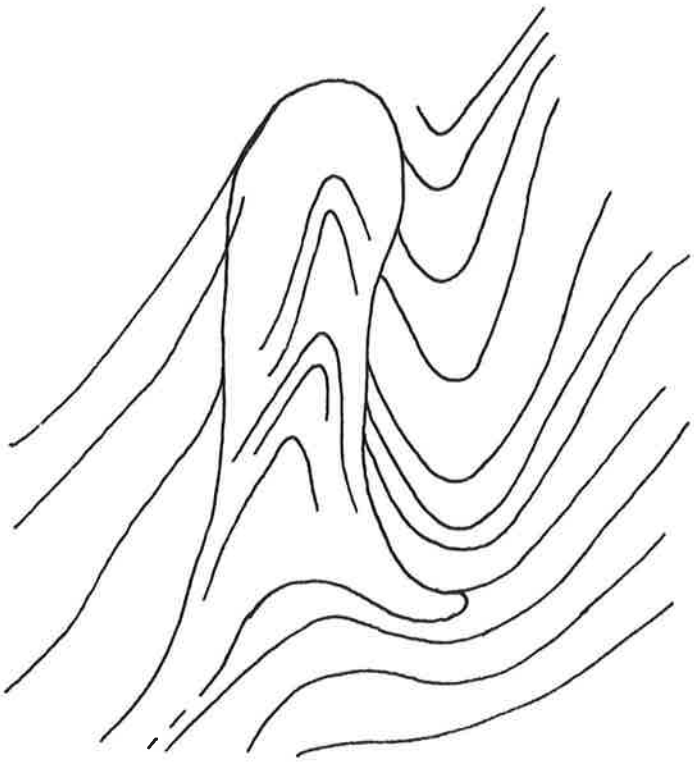

Fig. 3.2

Fig. 4.1 Interference pattern produced by the intersection of first, second and third generation folds. The axial trace of the first generation fold has been isoclinally folded by second generation folds and warped by third generation folds. Overprinting of first generation folds by second generation folds has produced type 2 interference patterns and overprinting by third generation folds has produced type 3 interference patterns.

Hammer 30 cm long.

Fig. 4.2a and 4.2b Details of type 2 interference patterns in Fig. 4.1, produced by the intersection of first and second generation folds. In the hinges of first generation folds, biotite is aligned parallel to first generation axial planes, but in the hinges of second generation folds, biotite is aligned parallel to second generation axial planes.

Fig. 4.3 Isoclinal second generation fold refolded by third generation fold. Biotite grains are aligned parallel to the axial plane of the/generation fold and have been crenulated by the third generation fold.

Lens cap 50 cm diameter.

Fig. 4.1

Fig. 4.2b

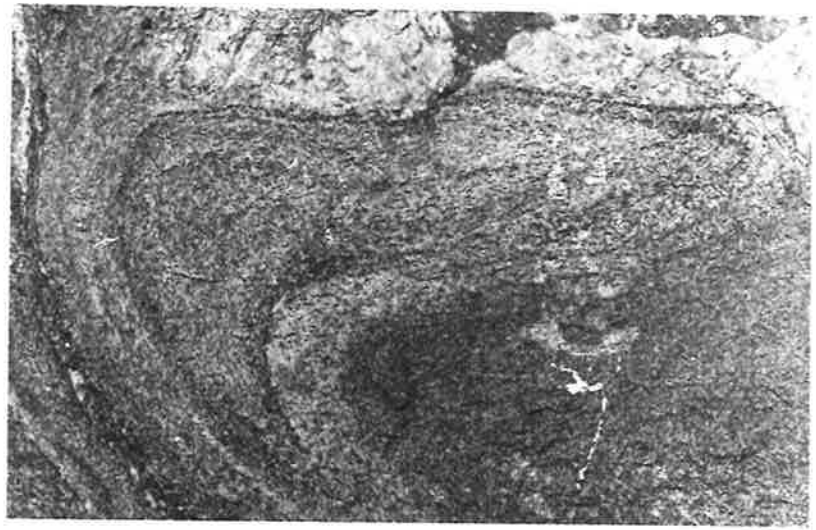

Fig. 4.2a

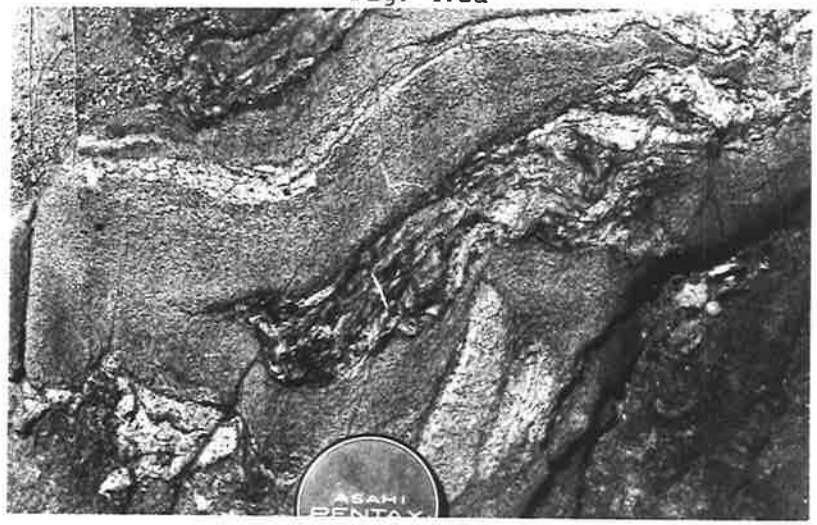

Fig. 4.3

Fig. 4.4 Isoclinal second generation fold in Epidote Schist with biotite grains aligned parallel to axial plane of fold.

Width of field 10 cm.

Fig. 4.5 Schistosity (S_{2B}) in Layered Schist showing mica-rich domains surrounding lenticular quartz grains and lenticular aggregates of quartz and chlorite in which the chlorite is aligned oblique to the main schistosity (S_{2B}).

(A470-066)

Width of field 25 mm; crossed polars.

Fig. 4.6 Schistosity curved around garnet porphyroblast in Chloritoid Schist.

(A470-009)

Field of view 1.0 mm; plane polarised light.

Fig. 4.7 Ellipsoidal aggregates of fine-grained muscovite, elongate parallel to second generation schistosity (S_{2B}) in schist. The aggregates are thought to have replaced original porphyroblasts.

(A470-071)

Scale in millimetres.

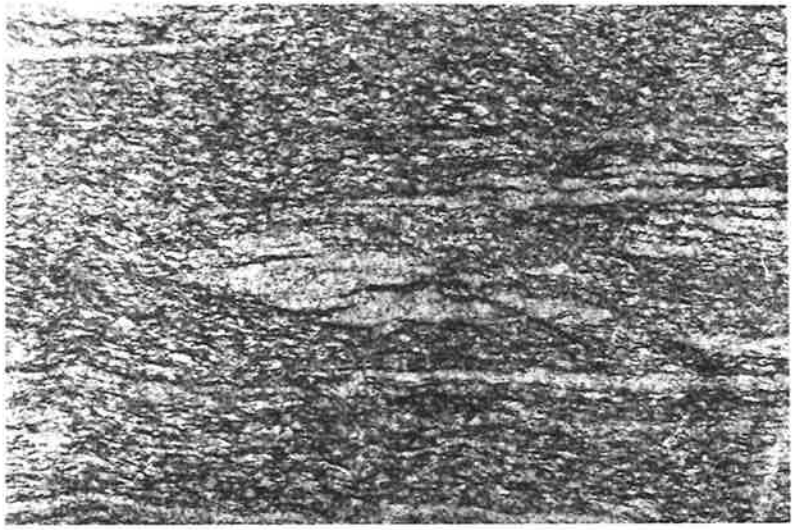

Fig. 4.4

Fig. 4.5

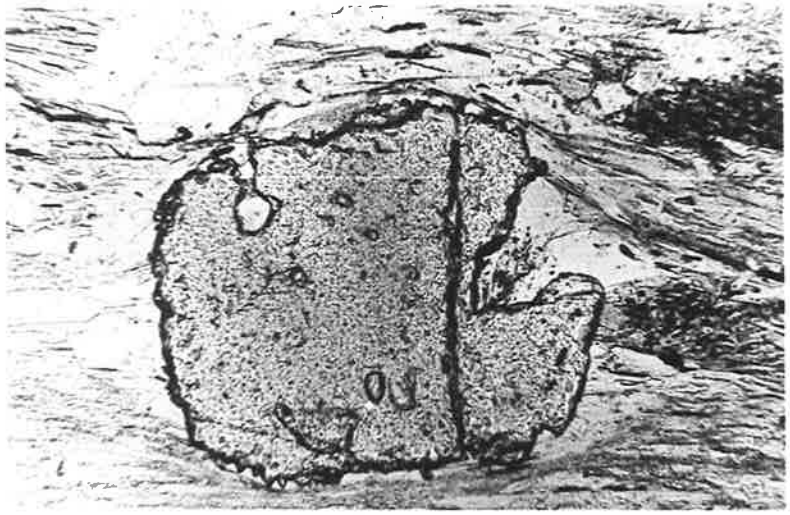

Fig. 4.6

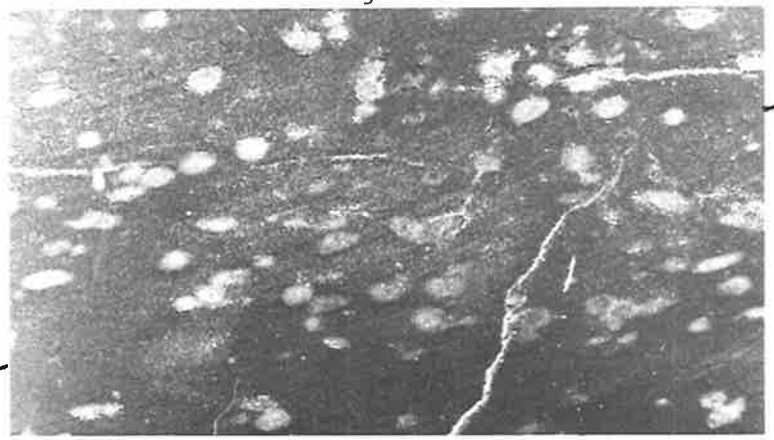

Fig. 4.7

Fig. 4.8 Schistosity (S_{2B}) surrounding lenticular aggregate of chlorite (dark) and quartz. The chlorite is aligned oblique to the schistosity (S_{2B}) in the rock.

(A470-009)

Field of view 5 mm; crossed polars.

Fig. 4.9 Tight asymmetric crenulations (axial plane, S_{3B}) folding second generation schistosity (S_{2B}) and producing lenticular aggregates of mica. In these lenses the basal cleavage of mica is oblique to the adjacent schistosity.

(A470-067)

Field of view 4 mm; crossed polars.

Fig. 4.10 Hornblende grains (dark) aligned defining a foliation (S_{2B}) oblique to the lithological layering (S_{OB}) in Quartz-Plagioclase-Hornblende Rock.

(A470-074)

Field of view 9mm; plane polarized light.

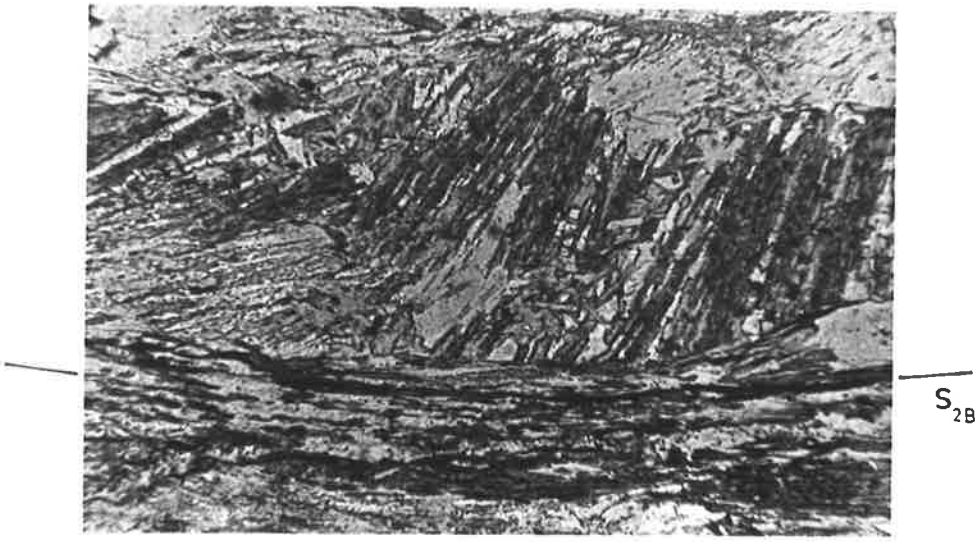

Fig. 4.8

Fig. 4.9

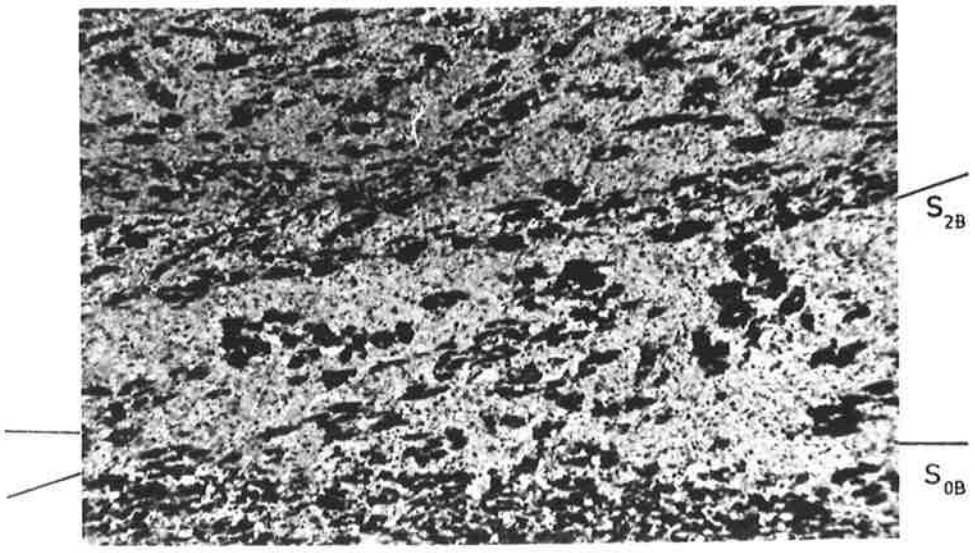

Fig. 4.10

Fig. 4.11 Isoclinal folds in Layered Gneiss showing extreme thickening in the hinge area.

Field of view 30 cm.

Fig. 4.12 Neosome of Older Migmatite displaying isoclinal second generation fold, folded by third generation fold to give a type 3 interference pattern. Biotite grains are aligned parallel to the axial of the second generation fold.

Pen 13 cm long.

Fig. 4.13 Ptygmatic folds in quartz vein in Epidote Schist.

Lens cap 5 cm in diameter.

Fig. 4.14 Ptygmatic folds in quartz vein showing boudinage of the vein in some limbs of the fold. The axial plane of the fold is parallel to the second generation schistosity in the enclosing Epidote Schist.

Field of view 15 cm.

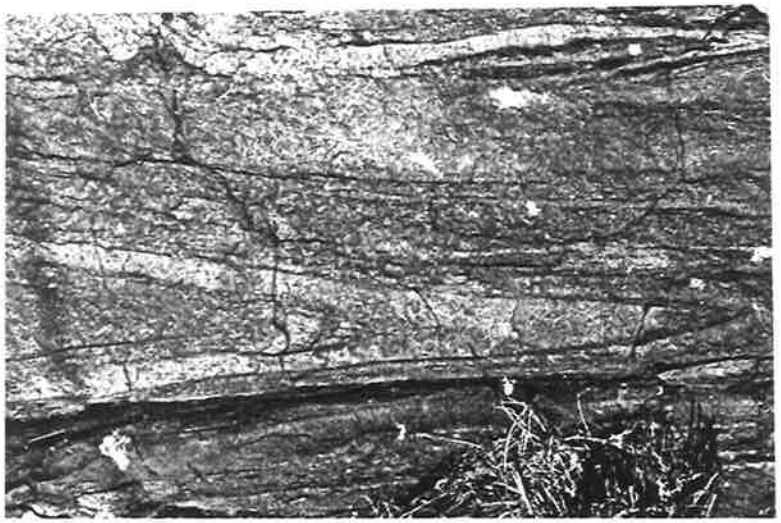

Fig. 4.11

Fig. 4.12

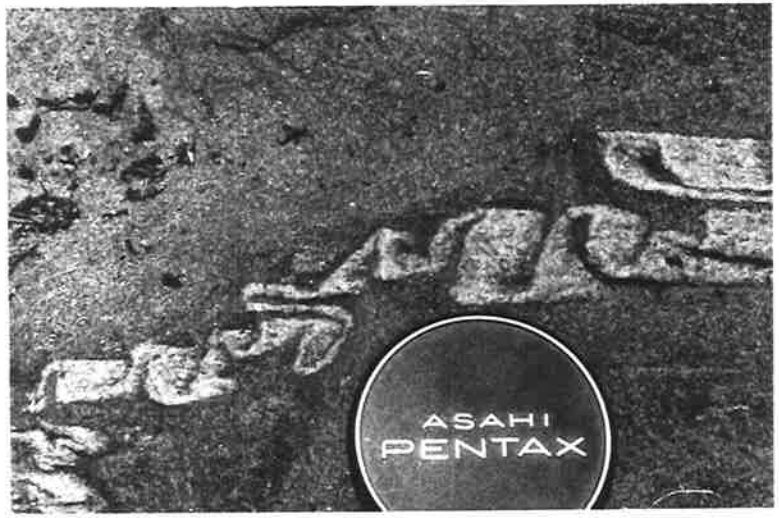

Fig. 4.13

Fig. 4.14

Fig. 4.15 Isoclinal fold in pegmatite showing boundinage in limb area.

Hammer 30 cm long.

Fig. 4.16 Details of boudins in Fig. 4.15 showing the 'blocky' nature of the boudins.

Hammer handle 15 cm long.

Fig. 4.17 Folds and 'pinch-and-swell' structure in pegmatite enclosed in Epidote Schist. Elongation indicated by 'pinch-and-swell' structure and axial plane of folds in pegmatite are parallel to schistosity (S_{2B}) in surrounding schists.

Scale 30 cm long.

Fig. 4.15

Fig. 4.16

Fig. 4.17

Fig. 4.18 Crenulations folding strongly developed schistosity (S_{2B}) in 'Bedded' Schist. Note the incipient development of a new foliation parallel to the axial plane of the third generation folds (upper left).

Field of view 30 cm.

Fig. 4.19 Second generation fold refolded by tight third generation fold to give a type 2 interference pattern.

Pen 13 cm long.

Fig. 4.20 Tight third generation folds in schist with development of a crenulation foliation (S_{3B}) parallel to the axial plane.

Scale in millimetres.

Fig. 4.21 Conjugate set of third generation crenulations crossing second generation schistosity surface.

Field of view 20 cm.

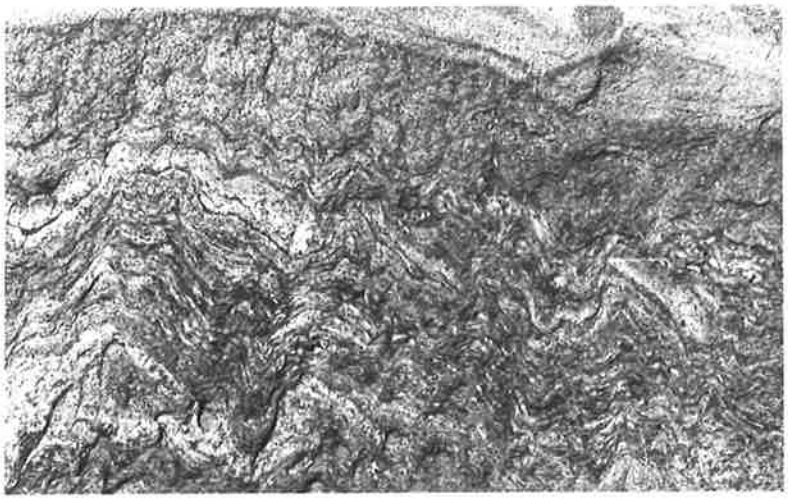

Fig. 4.18

Fig. 4.19

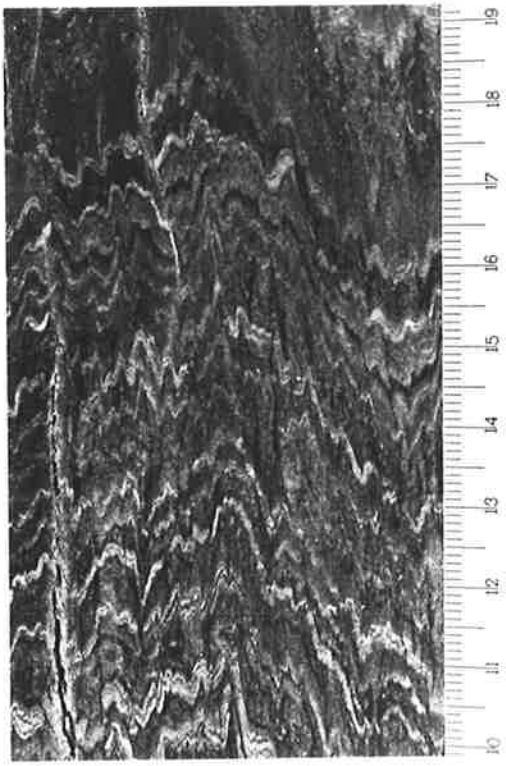

Fig. 4.20

Fig. 4.21

Fig. 4.22 Tight second generation fold in Layered Gneiss with superimposed open third generation fold, giving a type 3 interference pattern.

Fig. 4.23 Tight second generation fold in Albite Schist overprinted by open third generation fold giving a type 3 interference pattern.

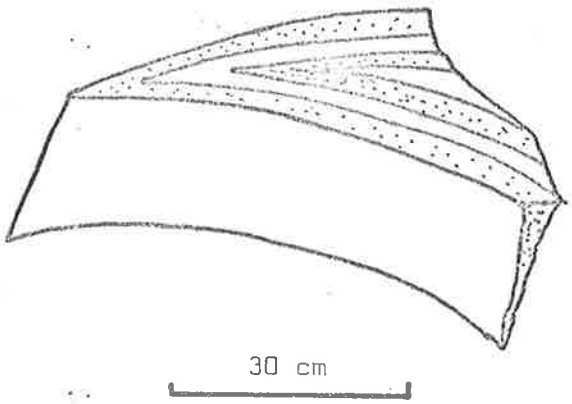

Fig. 4.22

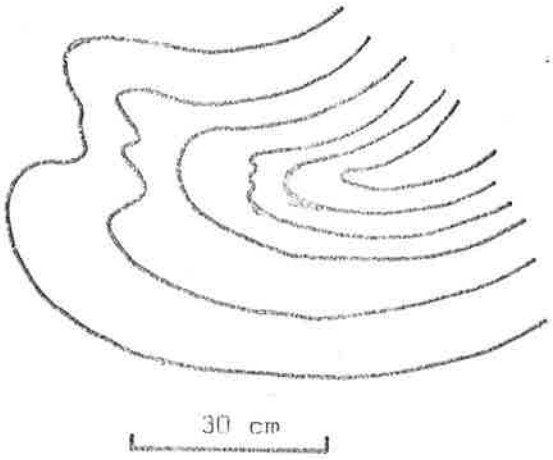

Fig. 4.23

Fig. 4.24 Open crenulation warping second generation schistosity, S_{2B}, in schist.

(A470-078)

Field of view, 9 mm; crossed polars.

Fig. 4.25 Second generation schistosity (S_{2B}) cut by narrow zone of micas aligned parallel to third generation crenulation foliation (S_{3B}) in mica schist.

(A470-077)

Field of view 2.7 mm; plane polarised light.

Fig. 4.26 Micas parallel to second generation schistosity (S_{2B}) curving into zone of micas aligned parallel to third generation foliation (S_{3B}).

(A470-078)

Field of view 2.7 mm; plane polarised light.

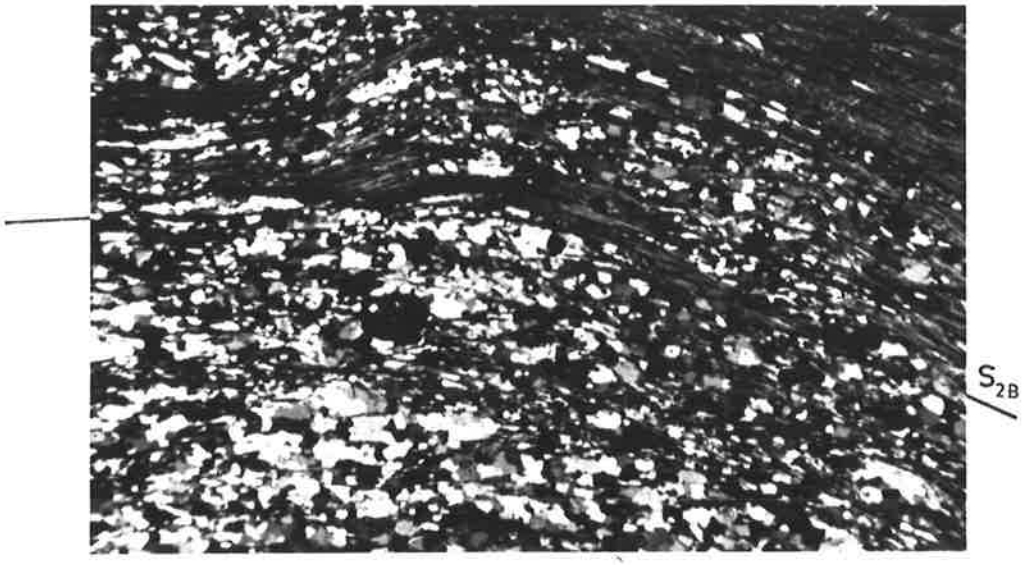

Fig. 4.24

Fig. 4.25

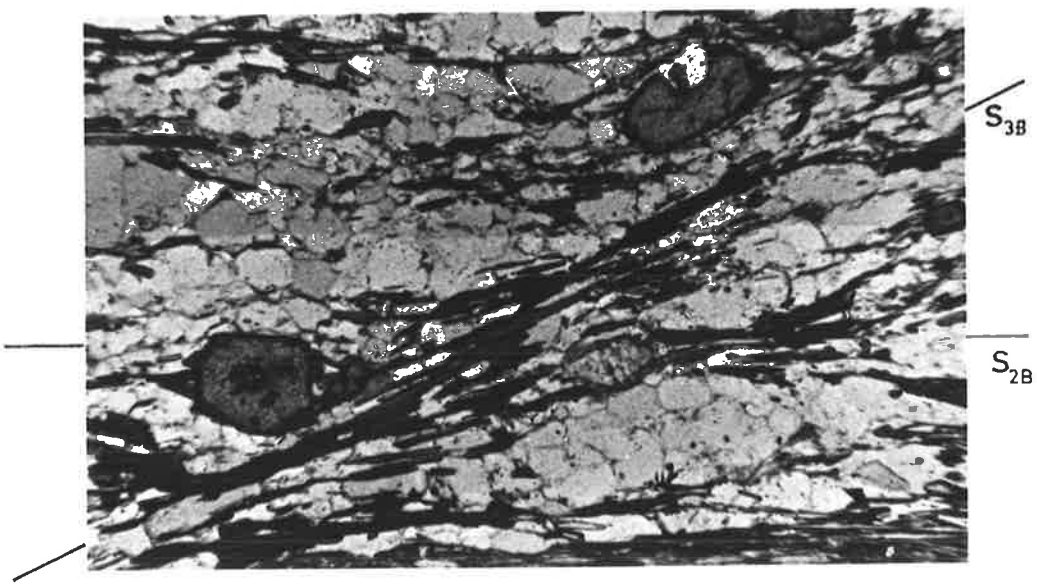

Fig. 4.26

Fig. 4.27 Crenulations of second generation schistosity showing curved hinge lines and individual crenulations extending for only short distances.

Match 4.5 cm long.

Fig. 4.28 Sharp crested crenulations folding second generation schistosity (S_{2B}) in schist.

(A470-079)

Field of view 4 mm; crossed polars.

Fig. 4.29 Smoothly rounded crenulations in schist folding second generation schistosity, S_{2B}, and with axial plane defining crenulation foliation, S_{3B}.

(A470-080)

Field of view 2.7 mm; crossed polars.

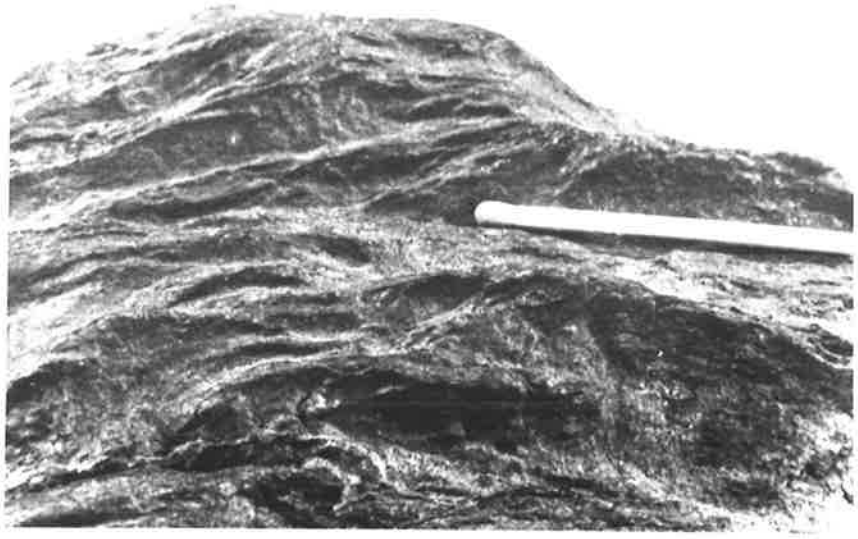

Fig. 4.27

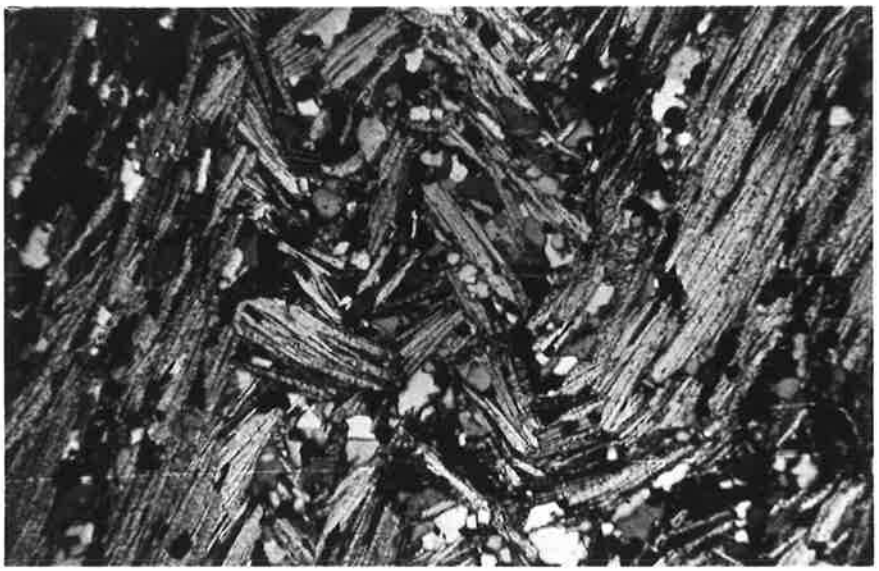

Fig. 4.28

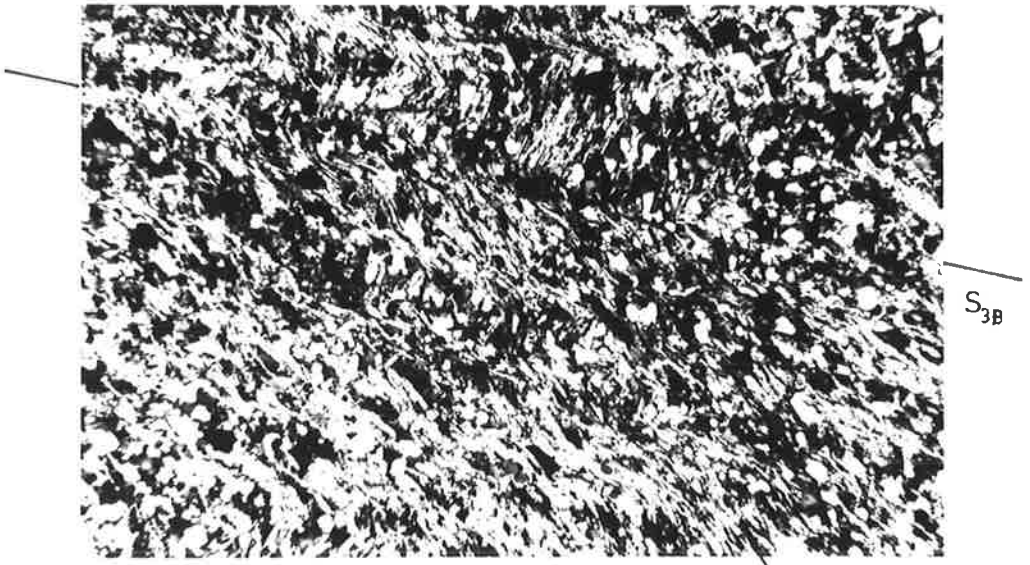

Fig. 4.29

Fig. 4.30 Faults with small displacement, cutting layering of the palaeosome of the Older Migmatites.

Hammer 30 cm long.

Fig. 4.31 Third generation fold in pegmatite with numerous, closely spaced fractures in the hinge area (to the right of the geological hammer).

Hammer 30 cm long.

Fig. 4.32 Thin pegmatite vein with tight third generation folds developed. In the enclosing epidote schist, crenulation foliation (S_{3B}) is developed and this is seen as a set of close-spaced fractures parallel to the axial planes of the folds in the pegmatite vein.

Hammer 30 cm long.

Fig. 4.33 Thin section of augen schist from a fault cutting basement rocks. Large quartz grains (e.g., lower centre) show undulose extinction and the development of subgrains (along boundaries between segments in slightly different orientations). Small quartz grains are polygonal and strain-free (e.g., upper left).

(A 470-068)

Field of view 4 mm; crossed polars.

Fig. 4.30

Fig. 4.31

Fig. 4.32

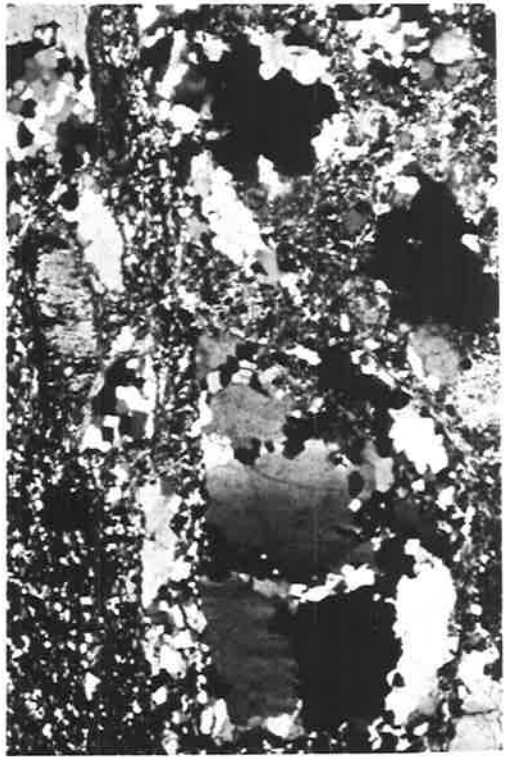

Fig. 4.33

Fig. 4.34 (a) Structural geology map of the Old Boolcoomata area, showing the location of subareas and the orientation of representative fabric elements.

Map held in pocket at rear of thesis.

Fig. 4.34 (b) Stereographic projections of orientations of fabric elements in the basement and cover rocks.

All data have been plotted on the lower hemisphere of equal area projections and where greater than 30 points occur on one diagram, the data has been contoured by the Schmidt method.

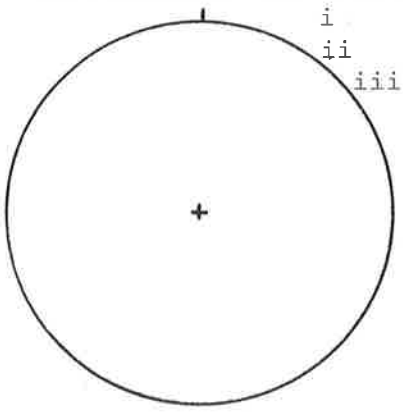

i — Total number of points

ii — contour values (in %/% area)

iii — M: orientation of a plane perpendicular to a point maxima

β: orientation of the pole to a great circle distribution.

N.B. Total $B_s^{S_{3B}}$ does not include data from subareas VIII and IX.

I II III

πS_{0B}

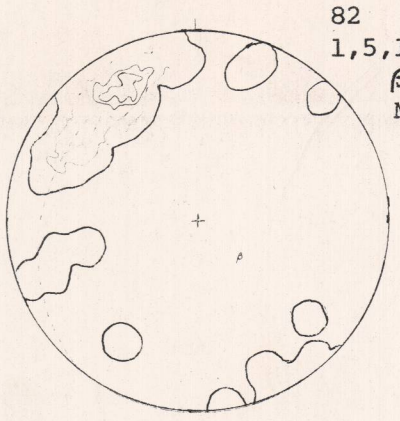

82
1,5,10,15,20
β:65-130
M:75-153

πS_{2B}

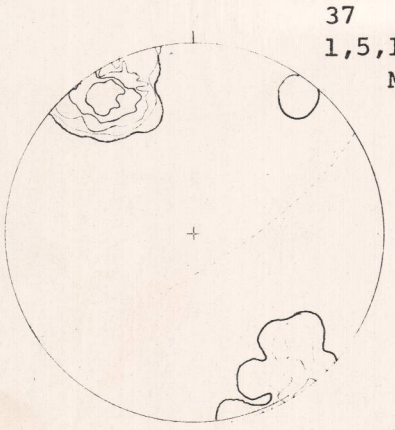

37
1,5,10,15,20
M:75-148

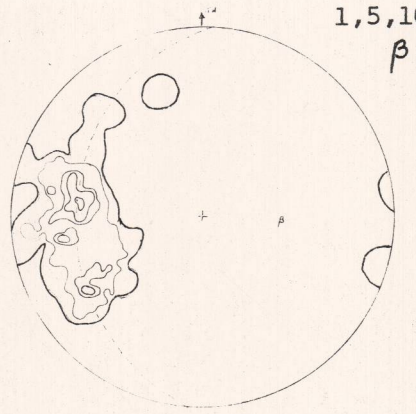

33
1,5,10,15,20
β:55-095

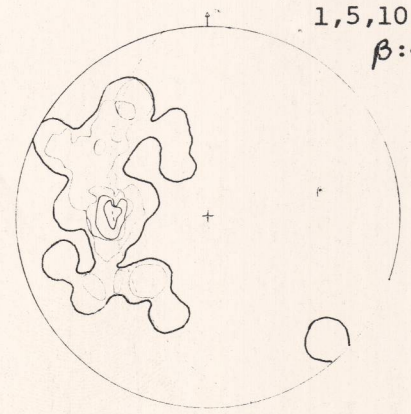

38
1,5,10,15,20
β:40-077

• πS_{3B} , 5

πS_{3B}

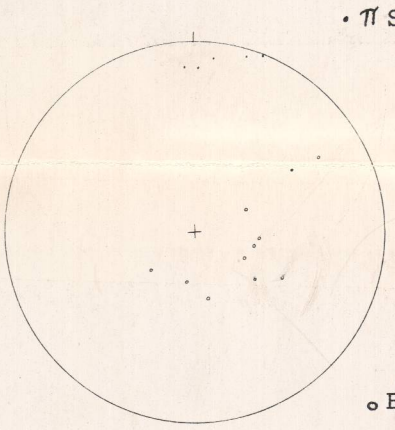

∘ $B^{S_{3B}}_{S_{0,2B}}$, 11

L

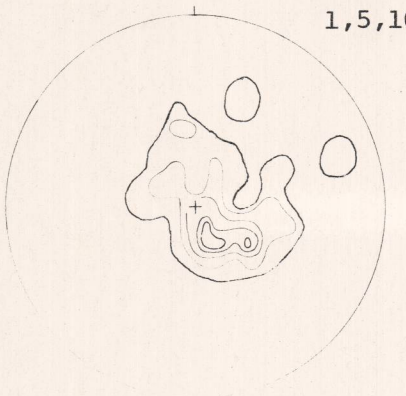

30
1,5,10,15,20

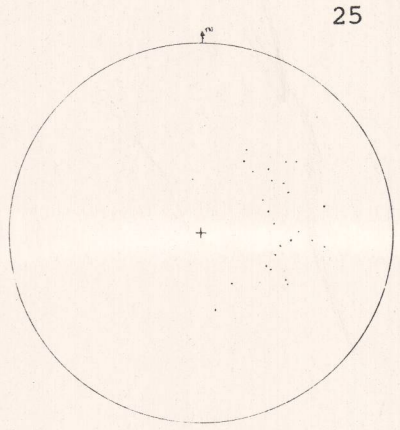

25

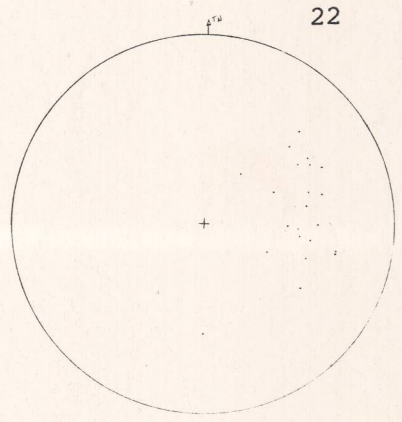

22

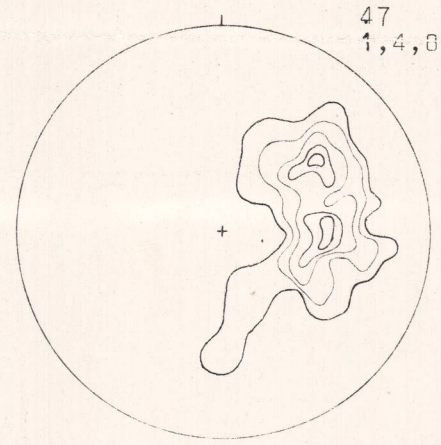

47
1,4,8,12,16

IV

V

VI

πS_{0B}

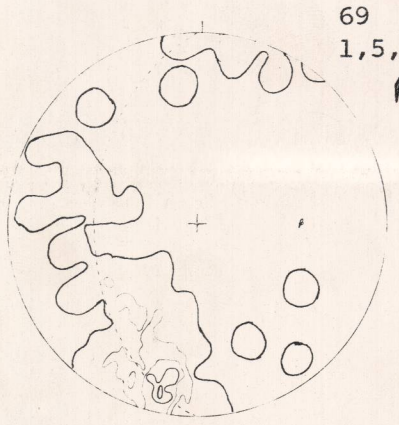

69
1,5,10,15,20
β :45-088

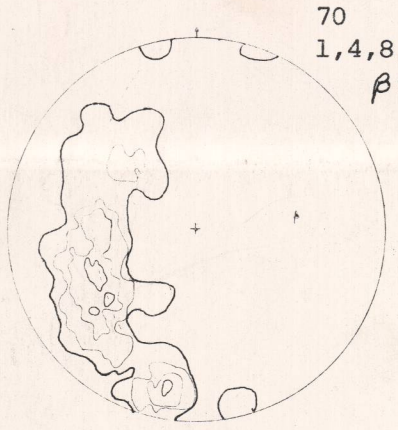

70
1,4,8,12,16
β :45-082

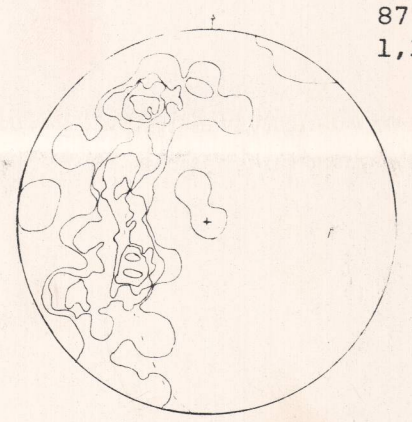

87
1,3,6,9,12
β :35-095

πS_{2B}

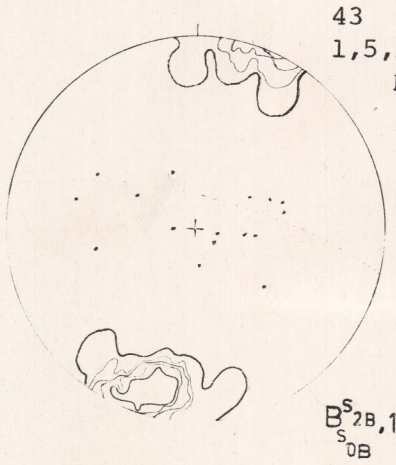

43
1,5,10,15,20
M:75-012

$B^{S_{2B}}_{S_{0B}}$,17

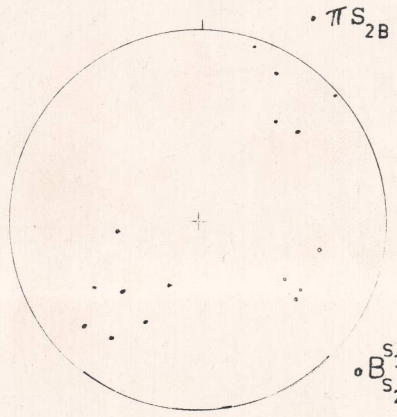

$\cdot \pi S_{2B}$, 12

$\circ B^{S_{3B}}_{S_{2B}}$, 4

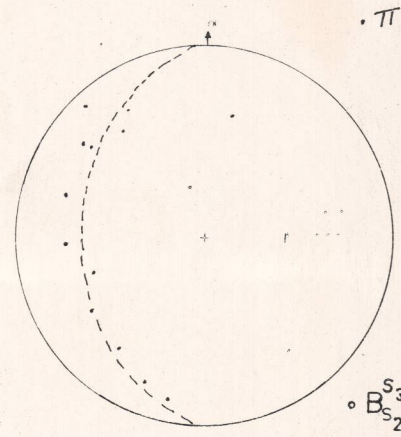

$\cdot \pi S_{2B}$, 14

β :55-087

$\circ B^{S_{3B}}_{S_{2B}}$, 7

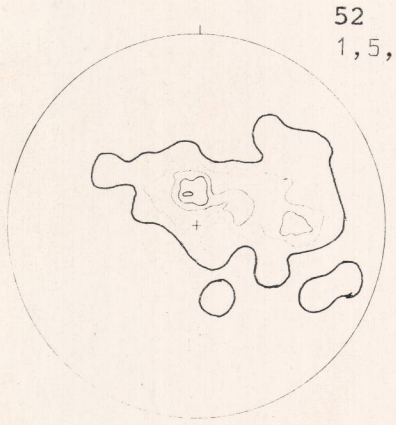

52
1,5,10,15,20

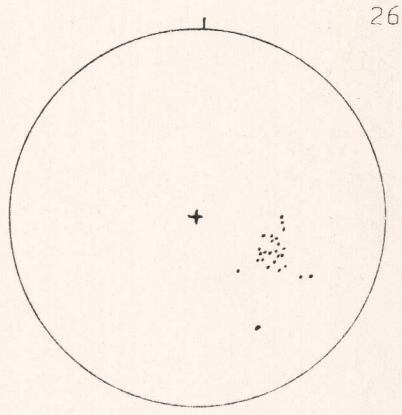

26

VII

VIII

IX

πS_{0B}

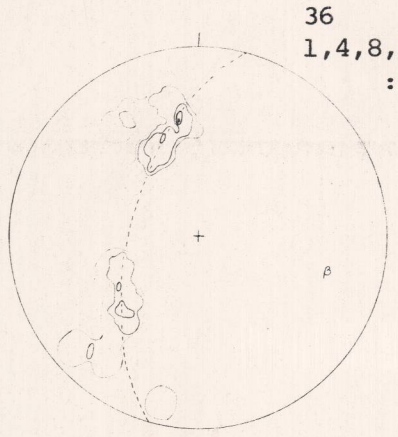

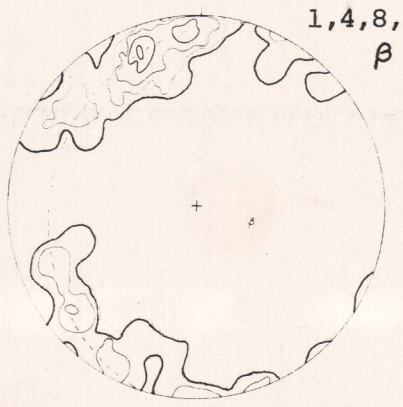

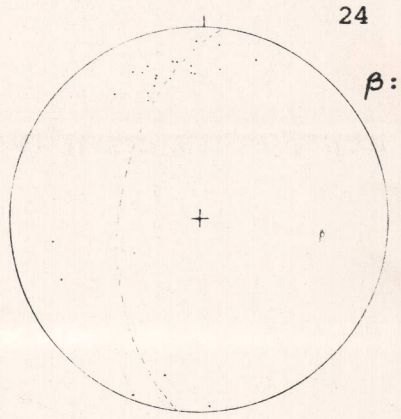

πS_{2B}

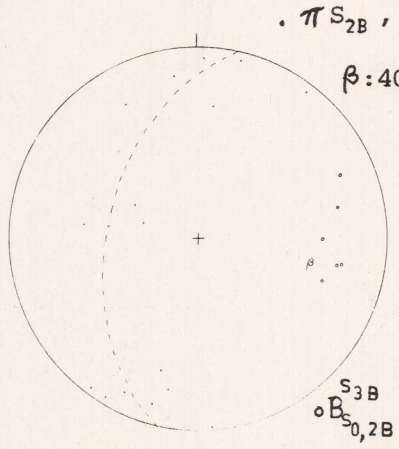

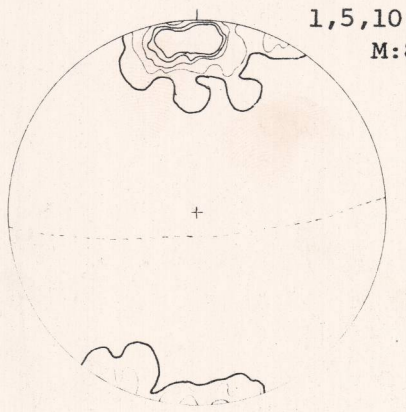

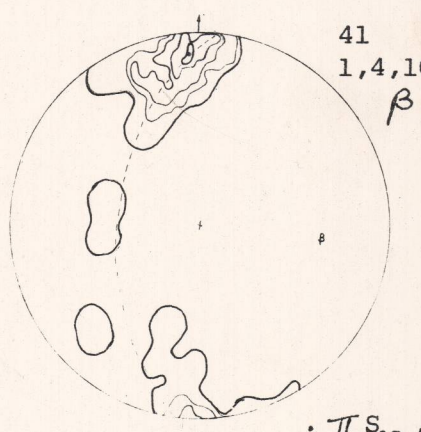

πS_{3B}

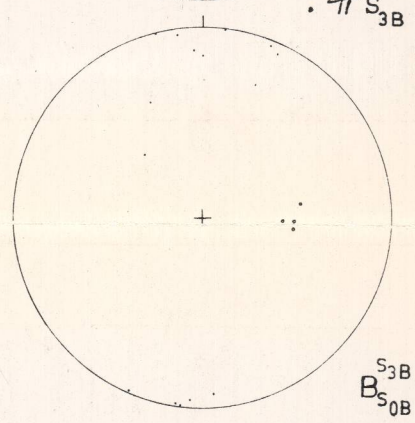

L

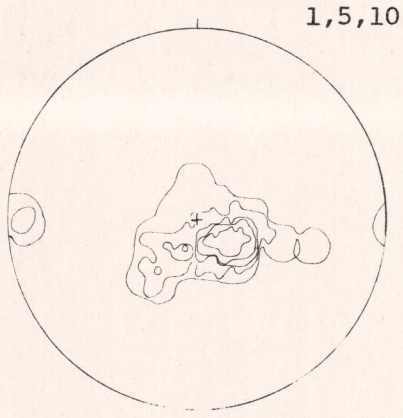

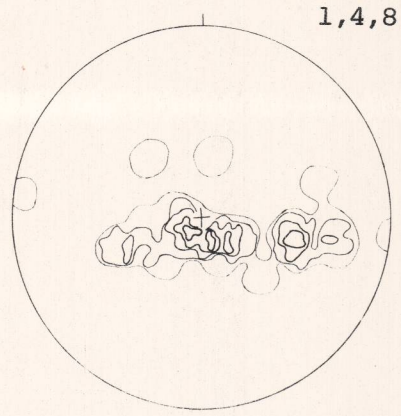

$B_{S_{2B}}^{S_{3B}}$

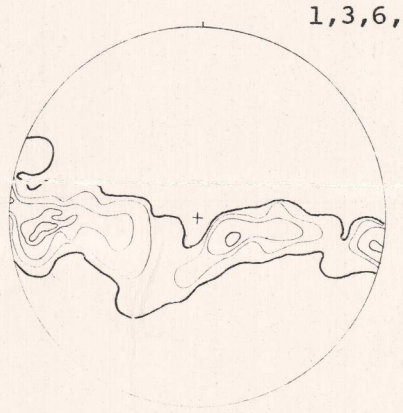

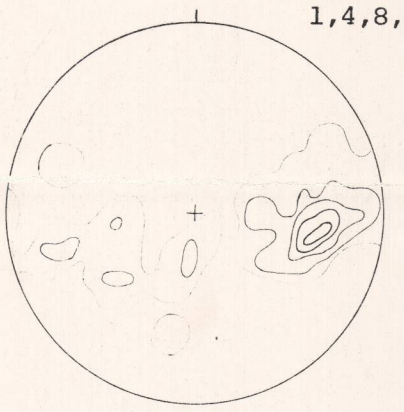

X

XI

XII

πS_{0B}

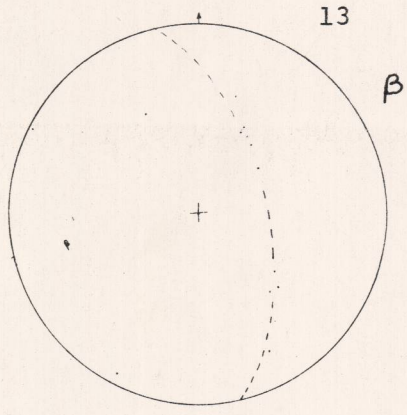

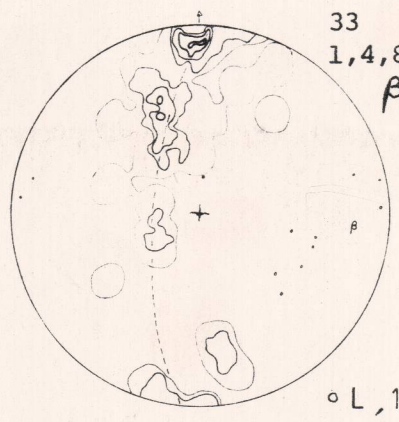

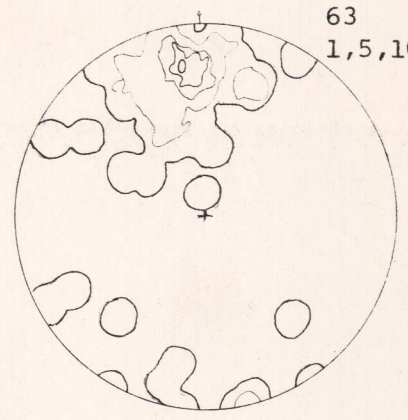

πS_{2B}

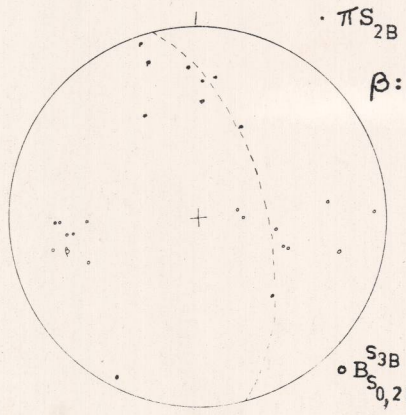

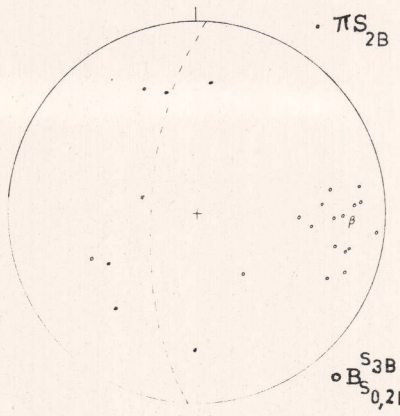

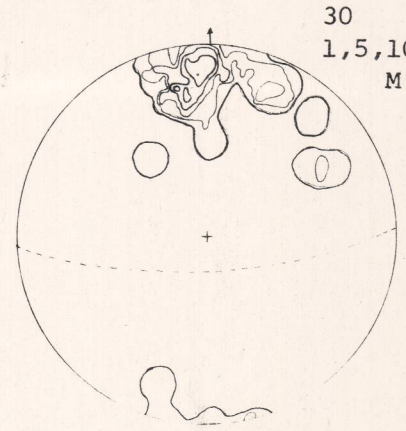

πS_{3B}

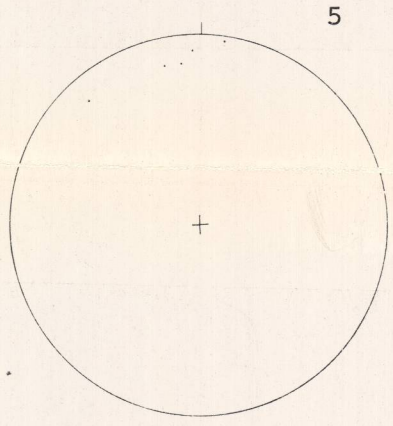

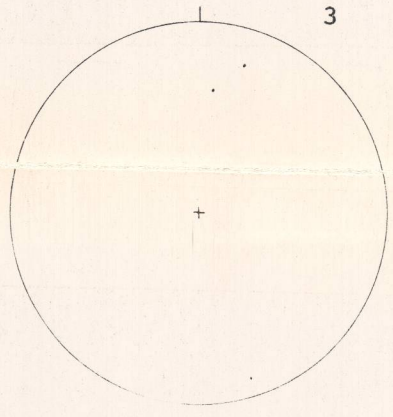

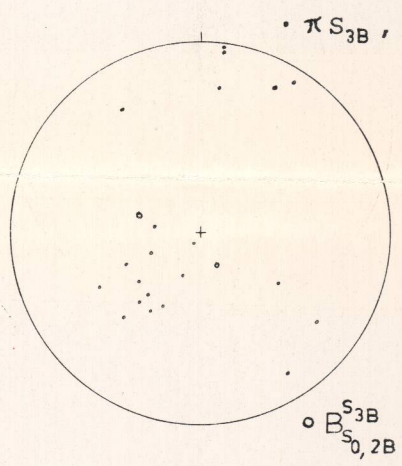

L

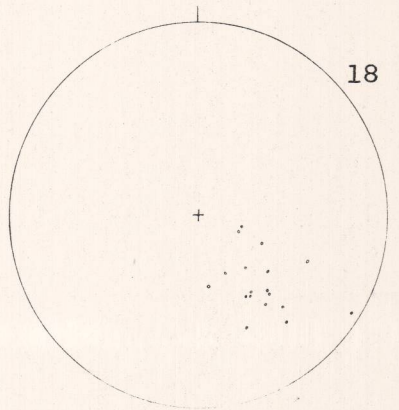

$B^{S_{2B}}_{S_{0B}}$

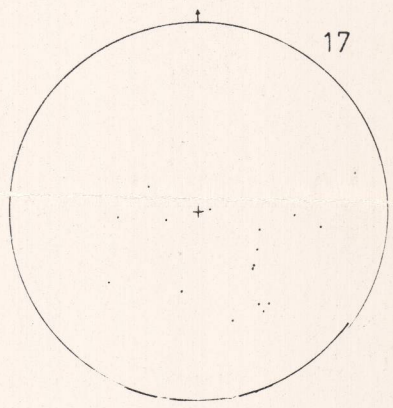

XIII

XIV

XV

140
1,2,4,6,8

πS_{0B}

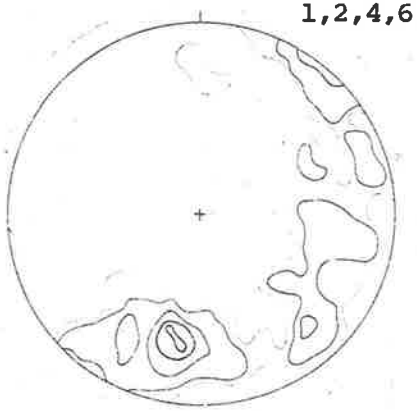

19

β :15-100

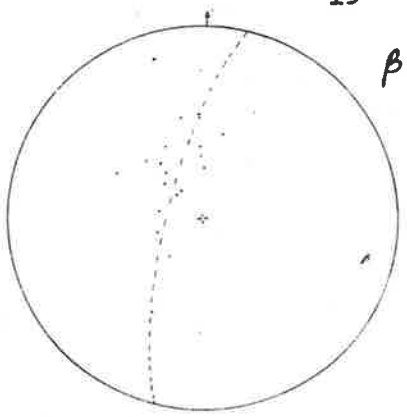

30
1,4,8,12,16

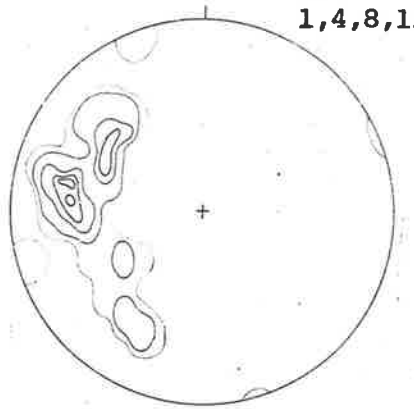

86
1,4,6,8,12

L

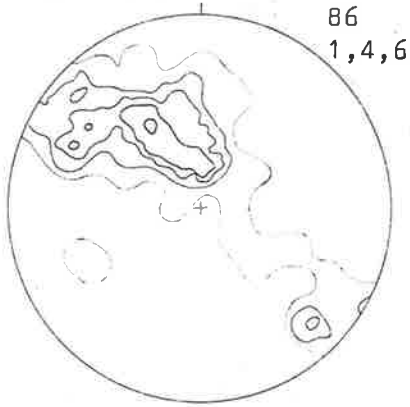

πS_{2B}

· πS_{2B}, 3

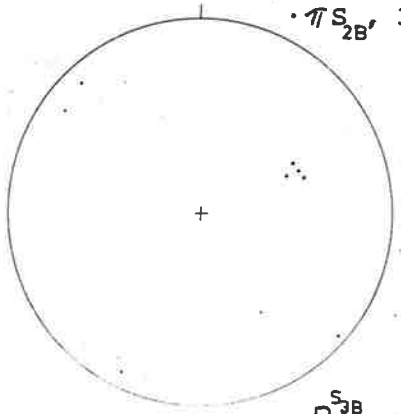

· $B^{S_{3B}}_{S_{0,2B}}$, 4

XVI

TOTAL

COVER

πS_{0B}

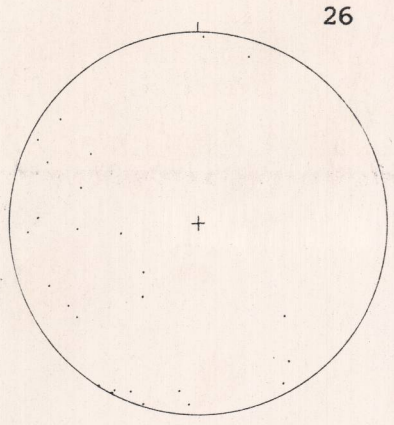

πS_{0C}

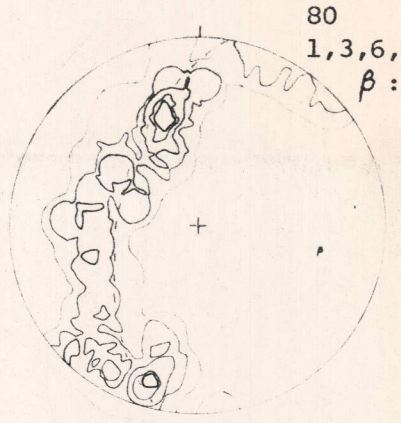

πS_{2B}

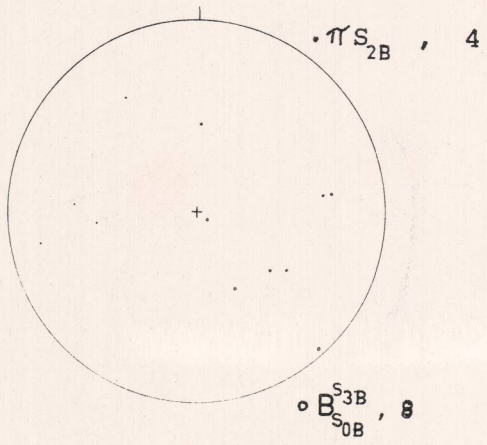

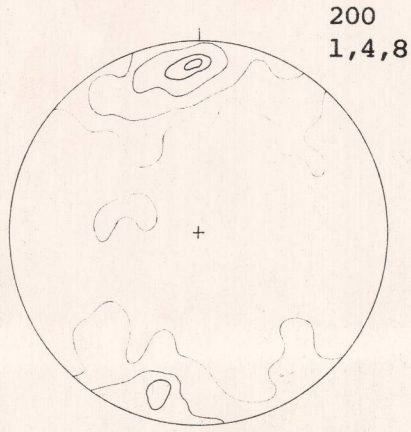

πS_{1C}

πS_{3B}

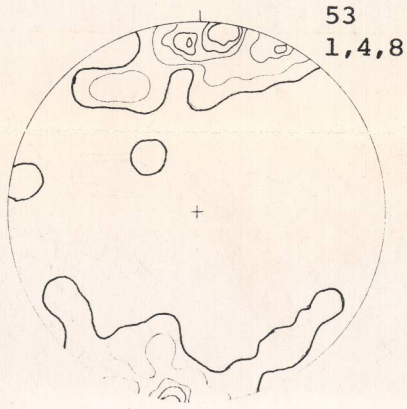

πS_{2C}

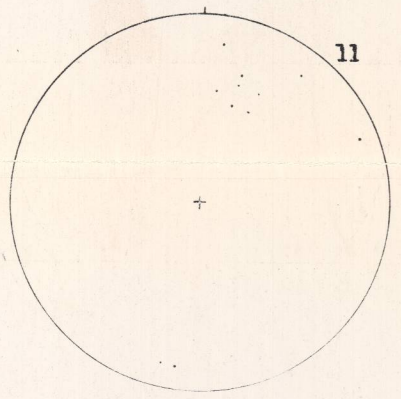

$B^{S_{2B}}_{S_{0B}}$

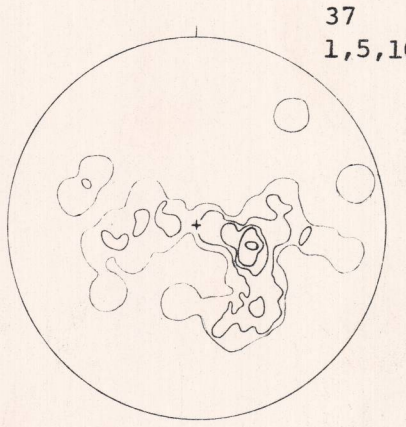

L_{1C}

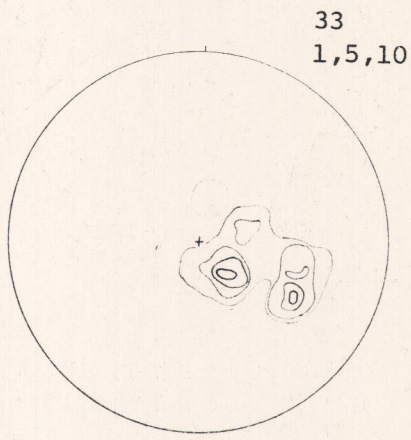

$B^{S_{3B}}_{S_{0,2B}}$

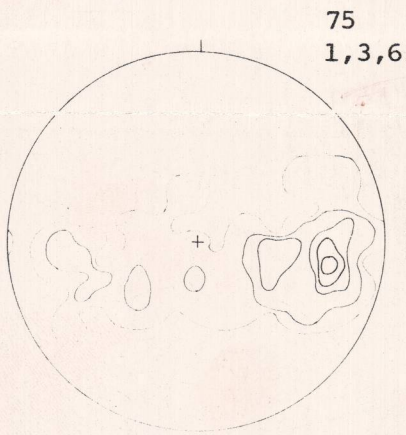

FOLIATION IN THE BOOLCOOMATA ADAMELLITE (Measurements taken on trace of foliation on outcrop surfaces)

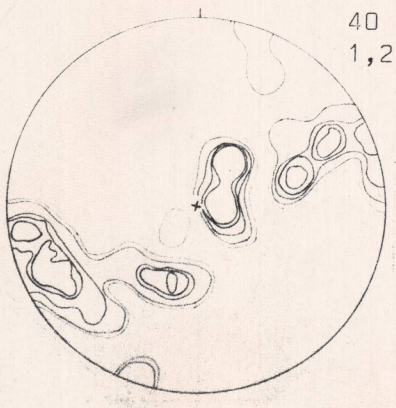

POLES TO FOLIATION (S_{1C}) AROUND SECOND GENERATION FOLD IN COVER AT 029056

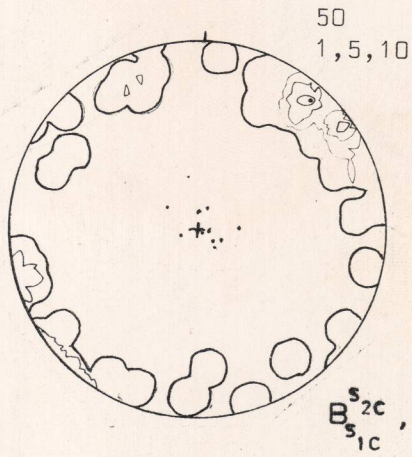

Fig. 4.35(a) Orthographic block diagram of the Old Boolcoomata area showing the structure of the basement and cover rocks. The basement and cover have been separated along the MacDonald Fault in the Diagram.

Basement rock units shown are the Granitic Gneiss which forms a third generation synform in the east of the area and the 'Bedded' Schist which forms an isoclinal first generation syncline refolded by second and third generation folds.

In the cover, Unit 3 and some prominent horizons in Unit 4 are shown.

The cube in the south western corner has sides 1 km long.

Fig. 4.35(b) Orthographic block diagram showing the structure of the 'Bedded' Schist.

(In back pocket.)

Fig. 5.1 Bedding lamination (about 1 mm thick) folded into dextral fold with slaty cleavage approximately parallel to the axial plane. Calcite occurs in thin veins (white) parallel to the slaty cleavage.

Scale in millimetres.

Fig. 5.2 Tight folds in quartzite bed in Unit 4. Cross-bedding is preserved (though distorted) in the hinges of these tight folds.

Field of view 30 cm wide.

Fig. 5.3 Elongate lenses of carbonate and mica in calcareous slate of Unit 4. The lenses are aligned parallel to the axial plane of microcrenulations.

Hammer 30 cm long.

Fig. 5.4 Chevron folds of bedding and cleavage in Unit 4.

Hammer 30 cm long.

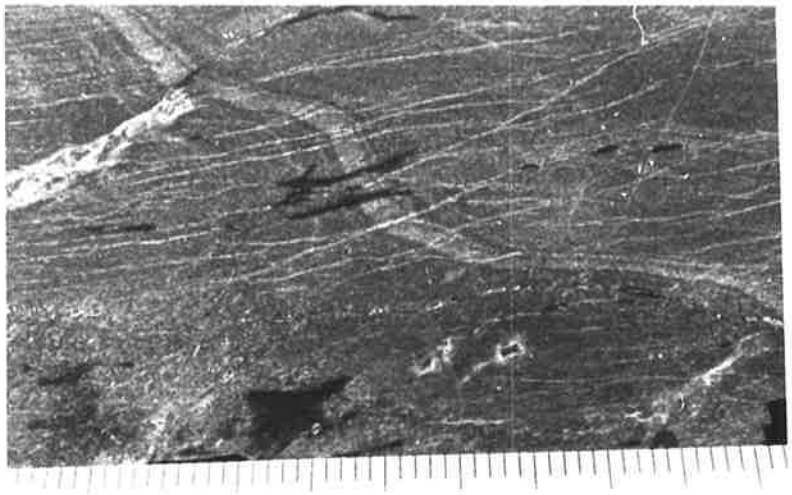

Fig. 5.1

Fig. 5.2

Fig. 5.3

Fig. 5.4

Fig. 5.5 Cross-section along the line A-B Fig. 2.1, showing the structure of the cover rocks.

(In back pocket.)

Fig. 5.6(a) Geological map of the basement inlier in Unit 4.

Adelaide Systems - grey (conglomerate indicated by circles)

Basement - yellow

Quartz veins - red

Fig. 5.6(b) Poles to bedding in Unit 4 at eastern end of inlier.

β: 30° - 100

Fig. 5.6(c) Poles to bedding in Unit 4 at western end of inlier.

β: 60° - 100

Fig. 5.6(d) Poles to lithological layering in basement inlier.

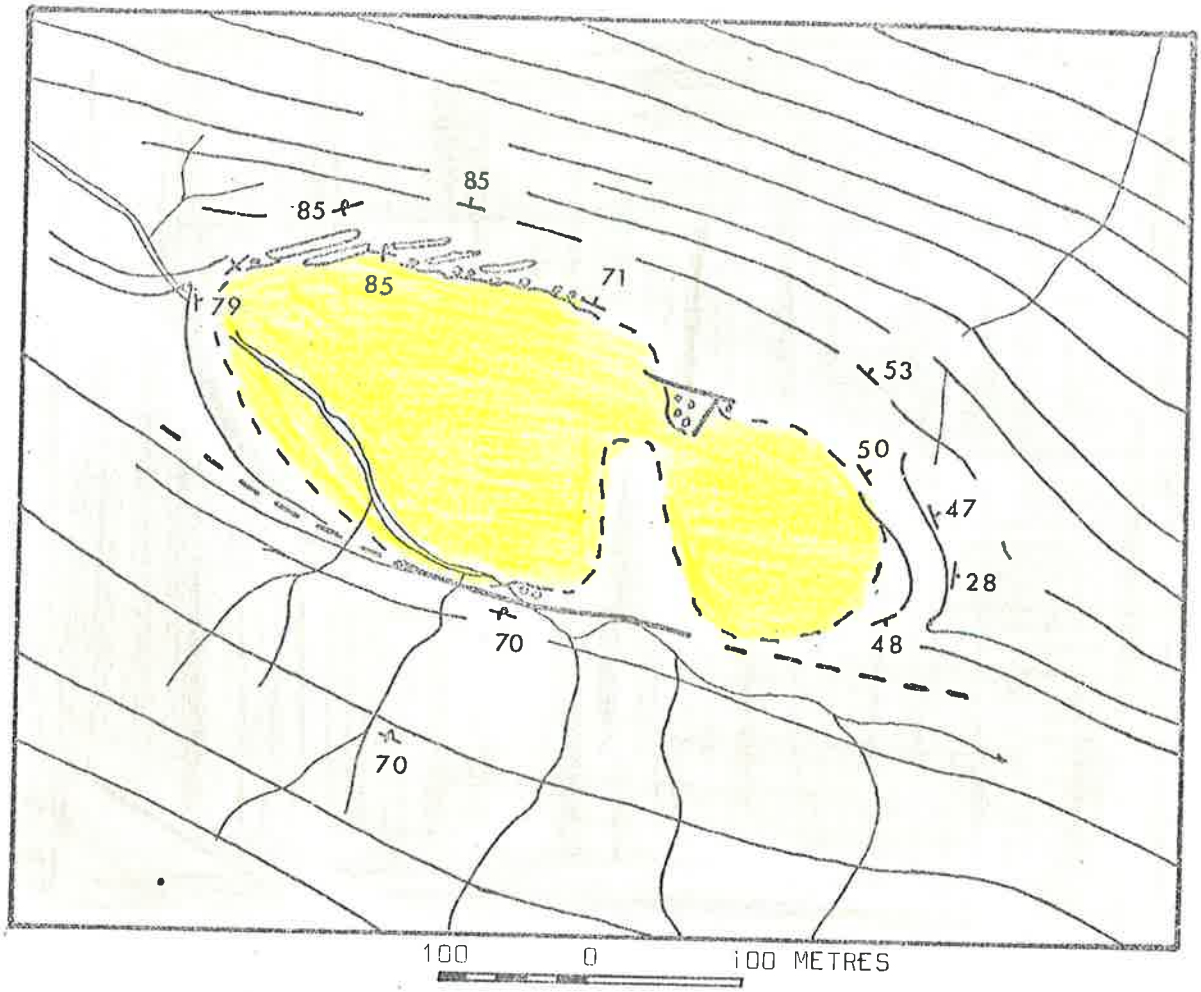

Fig. 5.6(a)

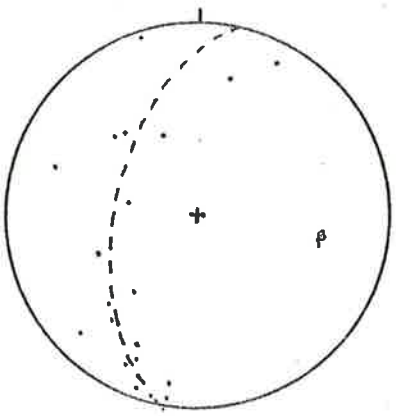

Fig. 5.6(b)

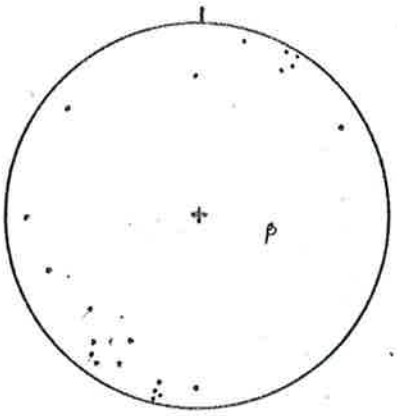

Fig. 5.6(c)

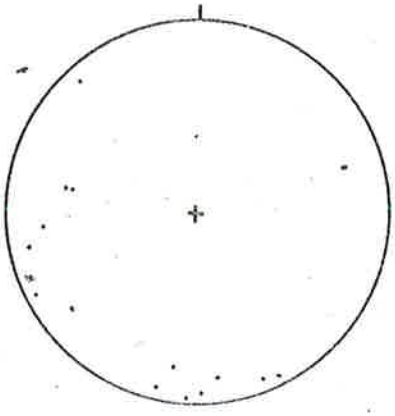

Fig. 5.6(d)

Fig. 5.7 Model for the development of the MacDonald Fault.

(a) Equal-area projection of the average orientation of the MacDonald Fault, the average orientation of foliation in the Adelaidean rocks in the Old Boolcoomata area and the maximum concentration of lineations (L_{1C}).

(b) Trace of axial plane foliation (S_{1C}) and MacDonald Fault in profile plane of fold. Shortening perpendicular to the foliation produces movement as shown which is in accord with the observations in the Old Boolcoomata area.

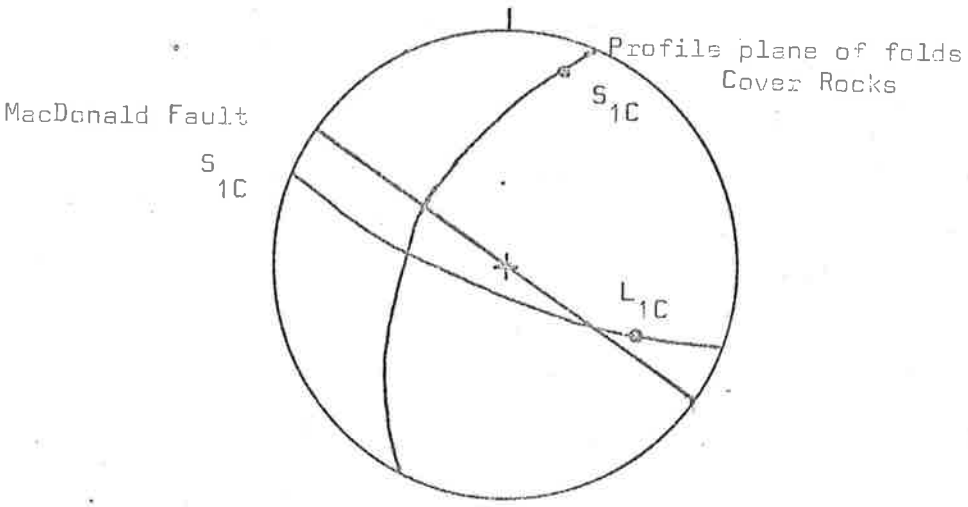

Fig. 5.7(a)

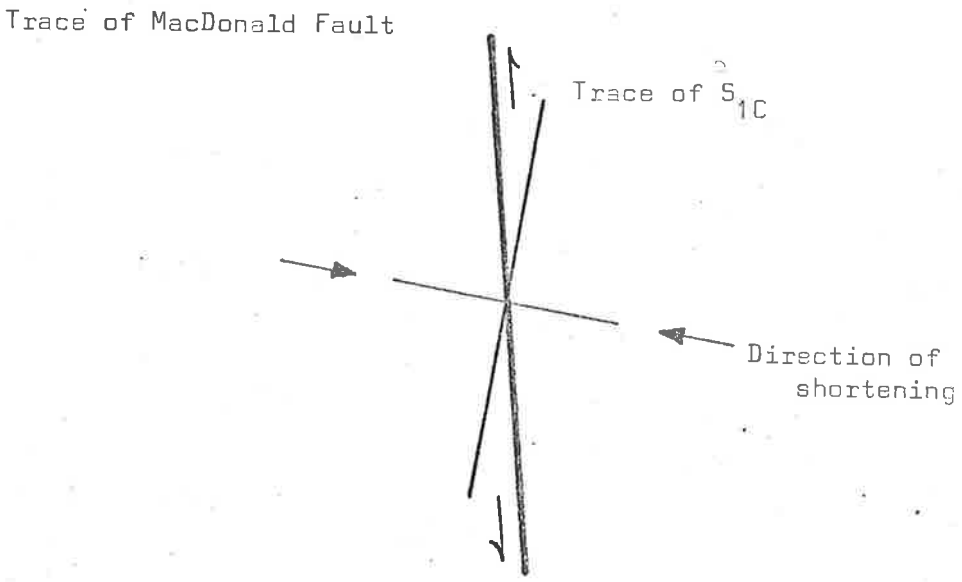

Fig. 5.7(b)

Fig. 5.8 Basement inlier (tree covered area) looking from the western end.

Fig. 5.9 Conglomerate unconformably overlying migmatites of the basement inlier (centre right). The unconformity turns through 90° and passes along the lower edge of the photograph. Quartzite bed (upper left) faces towards the unconformity.

Hammer 30 cm long.

Fig. 5.10 MacDonald Fault (F) separating basement schists (left) from cover slates (right). Schistosity in both rock types is parallel to the fault.

Hammer 30 cm long.

Fig. 5.8

Fig. 5.9

Fig. 5.10

Fig. 5.11 Mylonite from the MacDonald Fault with plagioclase grains showing bent twins and micro-faults.

(A 470-069)

Field of view 2 mm; cross polars.

Fig. 5.12 Mylonite from the MacDonald Fault showing large plagioclase grains and a fine-grained mosaic of quartz with the quartz occurring in narrow zones defining the mylonitic foliation.

(A 470-069)

Field of view 2 mm; crossed polars.

Fig. 5.11

Fig. 5.12

Fig. 6.1 R_f/ϕ plots of pebbles from Unit 1.

(a) Pebbles on horizontal face (approximately perpendicular to bedding) in Subunit 1a at 050 065.

19 pebbles.

(b) Pebbles on face dipping 10°-120 (approximately perpendicular to bedding) in Subunit 1a at 050 065.

20 pebbles.

(c) Pebbles on vertical face strike 045, in Subunit 1b at 054 065.

21 pebbles.

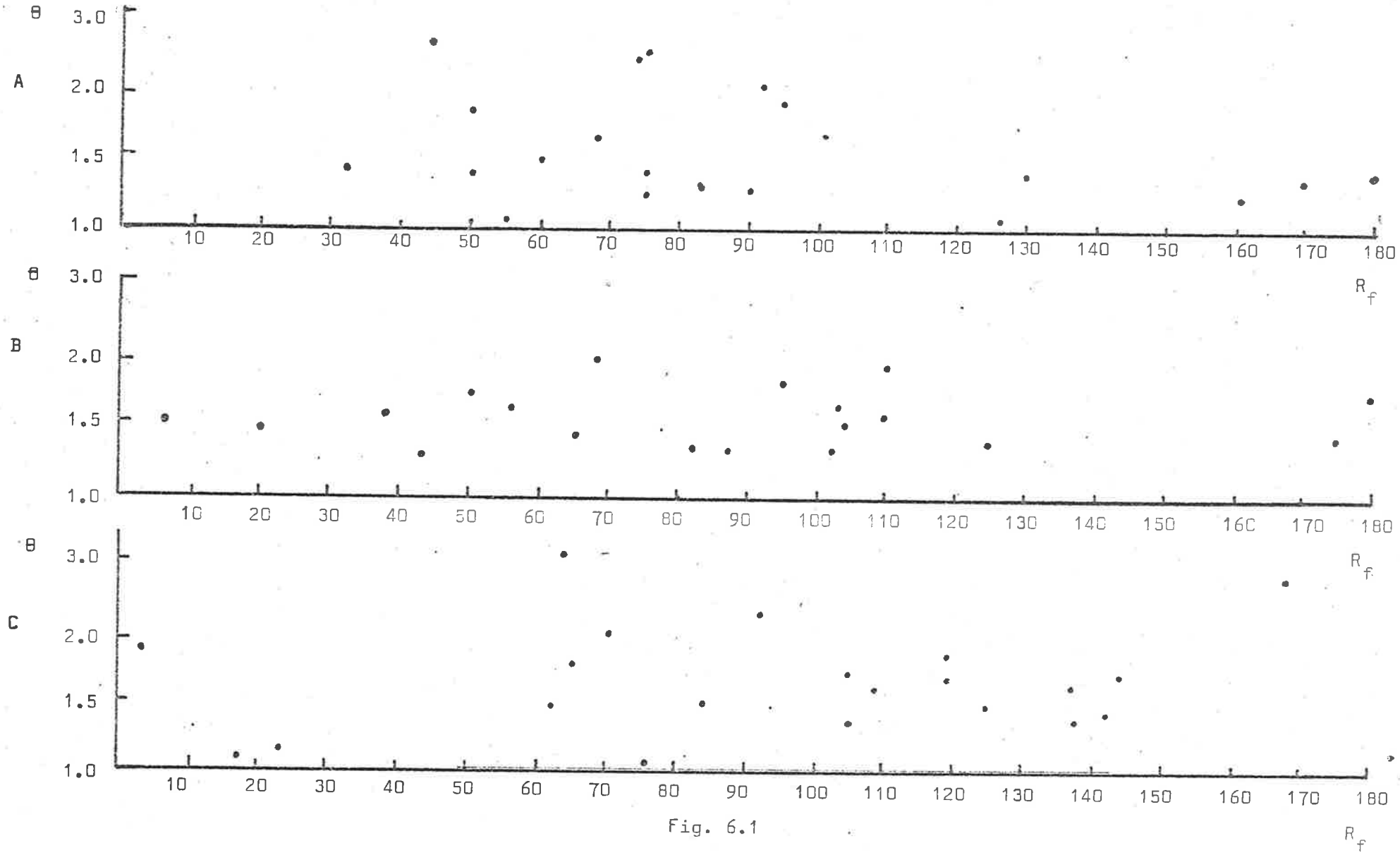
A
B
C
θ
3.0
2.0
1.5
1.0
10 20 30 40 50 60 70 80 90 100 110 120 130 140 150 160 170 180
R_f

Fig. 6.1

Fig. 6.2 Weakly developed cleavage in tillite (Unit 3) with sandy matrix, viewed parallel to cleavage and approximately parallel to fold axis.

Hammer 30 cm long.

Fig. 6.3 Well developed cleavage in tillite (Unit 3) with biotite-rich matrix. Pebbles are aligned subparallel to cleavage. View looking parallel to cleavage and approximately perpendicular to fold axis.

Scale: 30 cm long.

Fig. 6.4 Quartzo-feldspathic pebble curved around another quartzo-feldspathic pebble, possibly as a result of plastic deformation.

Hammer 30 cm long.

Fig. 6.5 Quartzite pebble deformed by slip on closely spaced parallel fractures oblique to the cleavage in the matrix of the tillite (Unit 3).

Hammer 30 cm long.

Fig. 6.2

Fig. 6.3

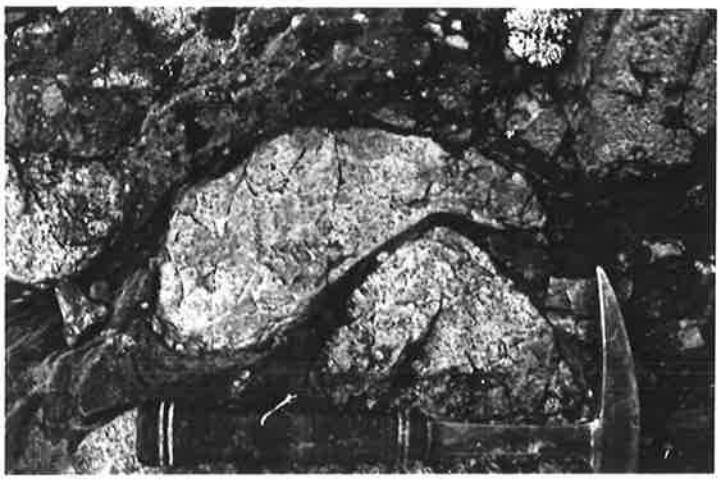

Fig. 6.4

Fig. 6.5

Fig. 6.6 Layered quartzo-feldspathic pebble deformed by slip parallel to lithological layering.

Lens cap 5 cm diameter.

Fig. 6.7 Layered quartzo-feldspathic pebble deformed by slip parallel to lithological layering.

Lens cap 5 cm diameter.

Fig. 6.8 Quartzo-feldspathic pebble deformed by slip on fractures parallel to layering and on oblique fractures.

Lens cap 5 cm diameter.

Fig. 6.9 Boulder displaying fracture filled with matrix.

Hammer 30 cm long.

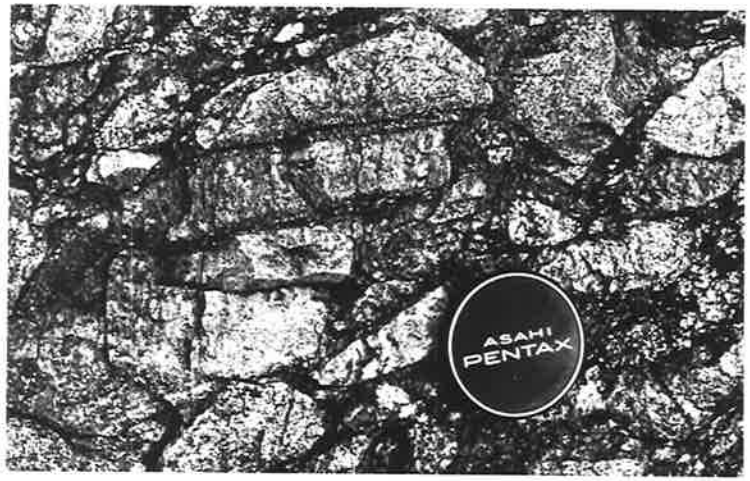

Fig. 6.6

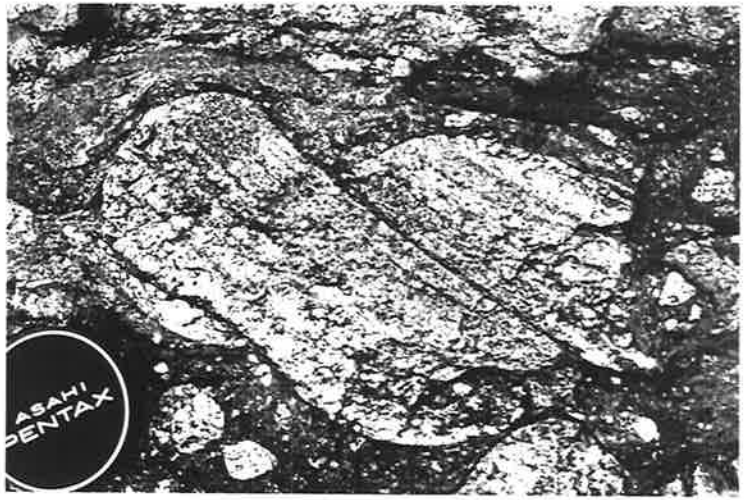

Fig. 6.7

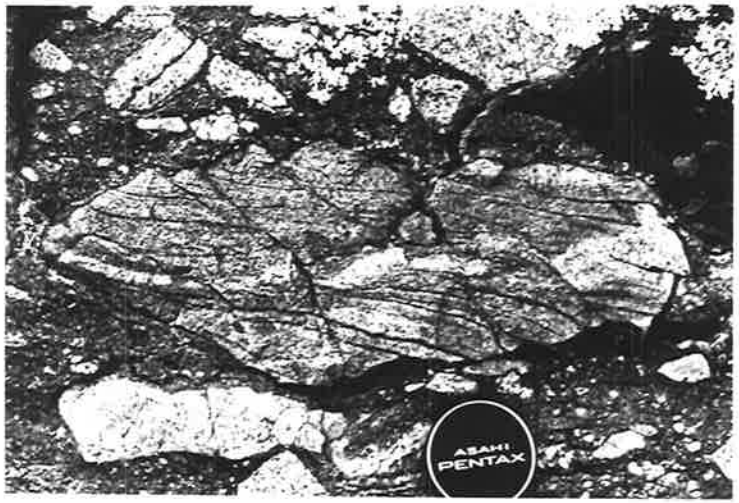

Fig. 6.8

Fig. 6.9

Fig. 6.10 Schist pebbles (black) aligned subparallel to cleavage in tillite (Unit 3). Some quartzo-feldspathic pebbles are elongate (especially the large one showing folded layering) but most quartzo-feldspathic pebbles show little evidence of deformation.

Hammer 30 cm long.

Fig. 6.11 Deformed schist pebble with cleavage parallel to the length of the pebble.

Coin 2.5 cm diameter.

Fig. 6.12 Schist pebble deformed between two quartzo-feldspathic pebbles. Schistosity parallel to the length of the schist pebbles is folded with the pebble.

Coin 2.5 cm diamater.

Fig. 6.13 Curved schist pebble with schistosity parallel to the length of the pebble.

Coin 2.5 cm diameter.

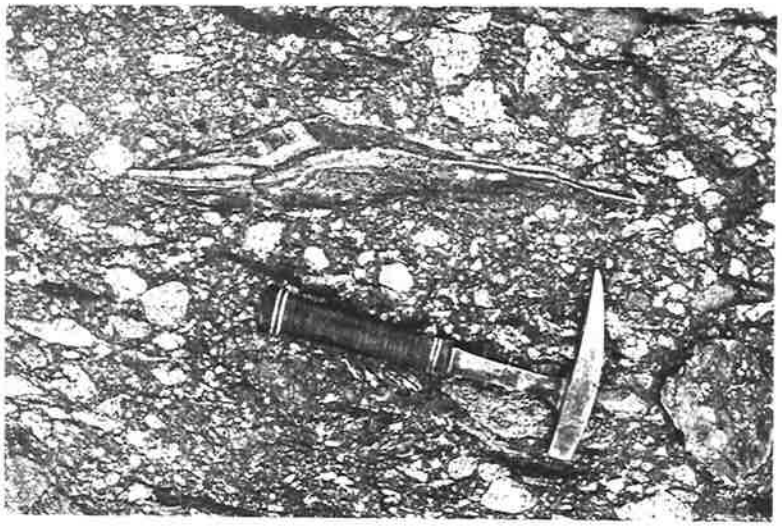

Fig. 6.10

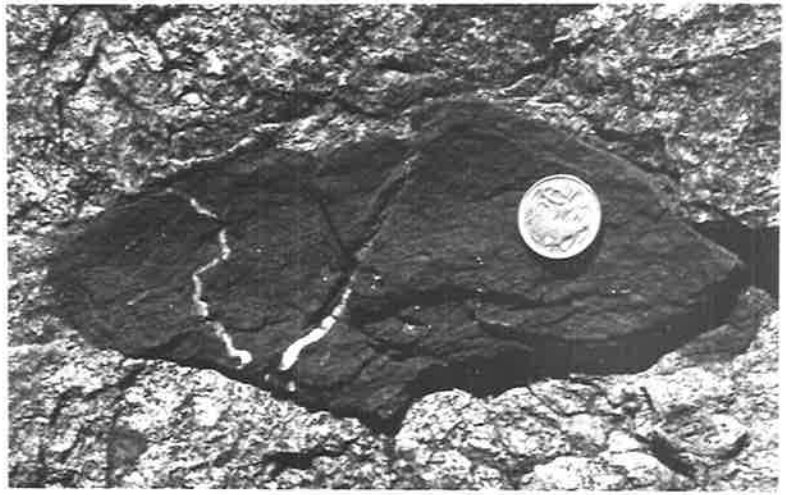

Fig. 6.11

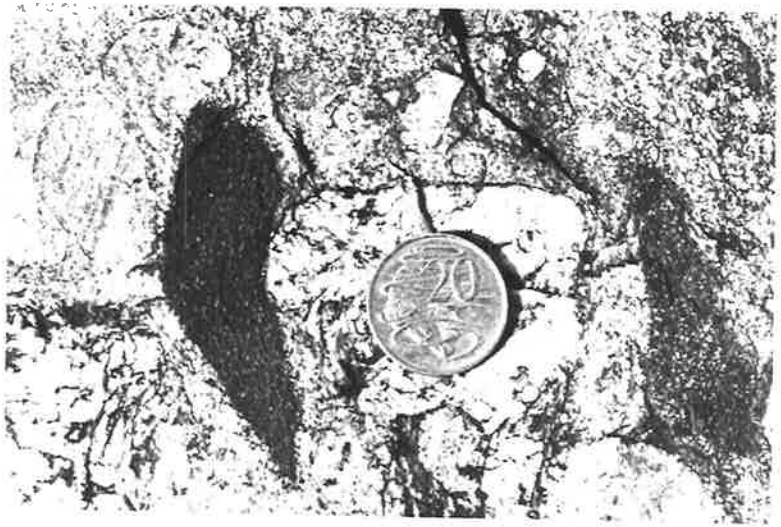

Fig. 6.12

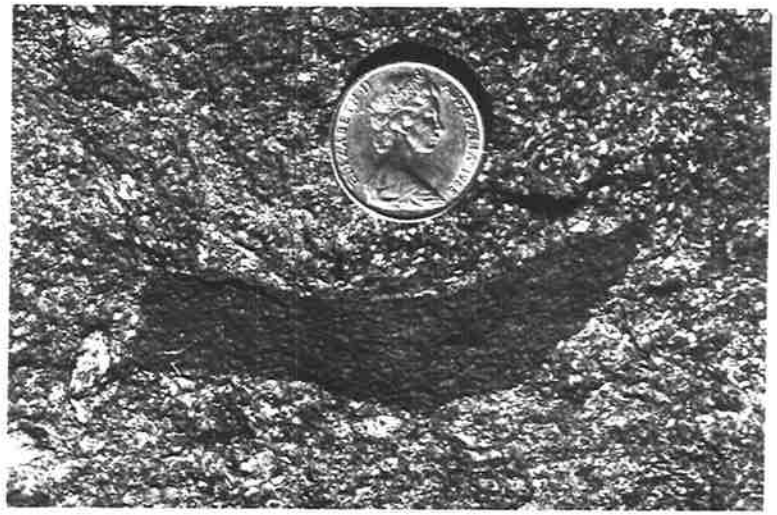

Fig. 6.13

Fig. 6.14 Schist pebble showing curved fractures which have been infilled with quartz. Adjacent schist pebbles are subellipsoidal and are elongate approximately parallel to the foliation in the matrix.

Hammer 30 cm long.

Fig. 7.1 Coarse muscovite (mottled grey) enclosing needles of sillimanite which outline a tight fold - this fold persists through the adjacent schist where it is delineated by biotite flakes.

(A 179-17 - specimen collected by R.L. Oliver.)

Field of view 2 mm; cross polars.

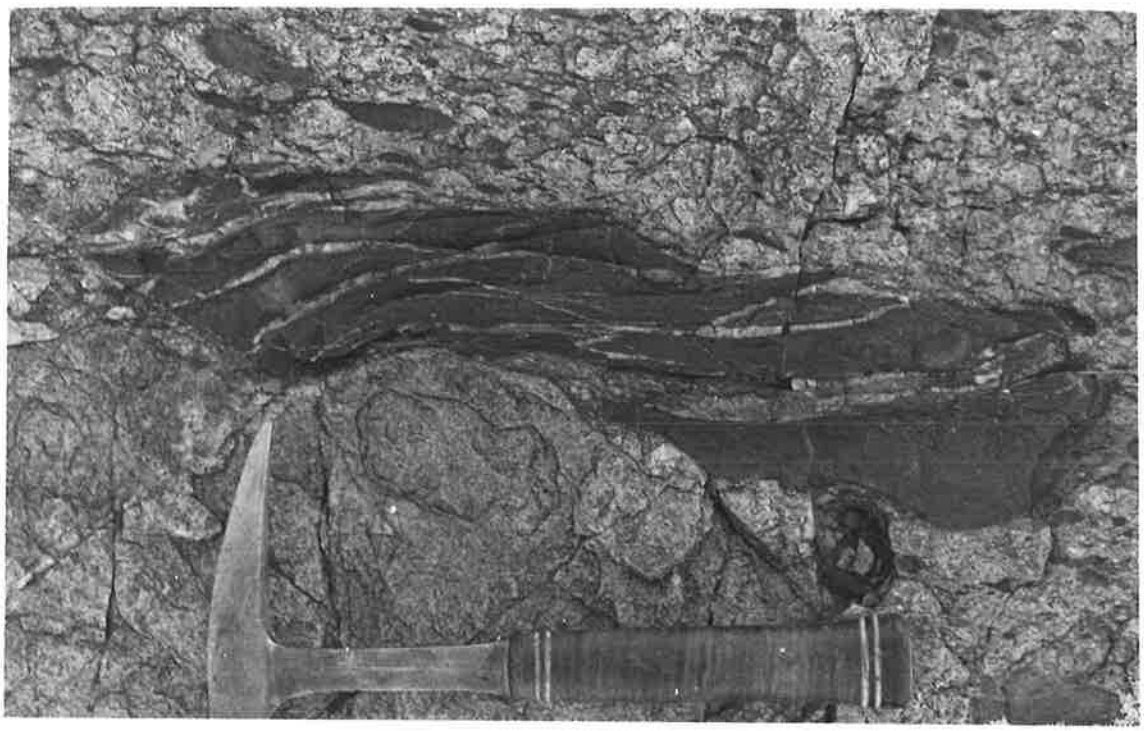

Fig. 6.14

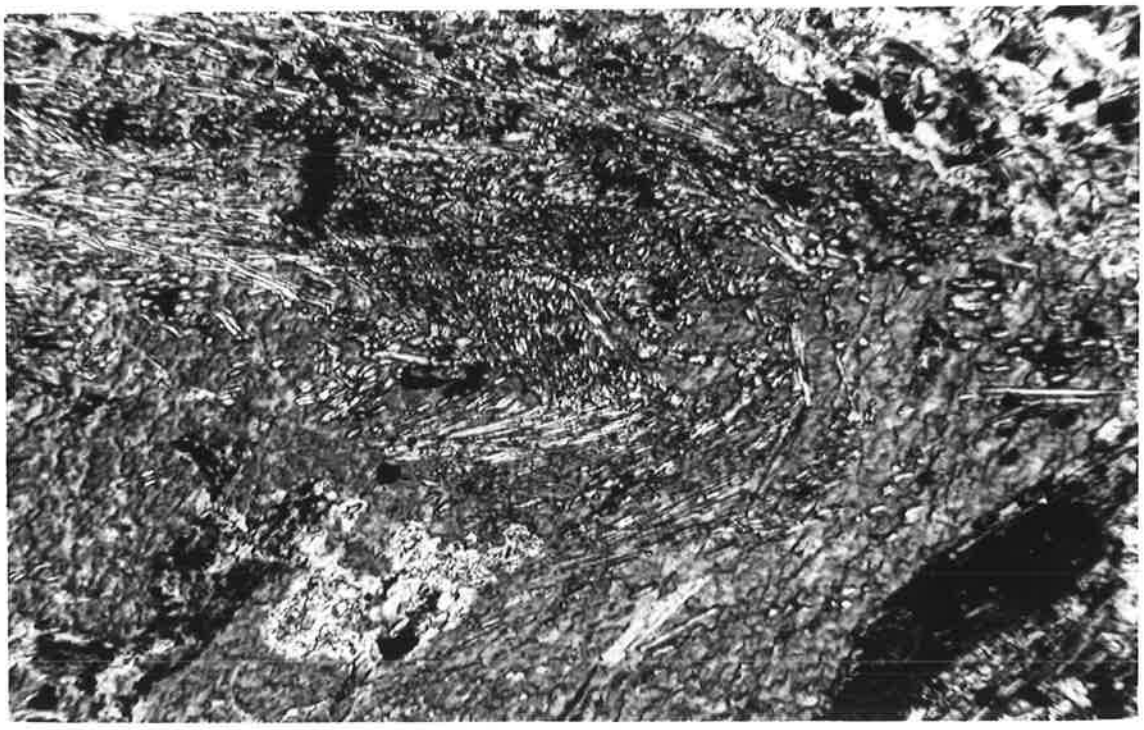

Fig. 7.1

Fig. 6.15 Polar graphs of long pebble axes (R_f) plotted against orientation (ϕ) for measurements taken in Unit 3. Distribution contoured by the Mellis method, contours show areas of 1, 2, and 3 circle overlap. Heavy line indicates orientation and amount of principal extension. Faint lines show the orientation of bedding (S_{OC}) and foliation (S_{1C}) where these could be determined.

(a) Unit 3 at 033020
face dipping 18°-186
50 pebbles

(b) Unit 3 at 033020
face dipping 87°-080
28 pebbles

(c) Unit 3 at 035018
face dipping 58°-250
50 pebbles

Fig. 6.15

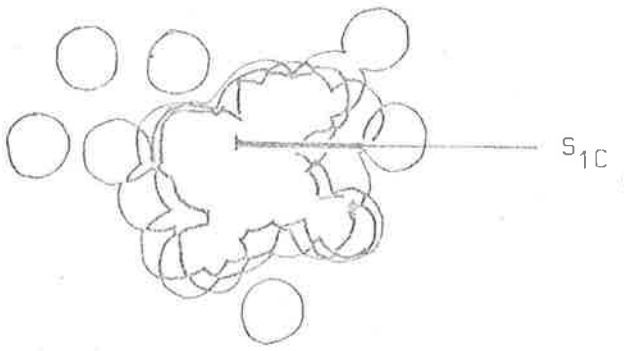

a

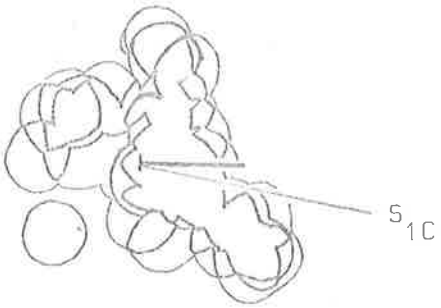

b

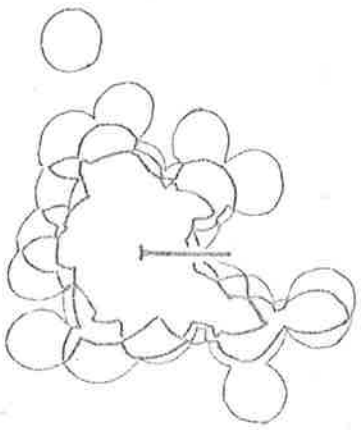

c

R_s

1.5 2 2.5 3 4 5

Fig. 6.15 (cont'd)

Unit 3, specimen A470-055, location 075013

(d) and (f) Quartzo-feldspathic pebbles on faces perpendicular to foliation

40 and 50 pebbles respectively

(e) Quartzo-feldspathic pebbles on face parallel to foliation

52 pebbles

(g) Schist pebbles, same face as Fig. 6.15d

30 pebbles

(h) Schist pebbles, same face as Fig. 6.15f

33 pebbles

Fig. 6.15(cont.)

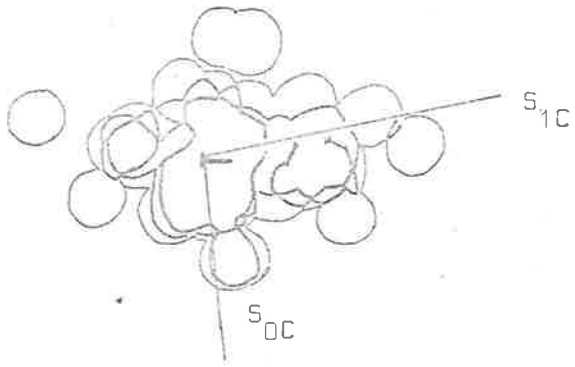

d

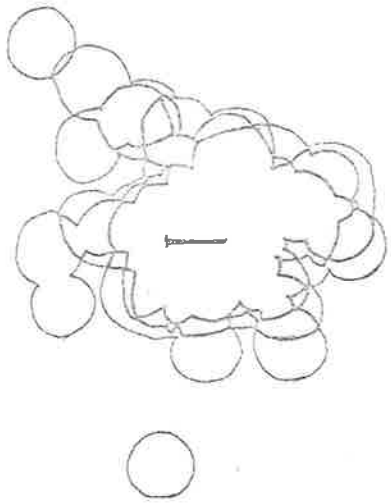

e

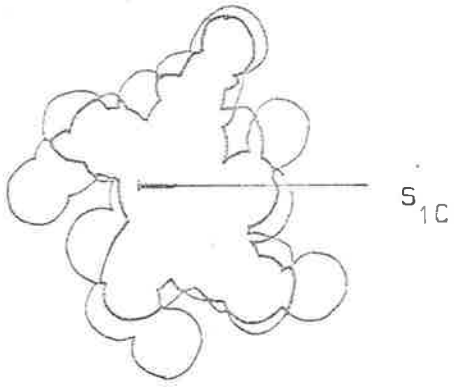

f

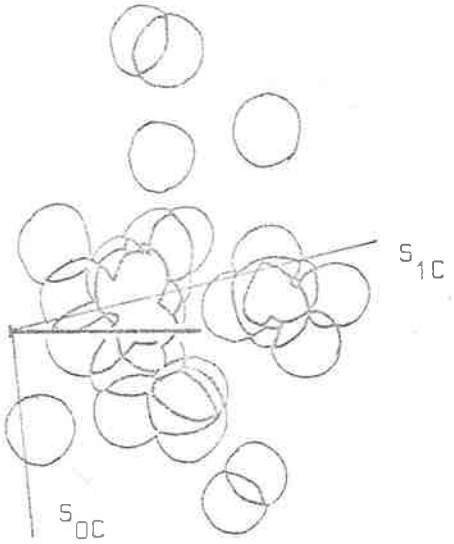

g

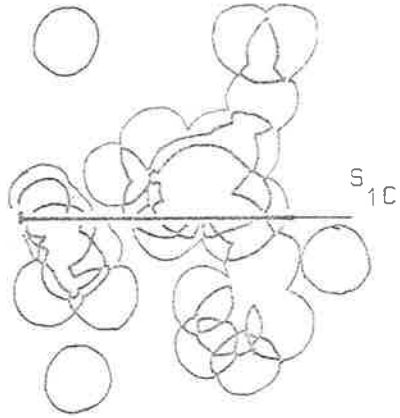

h

Fig. 6.15 (cont'd)

Unit 3, specimen A470-056, location 058018

(i) and (k) Quartzo-feldspathic pebbles on faces perpendicular to foliation

58 pebbles

(j) Quartzo-feldspathic pebbles on face parallel to foliation

60 pebbles

Unit 3, specimen A470-057, location 057016

(l) and (n) Quartzo-feldspathic pebbles on faces perpendicular to foliation

65 and 54 pebbles respectively

(m) Quartzo-feldspathic pebbles on face parallel to foliation

50 pebbles

Fig. 6.15(cont.)

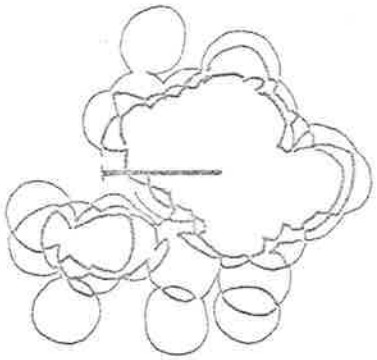

i

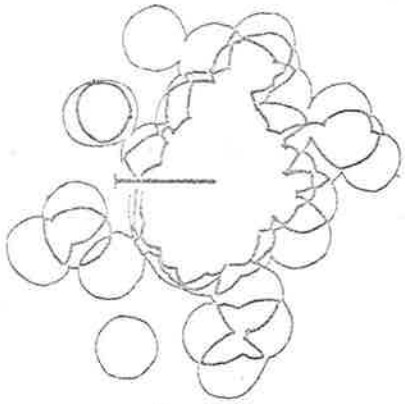

j

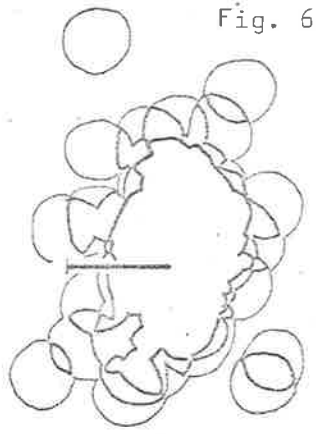

k

R_s

1.5 2 2.5 3 4 5

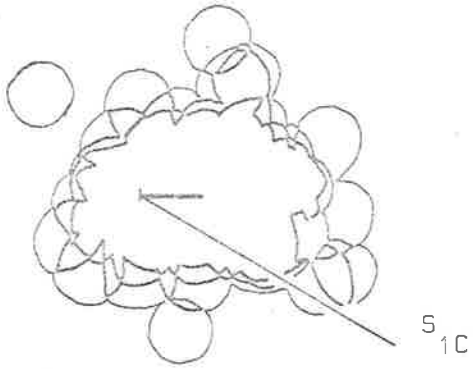

l

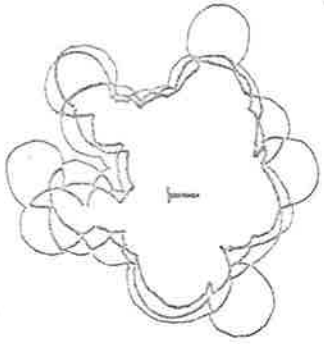

m

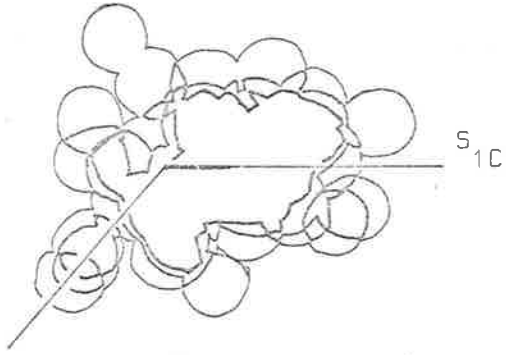

n

Fig. 6.15 (cont'd)

Unit 3, specimen A470-058, location 057012

(o) Quartzo-feldspathic pebbles on face parallel to foliation.

60 pebbles

(p) Quartzo-feldspathic pebbles on face perpendicular to foliation.

48 pebbles

(q) Schist pebbles on face perpendicular to foliation.

43 pebbles

(r) Schist pebbles on same face as Fig. 6.15p.

34 pebbles

Fig. 6.15 (cont.)

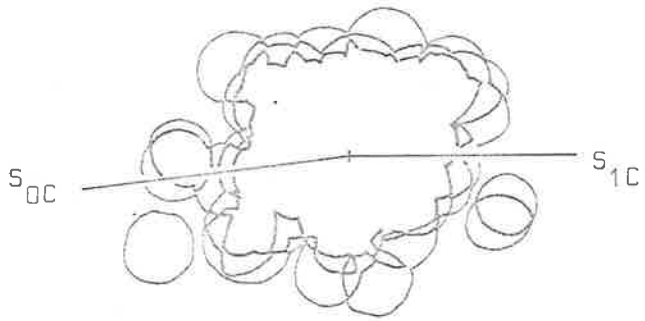

o

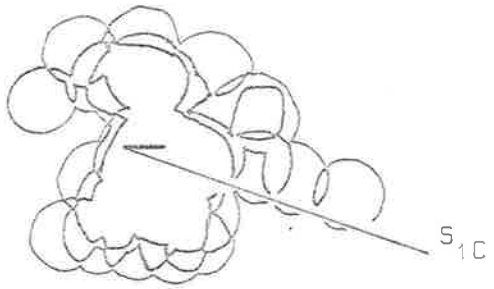

p

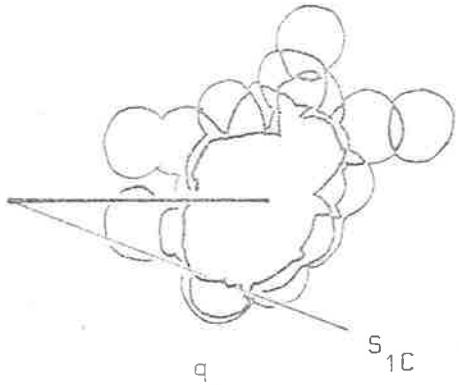

q

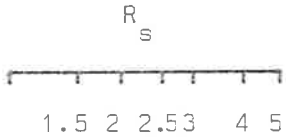

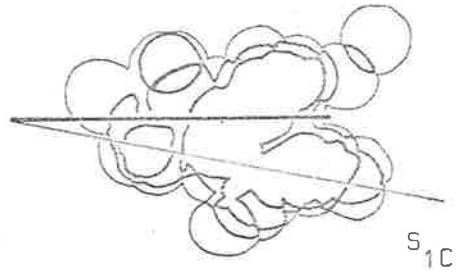

r

Fig. 6.16 Polar graphs of long pebble axes (R_f), plotted against orientation (ϕ) for measurements taken in Unit 5b. Distributions contoured by the Mellis method, contours show areas of 1, 2 and 3 circle overlap. Heavy lines indicate orientation and amount of principal extension. Faint lines show the orientation of foliation where it could be determined.

(a) and (b) Pebbles on faces perpendicular to foliation in specimen A470-065, location 064063.

68 and 70 pebbles respectively

(c) Pebbles on face parallel to foliation, specimen A470-065.

50 pebbles

(d) Pebbles on horizontal face perpendicular to foliation at 055061.

50 pebbles

(e) Pebbles on face dipping 55^{o}-085 (approximately perpendicular to foliation) at 055061.

57 pebbles

Fig. 6.16

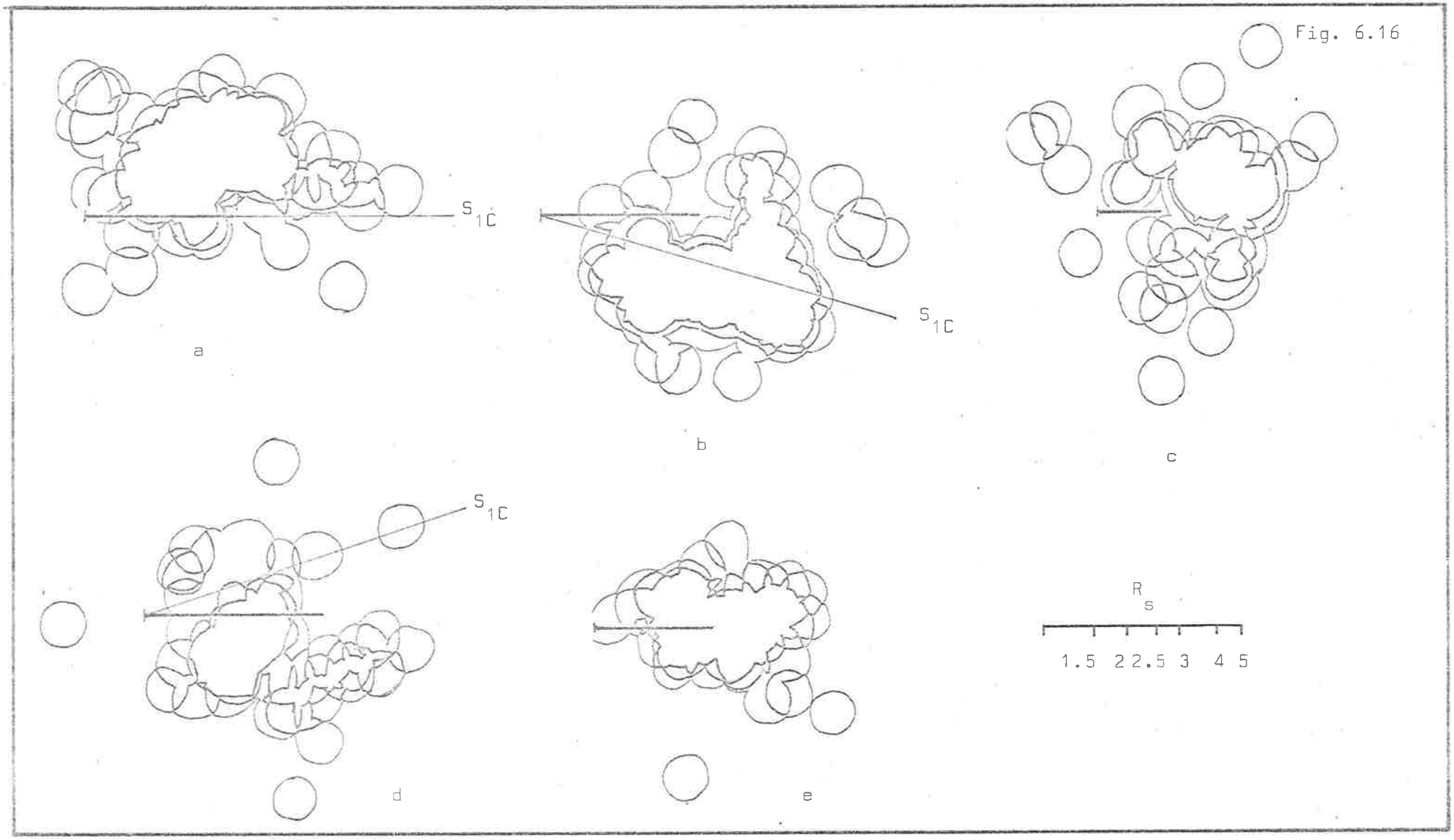

Fig. 6.17 Strain plots for basement schist A 470-071.

(a) and (b) Polar graphs of long axes (R_f) of 'porphyroblasts' plotted against orientation (ϕ) for faces perpendicular to schistosity (S_{2B}).

Contoured by Mellis method; 1, 2 and 3 circle overlap. Heavy line represents direction and amount of principal strain: light line represents orientation of schistosity (S_{2B}).

(c) Polar graph of long axes (R_f) of 'porphyroblasts' plotted against orientation (ϕ) for face parallel to foliation.

(d) and (e) R_f/ϕ diagrams for 'porphyroblasts' from faces of Fig. 6.17 (a) and (b) respectively, assuming principal direction of elongation is parallel to schistosity.

(f) Centre-to-centre method--distance between centres of adjacent 'porphyroblasts' (d) plotted against orientation (θ) for 'porphyroblasts' in same face as Fig. 6.17 (a) and (d).

Heavy line represents mean value of 'd' and light lines represent ± one standard deviation.

Maximum value of mean 'd' coincides with the trace of schistosity on this face.

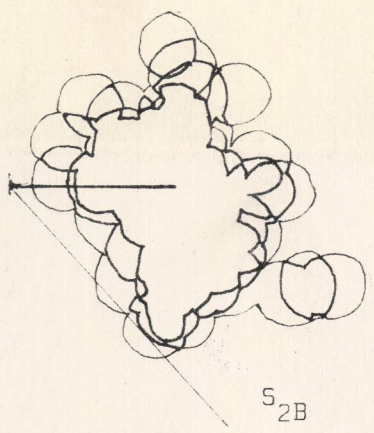

(a)

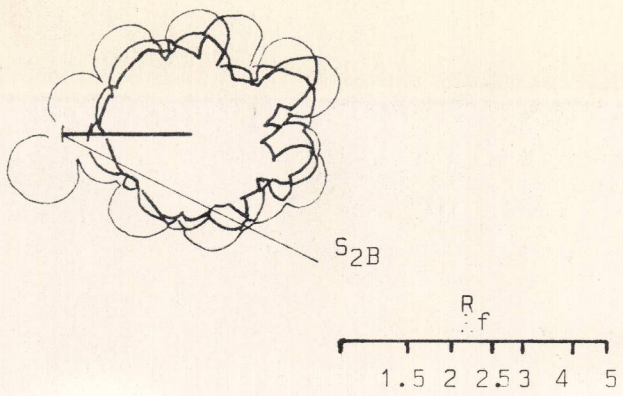

(b)

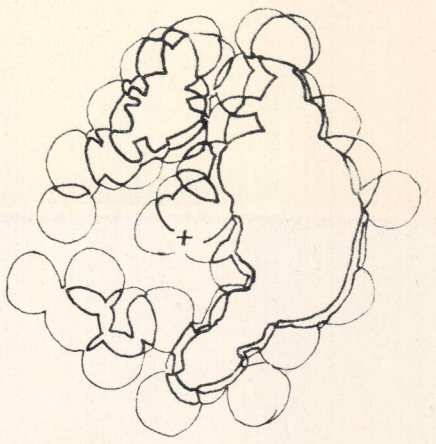

(c)

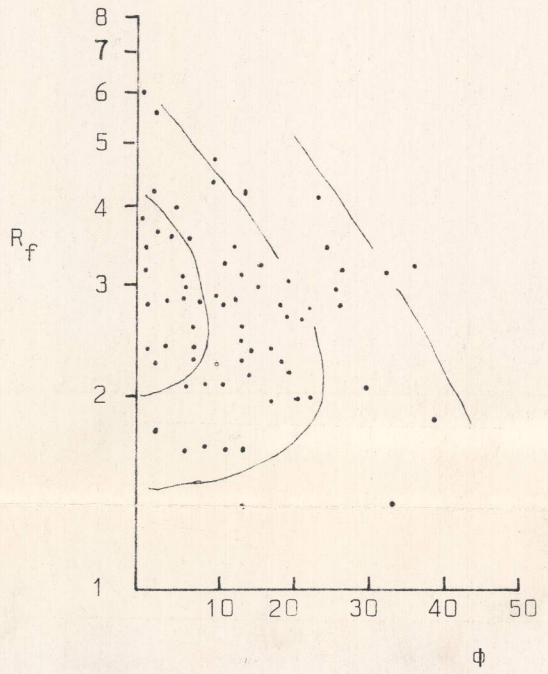

(d)

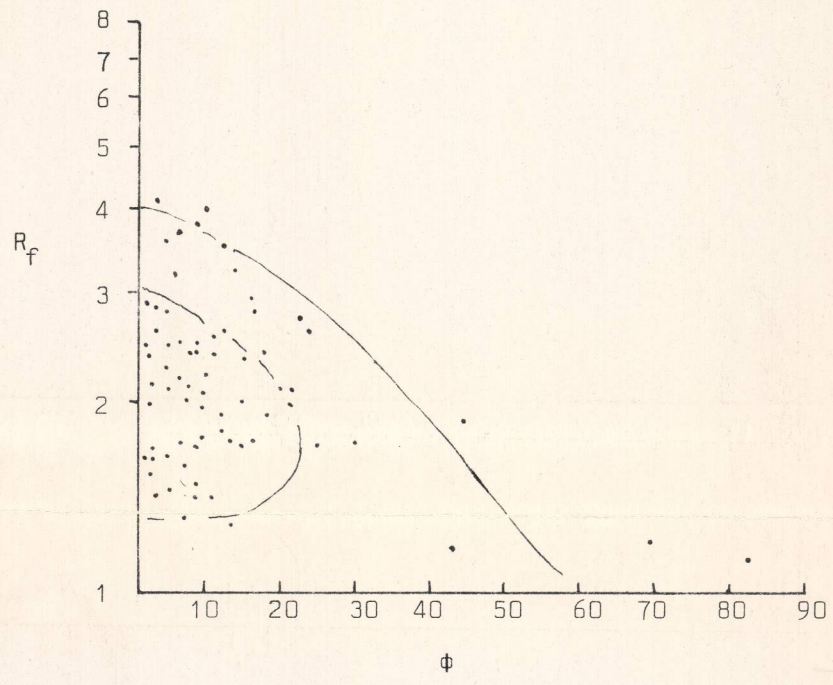

(e)

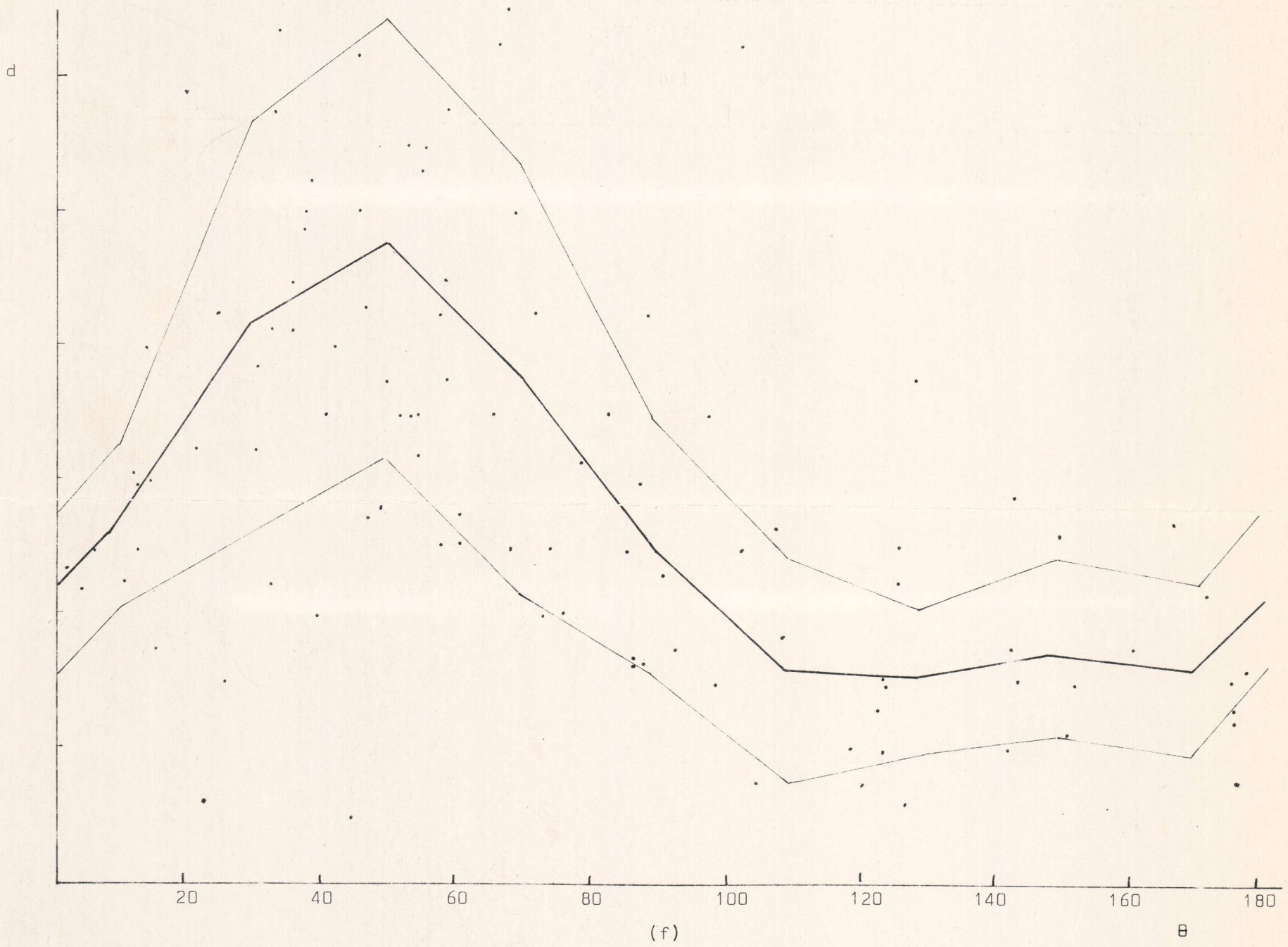

(f)

Fig. 6.17

Fig. 7.1 Mounted on plate with Fig. 6.14.

Fig. 7.2 Petrogenetic grid for minerals which outline the temperature pressure field (shaded) for the second episode of metamorphism (M_2) in the Old Boolcoomata area.

1 Kyanite ⇄ andalusite ⇄ sillimanite

2 Chlorite + muscovite + quartz ⇄ cordierite + biotite + H_2O

2a Biotite + sillimanite + quartz ⇄ cordierite + garnet + K-feldspar + H_2O

3 Calcite + quartz ⇄ wollastonite + CO_2

3a same reaction as 3 but with $X_{CO_2} = 0.25$

4 Muscovite + quartz ⇄ K-feldspar + aluminosilicate + H_2O

5 Minimum melting of granite

Equilibrium curves from Hyndman, 1972, figs. 7.11 and 7.12

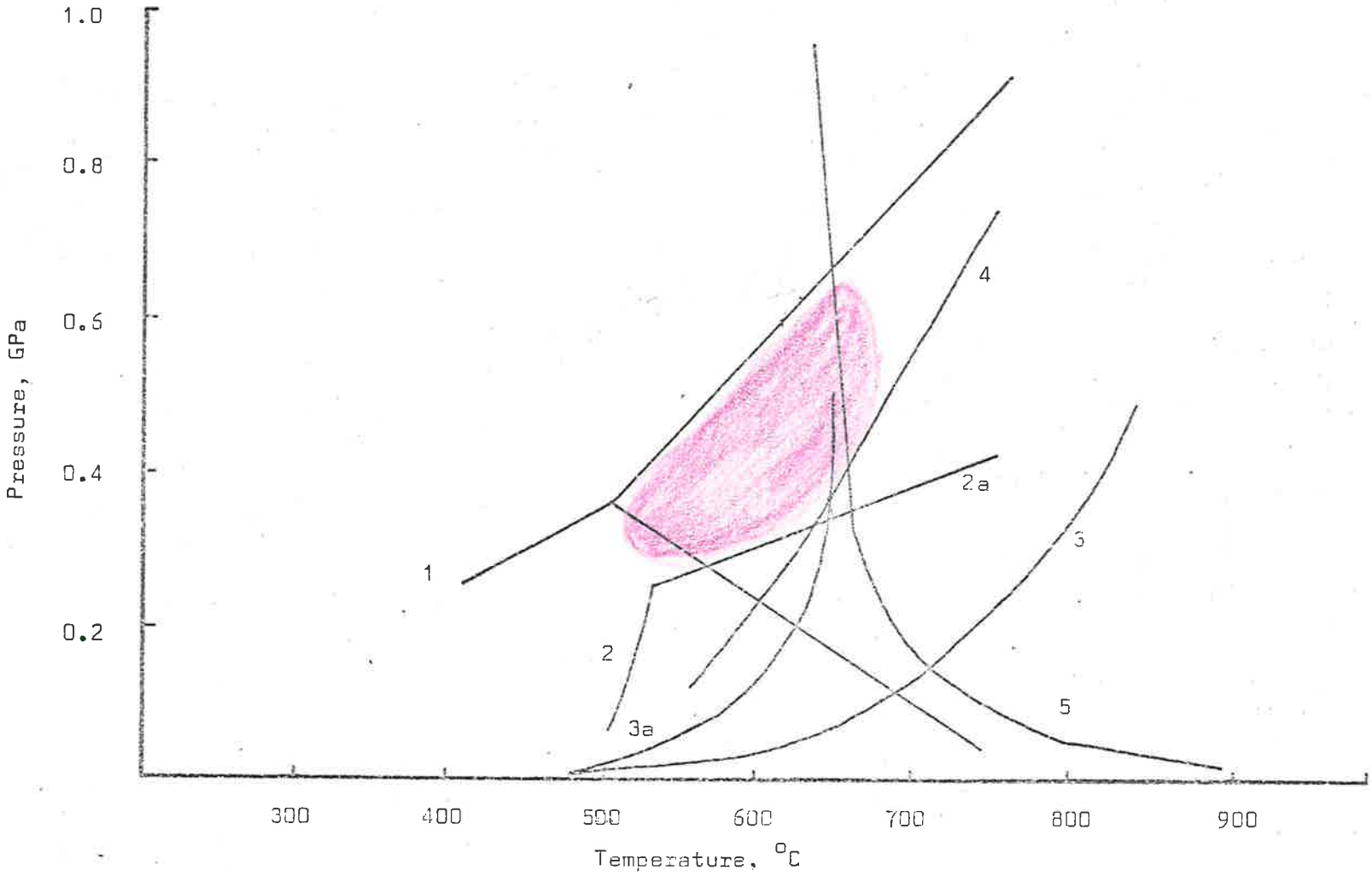
1.0
0.8
0.6
0.4
0.2
Pressure, GPa
1
2
2a
3
3a
4
5
300
400
500
600
700
800
900
Temperature, °C

Fig. 7.2

Fig. 7.3(a) Map of a portion of the Old Boolcoomata area showing the distribution of high grade mineral assemblages in the basement.

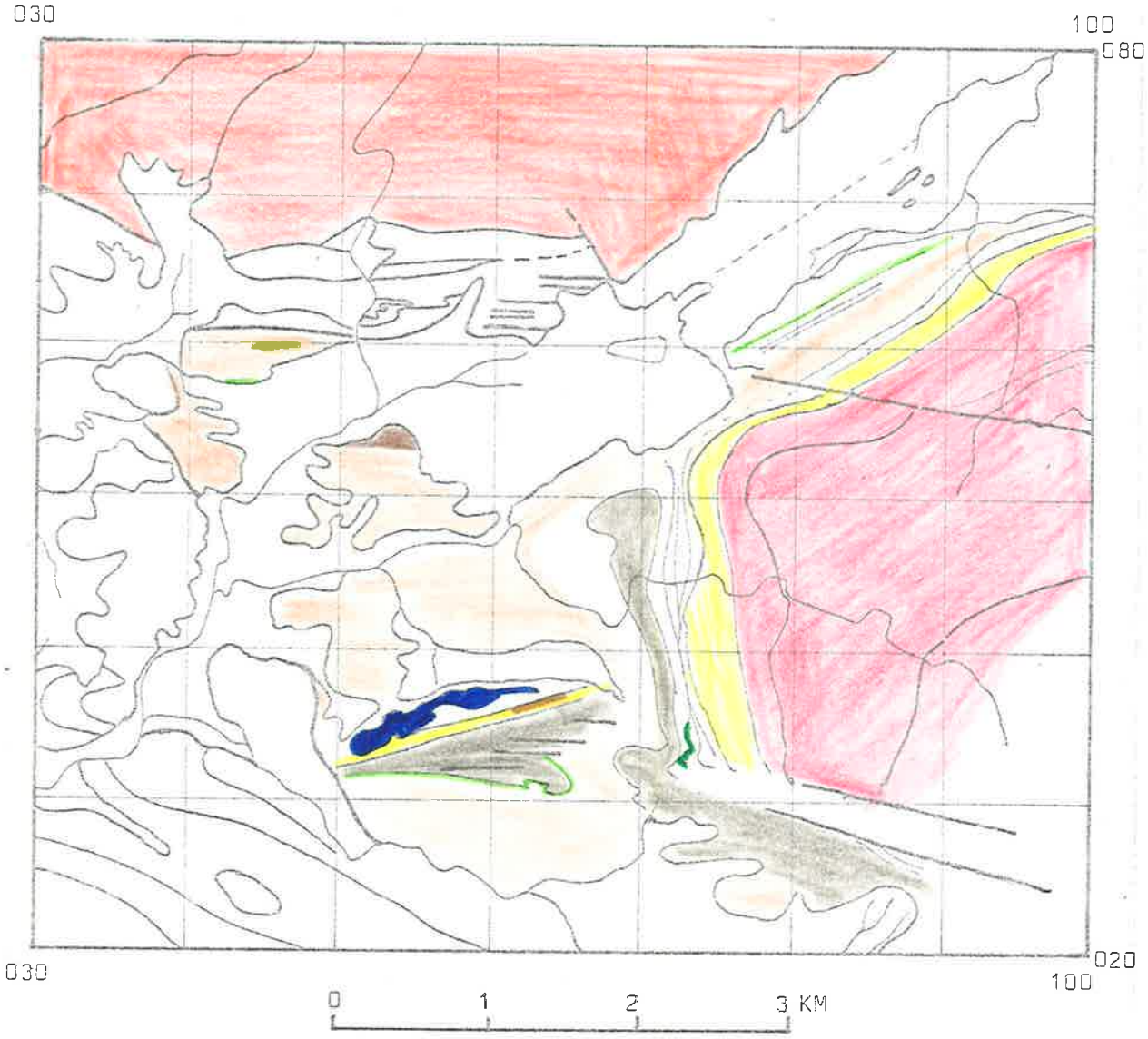

SCHISTS

- Muscovite-quartz-biotite
- Andalusite-muscovite-biotite-quartz
- Sillimanite-muscovite-garnet-quartz

CALCAREOUS ROCKS

- Plagioclase-hornblende-quartz
- Diopside-quartz
- Wollastonite-quartz-epidote-vesuvianite-garnet±diopside

GNEISSES

- Plagioclase-microcline-quartz-muscovite-biotite
- Corundum-biotite-albite-muscovite

AMPHIBOLITE

- Hornblende-plagioclase

GRANITIC ROCKS

- Adamellite
- Granitic gneiss and migmatite

Fig. 7.3(a) Distribution of High Grade Assemblages

Fig. 7.3(b) Map of a portion of the Old Boolcoomata area showing the distribution of low grade mineral assemblages in the basement.

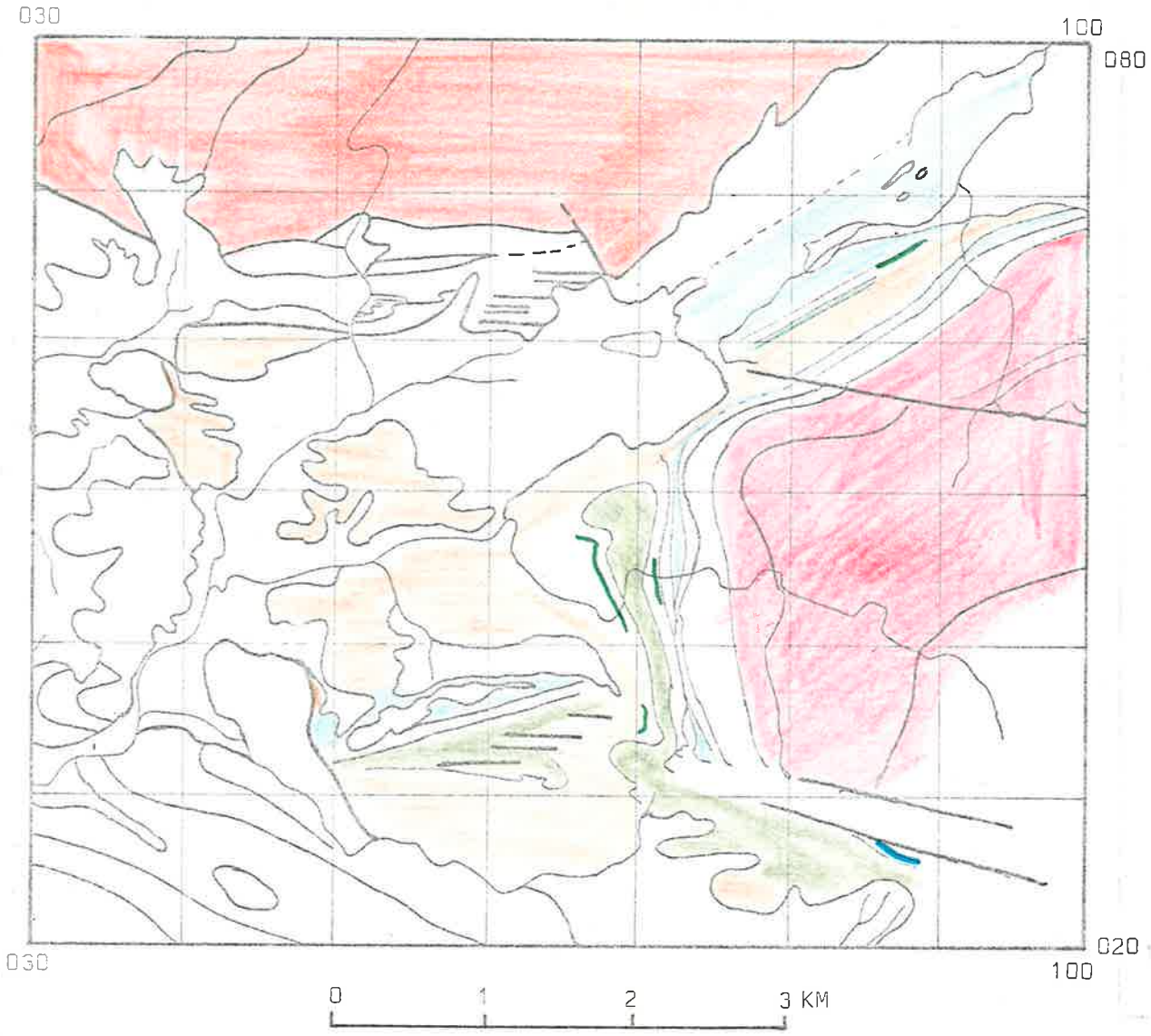

SCHISTS

- Muscovite-biotite-quartz
- Chlorite-muscovite-quartz
- Chlorite-chloritoid-muscovite-quartz

CALCAREOUS ROCKS

- Quartz-epidote-chlorite-calcite
- Calcite-chlorite-talc

ALBITE ROCKS

- Albite-actinolite-chlorite-calcite-quartz

GRANITIC ROCKS

- Adamellite
- Granitic gneiss and migmatite

Fig. 7.3(b) Distribution of Low Grade Assemblages

Fig. 7.4 ACF, AKF and Thompson's AFM diagrams for high and low grade mineral assemblages occurring in rocks from the Old Boolcoomata Area.

1. Chloritoid Schist

2. Layered Schist

3. Fine-grained and Medium-grained Mica Schists

4. Calcareous Rocks

5. Amphibolites

6. Cover slates

LOW GRADE ASSEMBLAGES

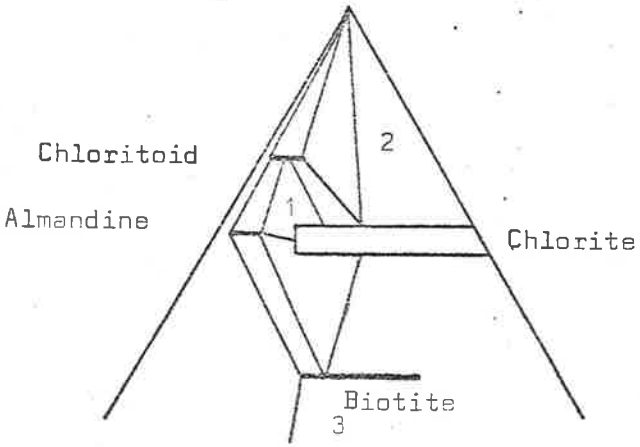

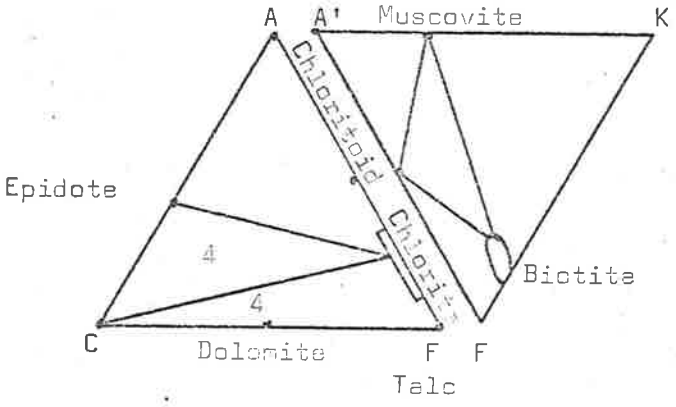

HIGH GRADE ASSEMBLAGES

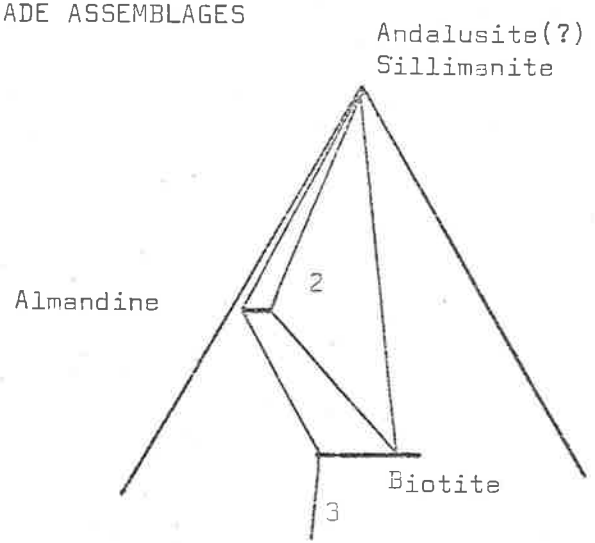

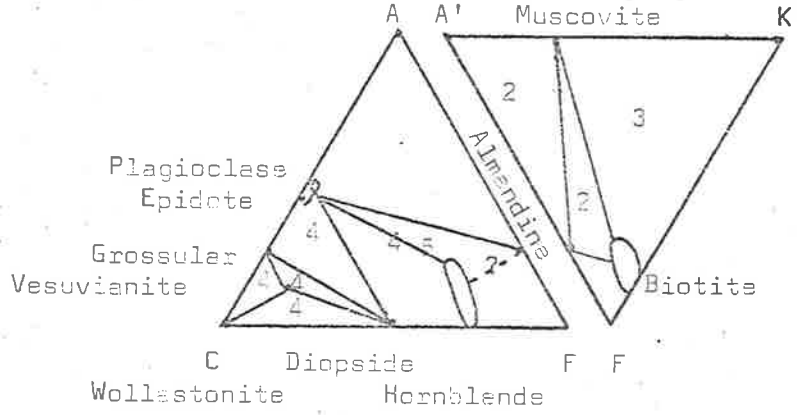

Fig. 7.4

Fig. 8.1 Model for the basement and cover deformation in the Olary Province.

(a) Adelaidean cover rocks deposited onto Willyama Complex basement.

(b) Shortening producing tight synclines and broad anticlines in the cover rocks due to competency difference between basement and cover.

(c) Further shortening leading to the production of faults and causing tightening of folds.

(Schematic cross-section from Whey Whey Creek area to Old Boolcoomata based on data from Campana and King, 1958; Talbot, 1962; and this study.)

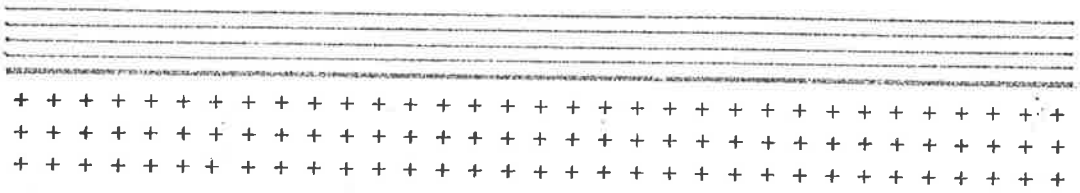

Fig. 8.1a

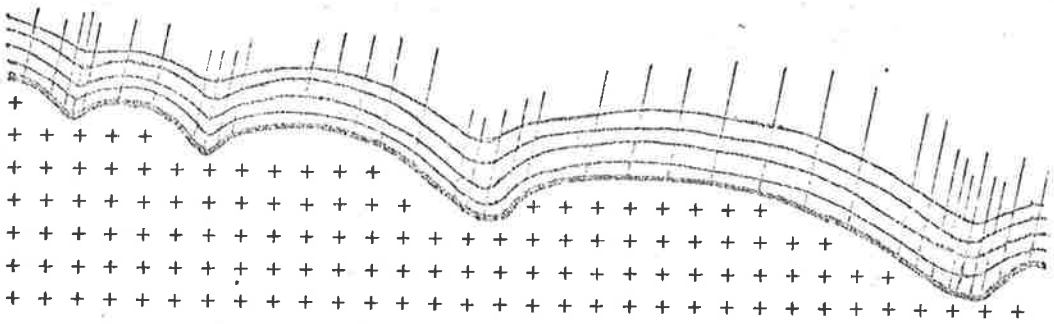

Fig. 8.1b

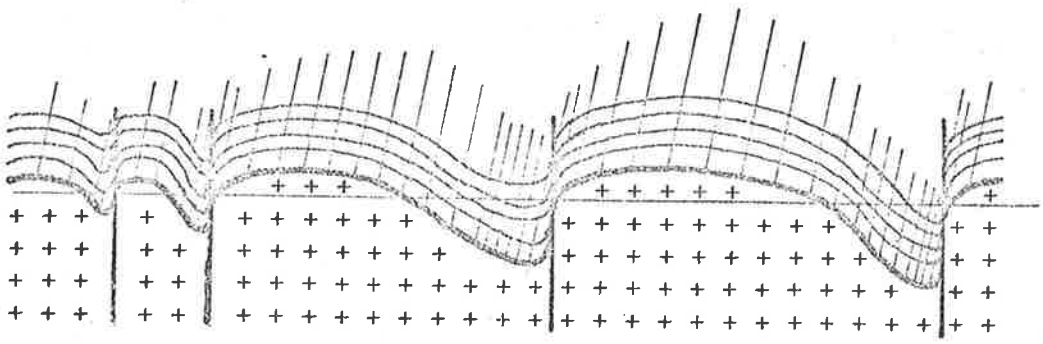

Fig. 8.1c